TUDelft

Delft University of Technology

Enhancing Virus Removal in Low-Cost Ceramic Pot Filters for Drinking Water Treatment

Soliman, Mona Youssef Moawad

Important note
To cite this publication, please use the final published version (if applicable).
Please check the document version above.

Enhancing Virus Removal in Low-Cost Ceramic Pot Filters for Drinking Water Treatment

Dissertation

For the purpose of obtaining the degree of doctor
at Delft University of Technology,
by the authority of the Rector Magnificus, Prof.dr.ir. T.H.J.J van der Hagen,
chair of the Board for Doctorates
to be defended publicly on
Monday 7 February 2022, at 17:30 o'clock

by

Mona Youssef Moawad SOLIMAN

Master of Science in Urban Water and Sanitation,
UNESCO-IHE, the Netherlands

Born in Cairo, Egypt

This dissertation has been approved by the promotors.

Composition of the doctoral committee:

Rector Magnificus	Chairman
Dr.ir. D. van Halem	Technische Universiteit Delft, promotor
Prof.dr. G.J. Medema	Technische Universiteit Delft, promotor

Independent members:

S. Murcott MSc	Massachusetts Institute of Technology, USA
Prof. dr. M.D. Sobsey	University of North Carolina at Chapel Hill, USA
Prof. dr. R.A. Buamah	KNUST, Ghana
Prof.dr. A.M. de Roda Husman	Utrecht University, The Netherlands
Prof.dr.ir. J.P. van der Hoek	Technische Universiteit Delft

Reserve member:

Prof.dr.ir. L.C. Rietveld	Technische Universiteit Delft

Author:	M. Y. M. Soliman
Printed by:	AIO; http://proefschrift-aio.nl
Cover art by:	Guss Gijben
Chapter photographs:	Frank Schuringa
Chapter drawings:	M. Y. M. Soliman

An electronic copy of this dissertation is available at the TU Delft Repository

Dedicated to all people who supported me when I couldn't stand on my own

SUMMARY

Access to safe drinking water is an essential human right and a crucial element to human survival. The quality of drinking water, has strong and direct impact on human health. Unless free of fecal contamination, water is unsafe to drink. Yet, to date, 2 billion people remain without access to safe drinking water [1]. Consequently, the burden of waterborne disease remains a global threat to public health especially in developing countries.

Fortunately, many interventions in the past decades aimed to provide safe drinking water in developing countries. Household water treatment (HHWT), provided individuals with a cheap and effective solution to treat water. Since its introduction, HHWT has dramatically improved the microbial quality of water, reduced the burden of waterborne diseases and its associated mortality [2]. In particular, ceramic pot filters (CPFs) were described as one of the most sustainable, popular and effective HHWT systems in reducing waterborne diseases[3–5]. In 2014, it was estimated that 4 million users rely on CPFs for water treatment [6]. CPFs provide consumers with an adequate protection against bacteria and protozoa which accounts for its reported protection against waterborne diseases. However, CPFs are not highly protective against all waterborne pathogens since they fail to remove viruses. The exceptionally small size of viruses enables them to pass through the filter pores.

Therefore, the objective of the thesis was to enhance virus removal in ceramic pot filters (CPFs). It was hypothesized that continued filtration of water through CPFs would lead to biofilm growth which might enhance virus removal. This hypothesis was examined using MS2 bacteriophage as ssRNA model virus. It was found that the growth of biofilm was dependent on the level of nutrients in raw water and as the subsequent virus (MS2) removal observed. The trade-off was the lower flow rates in high nutrient biofilms. Although high nutrient biofilms had better removal of virus (2.4 ± 0.5 logs), it reduced flow rates in the filters making them unusable.

This limitation in virus removal and flow rate called for alternative solution. Therefore, the use of metals, namely silver (Ag) and copper (Cu), was examined as potential additives to CPFs to enhance virus removal. Ag is already being applied to CPFs in many factories but its contribution to virus removal has been controversial

and only reported using model RNA virus (MS2). Cu is cheaper than Ag, hence it provided the possibility of an economical alternative or complementary addition.

To that end, Cu and Ag were examined for their antiviral efficiency; separately and combined. MS2 (ssRNA) and PhiX 174 (ssDNA) bacteriophages were tested as conservative model viruses for RNA and DNA waterborne viruses. Ag (0.1 mg/L) exhibited antiviral efficiency against MS2 and PhiX 174 (≤ 2 log inactivation over 6 hours), which was reduced in the presence of 20 mg C/L of natural organic matter (NOM) in water. Overall, Cu (1 mg/L) was a more potent disinfectant than Ag (0.1 mg/L). For example, in water containing NOM (20 mg C/L), Cu inactivated ≥ 6 logs of MS2 over 3 hours, and to lesser extent PhiX 174 (≥ 1 log in 3 hours). Moreover, significant synergy of Cu and Ag in combination was observed for MS2 in the absence of NOM and to a lesser extend in presence of low NOM at pH ≥7. A synergistic effect of Cu and Ag together in disinfecting PhiX 174 was observed, but only in presence of NOM in water. Overall to achieve ≥ 3 logs of inactivation by Cu and/or Ag, hours of interaction between the metal(s) and the virus were needed.

Because antiviral efficiency of Cu and Ag was observed, each was applied to ceramic filter discs (CFDs) according to the factory method (Filtron, Nicaragua) by painting metal ions solution using a hand brush. Virus removal by filtration through metal painted CFDs was examined. In addition, virus inactivation in the receptacles containing filtrate (in which there was leached Cu or Ag) was examined over 5.5 hours of storage. The contribution of Cu or Ag to enhancing virus removal by filtration was minor compared to the observed inactivation following hours of filtrate storage. This observation highlighted the value of utilizing virus inactivation as post treatment / post filtration option using Cu and/or Ag ions. Unfortunately, the rapid leaching of Cu from CFDs was an obstacle to testing Cu and Ag combination. It is therefore recommended to investigate alternative methods of Cu dosing other than painting.

This thesis quantified the contribution of biofilm growth to improving virus removal in CPFs, although the effect varied. With the in-depth assessment of Cu and/ or Ag antiviral efficiency, examining the effect of water quality parameters on the achieved virus inactivation, the potential of Cu and Ag was assessed. Post treatment or safe water storage relying on Cu and Ag ions can be applied in principle to provide safe drinking water in compliance with the WHO requirements.

SAMENVATTING

Toegang tot veilig drinkwater is een essentieel mensenrecht en cruciaal voor het voortbestaan van de mens. De kwaliteit van drinkwater heeft een sterke en directe impact op de menselijke gezondheid. Alleen wanneer water vrij is van fecale verontreiniging, is het veilig om te drinken. Toch, hebben tot op heden 2 miljard mensen geen toegang tot veilig drinkwater[1]. Hierdoor blijven in water overdraagbare ziekten een wereldwijde bedreiging voor de volksgezondheid, met name in ontwikkelingslanden.

In het afgelopen decennia, zijn er veel technologieën ontwikkeld die gericht zijn op veilig en schoon drinkwater in ontwikkelingslanden. Household water treatment (HHWT) of te wel huishoudelijke waterbehandeling, bood individuen een goedkope en effectieve manier om water te behandelen. Sinds de introductie heeft HHWT de microbiële kwaliteit van water drastisch verbeterd en de last van door water overgedragen ziekten en de daarmee samenhangende sterfte verminderd[2]. Met name de keramische potfilters (KP's) werden beschreven als een van de meest duurzame, populaire en effectieve HHWT-systemen om water overdraagbare ziekten te verminderen [3–5].

In 2014 waren naar schatting 4 miljoen gebruikers afhankelijk van KP's voor waterbehandeling [6]. KP's bieden gebruikers bescherming tegen bacteriën en protozoa, wat de gerapporteerde bescherming tegen de door water overdraagbare ziekten verklaart. Echter, KP's bieden geen bescherming tegen virussen. Virussen kunnen dankzij hun kleine omvang door de filterporiën van KP's heen. Voor deze reden heeft dit proefschrift de doelstelling om de virusverwijdering in keramische potfilters te verbeteren.

In de literatuur werd er verondersteld dat continue waterfiltratie door KP's zou leiden tot biofilmgroei die de virusverwijdering zou kunnen verbeteren. Deze hypothese werd onderzocht met behulp van het ssRNA-modelvirus, de MS2-bacteriofaag. De groei van biofilm is afhankelijk van de nutriënten concentratie in het ongezuiverde water en kon worden gerelateerd aan de verwijdering van het virus (MS2). Dit ging echter ten koste van de stroomsnelheid door het filter. Alhoewel biofilms bij een hoge nutrienten concentratie het virus beter konden verwijderen (2.4 ± 0.5 log), verminderde de doorstroomsnelheden in zo'n mate waardoor de filters onbruikbaar werden.

De gelimiteerde verwijdering van virussen en de verlaagde stroomsnelheid vroeg om een alternatieve methode om virussen te verwijderen. Daarom werd onderzocht of zilver (Ag) en koper (Cu) kunnen dienen als mogelijke toevoegingen aan KP's om de virusverwijdering te verbeteren. Ag wordt al toegepast op KP's. Echter de bijdrage van Ag aan het verwijderen van virussen is discutabel en wordt alleen gerapporteerd met behulp van model RNA-virus (MS2). Cu is een goedkoper alternatief dan Ag. Cu kan daarom dienen als een (complementaire) toevoeging aan KP's.

Daartoe werden Cu en Ag onderzocht op hun antivirale efficiëntie; afzonderlijk en gecombineerd. De bacteriofagen MS2 (ssRNA) en PhiX 174 (ssDNA) werden getest als modelvirussen voor RNA- en DNA- virussen. Ag (0,1 mg/L) vertoonde antivirale activiteit tegen MS2 en PhiX 174 (≤ 2 log-deactivatie gedurende 6 uur). Deze activiteit werd verminderd in aanwezigheid van 20 mg C/L natuurlijk organisch materiaal (NOM) in water.

In het algemeen werkte Cu (1 mg/L) beter dan Ag (0.1 mg/L). Bijvoorbeeld, in water dat NOM (20 mg C/L) bevatte, inactiveerde Cu ≥ 6 log MS2 gedurende 3 uur, en in mindere mate PhiX 174 (≥ 1 log in 3 uur). Verder werd een significante synergie in Cu- en Ag-combinatie waargenomen voor MS2 verwijdering in afwezigheid van NOM en in mindere mate in aanwezigheid van NOM bij pH ≥7. Een synergetisch effect van de Cu en Ag combinatie op de verwijdering van PhiX 174 werd alleen waargenomen in aanwezigheid van NOM in water. Om ≥ 3 logs virus deactivatie door Cu en/of Ag te bereiken, zijn vele uren interactie tussen het metaal/de metalen en het virus nodig.

Omdat de antivirale efficiëntie van Cu en Ag was bewezen, werd elk metaal, volgens de fabrieksmethode (Filtron, Nicaragua), aangebracht op keramische filterschijven (KFS's). Dit werd gedaan door de filterschijven te beschilderen met een metaalionenoplossing. Vervolgens werd de virusverwijdering door filtratie voor deze beschilderde KFS's onderzocht. Hiernaast werd ook de virus deactivering in het filtraat, die ook uitgeloogd Cu of Ag bevat, onderzocht gedurende 5,5 uur opslag. De resultaten lieten zien dat de bijdrage van Cu of Ag aan het verbeteren van de virusverwijdering door filtratie gering was in vergelijking met de waargenomen inactivatie na opslag van het filtraat.

Deze resultaten benadrukken de toegevoegde waarde van het voor of na behandelen met Ag en/of Cu ionen voor virus deactivatie. Het is aanbevolen om

een andere methode voor Cu dosering te onderzoeken dan schilderen. De snelle uitloging van Cu uit de KPS maakte het testen van de Cu en Ag combinatie lastig.

Dit proefschrift liet zien dat de biofilmgroei in KPF kan bijdragen aan de verwijdering van virussen. Ook werden de antivirale efficiëntie van Cu en/of Ag aangetoond dat in relatie met andere water kwaliteitsparameters. Nabehandeling of veilige wateropslag op basis van Cu- en Ag-ionen kan worden toegepast om veilig drinkwater te leveren in overeenstemming met de WHO-vereisten.

ACKNOWLEDGEMENTS

In 2016, I started the journey of my PhD funded by Delft Global initiative to work on this challenging topic. I am grateful to Delft Global initiative not just for their interest in research aimed for developing countries but also for their continuous support of their fellows. I want to start by thanking my team, Dr. Doris for her young fun spirit, endless enthusiasm, and passion for water research. Prof. Gertjan for his critical mind, passion for science, patience, and humorous soul.

I also would like to thank my first office mates, Katie, Heloise, Steef and Franka. I am so lucky to have met you. Your laughs and their continuous support made tough days enjoyable. Steef, thank you for your help with my thesis and for being crazy. I would like to thank Katie for making the journey of starting the white lab enjoyable. After many frustrating failed attempts to run bacteriophage assays in the red lab, we started the exciting journey of setting up the area for clean water analysis (known now as the white lab).

It is hard to imagine for my first two years of my PhD and my first publication was on such simple set-up (left picture); small incubator, water bath and a fridge. The troubleshooting to set up phage assays, grow bacterial host stocks, without laminar flow cabinet, were endless. As time passed, the lab grew (right picture), others joined and added to knowledge and the fun of working in the white lab.

It was such challenging task to kick off my PhD with but gives me pride of to have contributed to such facility that also impact the work of others. It wouldn't have been possible without Doris, Gertjan, Thom, Jules, Armand, Patricia, and Mohammed who provided continuous support, lots of effort, fund, dealt with the tough logistics, pushed for approvals and endless meetings and paper work.

TABLE OF CONTENTS

1
INTRODUCTION

1.1 Water Safety and waterborne diseases

Water is essential for human survival. In 2010, the UN recognized access to safe drinking water as a human right[7]. Yet, to date, 2 billion people remain without access to safe drinking water. These numbers are predicted to further escalate because global warming is aggravating the situation due to flooding and droughts. Moreover, the COVID-19 pandemic has restricted people's access to safe drinking water, leading to increased human suffering[8].

In the absence of safe drinking water, people can be forced to rely on contaminated water to meet their needs. Unless the biological and chemical safety of water are guaranteed, water can become a threat to human health and economic prosperity. In fact, more than 10% of the global population consume untreated surface water[9]. This is particularly concerning because 80% of wastewater is discharged untreated in open water bodies, hence increasing fecal contamination of water. Drinking untreated water or fecally contaminated water exposes consumers to harmful and disease-causing organisms. The most common waterborne disease is diarrheal diseases which vary in severity from recoverable to deadly.

It was estimated that 35% of death caused by diarrheal diseases is due to unsafe drinking water (WHO, 2019). Waterborne diseases are mostly caused by 6 RNA virus families such as Picornavirus (enterovirus, poliovirus, hepatitis A virus), Caliciviridae (norovirus, sapovirus) and Reoviridae (rotaviruses) [10]. dsDNA adenoviruses also cause waterborne diseases and can be more resistant to disinfectants (such as UV) than RNA viruses [10]. Diarrheal diseases are one of the major causes of child mortality especially of children under the age of 5. Rotavirus causes acute diarrheal disease among young children [11]. Hepatitis A and E can cause severe liver disease, resulting in patient's death [12]. It was estimated that 90% of children under the age of 10- who lack access to safe water or sanitation- were infected with hepatitis A[12,13]. Moreover, the mortality rate of hepatitis E infection is 25% in pregnant women [12,13].

Surviving diarrhea or waterborne diseases is not the end of the problem. Guerrant (1999) conducted a study in an urban poor community in Brazil and found that children under age 2 who were infected with the waterborne protozoan parasite *Cryptosporidium,* developed a lower fitness between the age of 6-9 years [14]. Moreover, early diarrhea was correlated with impaired cognitive function, lower

physical fitness and long term retardation[14,15]. The situation is more critical in children suffering from HIV, in whom the death rate is 11 times higher than in those who are not infected with HIV [16].

Not surprisingly, a recent study by Adelodun et al. (2021)[17] identified ingestion of virus-contaminated water as a cause for socioeconomic inequality and poverty in developing countries. Economically, lack of access to safe water results in substantial cost in health care, loss of life and loss in productive work days or school attendance due to sickness [18]. Although medical interventions such as rotavirus vaccination exist, their impact is not sufficient without serious improvements in water and sanitation conditions [16,19]. A meta-analysis for 144 studies suggested that child mortality dropped by 55% when water and sanitation conditions were improved [20].

1.2 Household water treatment system

Over the past decades, tremendous efforts were dedicated to improve water, sanitation, and hygiene (WASH) conditions to compact the global burden of waterborne diseases. Between 2015 and 2020, 193 million people gained access to safe drinking water[1].

Despite the progress and the global efforts to improve water conditions, to date, 2 billion people remain without access to safe drinking water[1]. Moreover, recontamination of water in low-income countries often still occurs. Treated piped water can be re-contaminated when supply is interrupted[21,22]. In addition, when treated water is collected by community members, transported and stored, recontamination can happen during any stage of this process [21,22]. For example, collection containers could be unclean or containers left open without a lid can attract animals or birds[22,23]. Moreover, the behavior in handling water during storage is detrimental in its safety (i.e., by dipping unclean hands in a drinking water bucket)[22].

To address these household water conditions, household water treatment (HHWT) systems enabled consumers to treat or re-treat their water inhouse to improve its safety. HHWT provides safe low cost technology for water provision in many countries, independent from governmental or community services[24–31]. Its impact has been clearly demonstrated to improve public health and significantly reduce diarrheal disease [26,32,33].

There are a number of systems available for HHWT. They vary in energy requirements, chemical use, price, and treated water microbial or chemical quality. Most HHWT focus on improving the microbial quality of water as it has direct impact on the global burden of disease.

1.3   Ceramic pot filters

Ceramic pot filters (CPF) are one of the most promising and accessible technologies for HHWT [34]. CPF's role in reducing waterborne diseases, especially diarrheal disease among children and low income consumers has been well documented [3,4,35–38]. Its impact is well documented as more effective in reducing diarrhea disease compared to other HHWT systems [3,4]. Abebe et al. (2014)[39] reported a significant contribution of CPFs in improving the quality of life of people living with the human immunodeficiency virus in rural South Africa by reducing diarrhea. In addition, CPFs gained popularity in areas where water boiling or chemical disinfection are not suitable to adopt [40].

CPFs are produced using local materials which provides an additional economical advantage in terms of low cost, creating micro investments and job opportunities [14,19,24,41]. There are 35 CPFs factories located across 18 countries and producing over 40,000 filters monthly [42,43]. The production process of CPFs starts by mixing clay with burnout material and water [32,41,43,44] (**Fig.** 1-1). Burnout material could be sawdust or rice husk. After mixing, the mixture is molded into a pot shape and fired in a klin [32,41,43,44]. The firing process turns the burnout material into ash, hence creating the CPF's pores. The created pores are responsible for the filtration mechanism of CPFs and to a great extent, the improved microbial quality of the treated water [45–47].

Possible inconsistency in the materials used such as: types of burn-out material or firing temperature can lead to variation in the pore structure of CPF units. It was reported that majority of CPFs' pores are < 20 μm [48,49] in size. However, some pores can reach 100 μm in size. Depending on the production conditions, microcracks can form inside the filter. Microcracks can effect interconnectivity of pores and the filter flow rates [50]. Hence, microcracks effect the relationship between flow rates and microbial performance of CPFs. This is a troubling issue because water flow rate checks are the main quality control step reported from CPF factories (**Fig.** 2-1).

Although some factories add an additional pressure test[51], quality control by measuring the flow rate (1-3 L/h) remains the prevailing practice.

The material used in producing CPFs plays an important role in the structure and the microbial performance of the pots[47,52]. For example, clay minerology impacts the shrinkage rate of the pots during the firing process and the final pore structure[49]. Moreover, it has an impact on the microbial adsorption capacity of the filter[52]. Although important, controlling the clay type used is a problem because maintaining a local clay supply is crucial for sustainable low cost production [47]. In addition, the impact of other filter production variables such as burnout material size and burnout to clay ratio have been contradictory in their effect on CPF microbial performance according to different reports in literature [47].
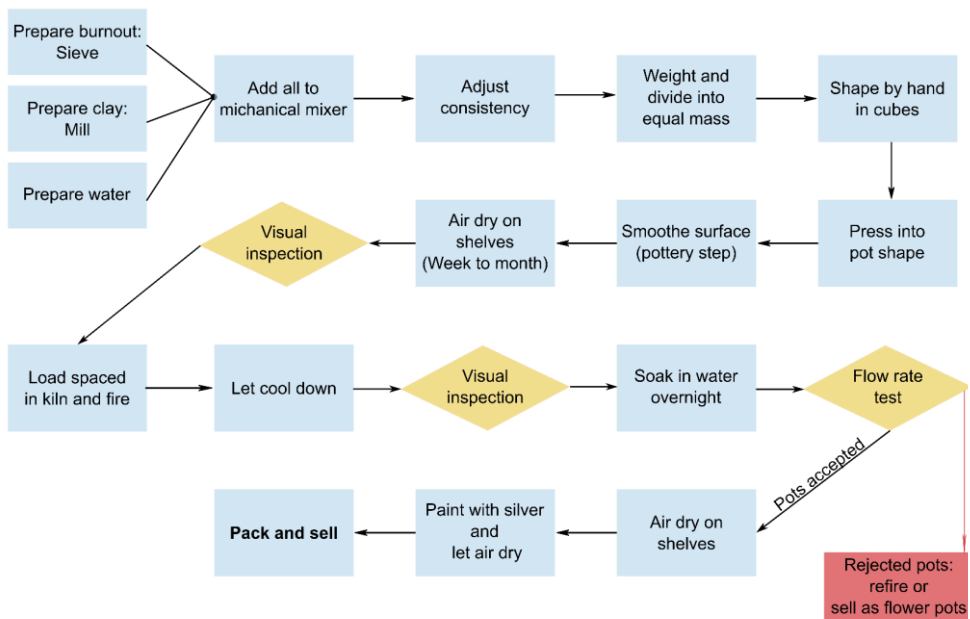
Figure 1-1: Manufacturing process steps for CPFs according to data from the Filtron factory, Nicaragua.

1.3.1 Microbial performance of ceramic pot filters

Water filtration by CPFs (**Fig.** 2-2) can be described by two stages: the contact between water and the filter's surface layer (surface filtration), followed by deep filtration. In surface filtration, microbes and contaminants larger than the surface

pore size are retained inside the filter. As water passes through the filter, microbes can get trapped in dead-end pores, be removed by further straining or adhere to the filter medium by electrostatic interaction[47].

Figure 1-2 Illustration of CPF in use, adapted from WHO (2016) [53]

It is important to distinguish between the size of different microbial contaminants: protozoa, bacteria, and viruses. Protozoa range in size from 10 to 200 µm, bacteria from 0.2 to 2 µm and viruses from 0.02 to 0.1 µm[54]. Considering that CPFs can contain pores as small as 0.1 µm, protozoa and bacteria can be removed by size exclusion but not viruses. In CPFs viruses can only be removed by means of dead-end pores entrapment or adsorption[47,51,55].

The reported removal of protozoa range from 2 to 5 logs[51,56–58]. The removal of E. coli bacteria was an average of about 2 logs without silver (Ag) and 4 logs with Ag[47,51,58]. However, virus removal was unsatisfactory by CPFs at ≤ 1 log, regardless of Ag presence[6,55,58–60]. According to the WHO, house hold water technologies need to achieve 2-star performance criteria for two classes of pathogens to qualify as accepted-protective technology for water treatment (**Table** 2-1). While for protozoa and bacteria CPFs achieve high to very high pathogen removal, the failure to remove viruses reduces CPFs to minimally acceptable technology having only targeted protection.

Table 2-1 WHO recommended microbiological performance criteria for HWT technology performance classification- adapted from WHO (2016)

performance classification	Protozoa (log10 reduction required)	Bacteria (log10 reduction required)	Viruses (log10 reduction required)	Interpretation (assuming correct and consistent use)
★★★	≥ 4	≥ 5	≥ 4	Comprehensive protection (very high pathogen removal)
★★	≥ 2	≥ 3	≥ 2	Comprehensive protection (high pathogen removal)
★	Meets at least 2-star (★★) criteria for two classes of pathogens			Targeted protection
–	Fails to meet WHO performance criteria			Little or no protection

Improving CPFs to provide protection against viruses is crucial for the health and safety of consumers. Viruses are obligate parasites, and once a host is found they replicate inside the host before being released in feces to repeat the cycle in another host [61–64]. . Viruses can be shed in feces at high concentrations – up to 11 logs- and persist in water for long periods [63,64]. Unless viruses are properly treated in water and prevented from reaching other consumers, disease outbreaks can occur [63,64]. This is particularly concerning, because successfully overcoming viral infection is dependent on the human immune system. Due to reduced immunity, viral infection can be fatal to children and individuals with HIV.

1.4   Virus removal in CPFs – identifying research gaps

Due to the exceptionally small size of viruses, CPFs fail to remove viruses by size exclusion. This has been consistent according to literature reporting negligible virus removal (<1 log) in CPFs[6,55,58–60]. . However, a few exceptions in literature have been reported for studies with relatively long term filter usage, which was hypothesized to be due to slime layer -biofilm- growth in the filter[50,60]. Over the past decades, multiple efforts have aimed to improve virus removal in CPFs. For example, changing the firing process or adding metals before or after firing. Those attempts rely on one or two processes to enhance virus removal: adsorption and/ or inactivation[65]. The adsorption process considers viruses as colloidal matter for which surface charge, surface area or hydrophobicity are the determining factors of virus removal. Meanwhile, inactivation of virus relies on chemical or physical destruction of the virus particle causing loss of infectivity. Here, we discuss the

major efforts to improve virus removal in CPFs, their related mechanisms, extent of success and identify the present gaps in research.

1.4.1 Biofilm growth in CPFs

As mentioned, a few improved LRVs were reported for virus removal in CPFs. Van Halem, (2006)[50] reported 3 logs removal values (LRVs) of MS2 bacteriophage (used as conservative RNA virus indicator). This removal was recorded after 13 weeks of filtering canal water. The author observed a growth of "slime layer" inside the filter after long usage. Farrow et al. (2014)[60] also reported increase in MS2's LRVs from 0.2 to 2 logs following 2 weeks of turbid water filtration. Larimer (2013)[66] demonstrated that in absence of Ag, CPFs are susceptible to bacterial colonization and biofilm growth. Biofilm growth was only inhibited at high concentrations of Ag and dominating surface coverage with Ag[66]. However, the constant leaching of Ag from CPFs diminishes its effectiveness for virus reduction after a few month of usage[58]. Hence, it is likely that the retained bacteria inside the filter along with the absence of or diminished Ag, would lead to biofilm growth during the long-term usage of CPFs. **Yet, assessing the relationship between biofilm growth in CPFs and virus removal remains a clear gap in literature.**

1.4.1.1 Biofilms and viruses

Biofilm growth is initiated when bacteria present in water adheres to a solid surface[67]. Depending on the available organic nutrients and surrounding conditions, a biofilm develops[68–70]. Growth of bacteria in biofilms produces extracellular polymeric substances (EPS) which defines the physiochemical and biological properties of the biofilm[71]. EPS is an integral constituent of biofilms and is physically recognized by its "slime" feeling which was mentioned in the report of Van Halem, (2006).

The interaction between biofilms and viruses has been studied in water pipelines, membrane reactors and slow sand filters. In pipelines, $3 - 4$ logs/cm^2 of bacteriophage were removed by biofilms and persisted as viable for at least a week[72]. In membrane bioreactors around 3 LRVs of bacteriophages were observed following biofilm growth[73,74]. In slow sand filters, 0.1 to 3 LRVs of bacteriophages were reported, depending on the biofilm age[75].

Hence, it can be anticipated that biofilm growth in CPFs will lead to enhanced virus removal. However, none of the cited $\log_{10}$ reductions values (LRVs) can be generalized to CPFs because of variations in hydralic flow, material characteristics and water quality conditions would lead to structural differences between biofilms. **These knowledge gaps call for a dedicated study examining biofim growth in CPFs in relation to virus reductions. Factors such as: nutrient content in water, biofilm age, filter usage period, filter cleaning practices and possible persistence of viruses in CPFs are important to account for (as research gaps).**

1.4.2 Metal additives and virus removal in CPFs

The widely applied metal additive in CPFs is silver, Ag. Ag application has been advised by the ceramics manufacturing working group to improve microbial performance of the filter and control biofilm growth[47,76]. There is abundant study in evaluating the effect of Ag addition on *E. coli* removal in CPFs. It was concluded that the main contribution of Ag to enhance *E. coli* LRVs takes place in the receptacles[6,47]. Leached Ag from CPFs inactivates *E. coli* that penetrated the CPF and is present in filtered water in a time dependent manner[6,47].

On the other hand, limited studies had evaluated the impact of Ag additives on virus removal by CPFs and was mostly limited to examining RNA viruses using MS2 as a ssRNA model virus. The reported results only focused on direct filtration, overlooking the interaction between viruses and Ag ions in the receptacles. Brown and Sobsey (2010) and Van der Laan et al. (2014) reported no improvement in LRVs of MS2 in samples directly collected from Ag amended CPFs compared to Ag free CPFs[6,41]. However, the study of Salsali et al. (2011) demonstrated that the quality of filtered water (i.e., deionized vs surface water) significantly contributed to higher MS2 LRVs by Ag amended CPFs rather than the type of Ag (ions or nanoparticles) applied in the filter[59].

Recently, copper (Cu) additives have been introduced to CPFs as possible cheaper alternative to Ag. Ehdaie et al. (2020) showed improvement in MS2 removal by ceramic tablets amended with Cu compared to controls[77]. Friedman (2018)[78] also reported increase in overnight LRVs of MS2 (almost reaching 3 logs) when Cu was combined with Ag to amend CPFs before firing. On the other hand, Lucier et al. (2017) reported similar MS2 LRVs (> 3 logs) in metal free CPFs and those amended with Ag or Cu.

These findings highlight the following gap in examining Ag or Cu contribution to virus removal by CPFs: the efficiency of Cu or Ag in removing DNA viruses versus RNA viruses in CPFs needs assessment. Moreover, distinguishing virus removal by direct filtration from time dependent inactivation of viruses by leached metals in the receptacles is important. Also, understanding the impact of water quality parameters on Cu and Ag inactivation of DNA and RNA viruses is important to their application in CPFs.

1.4.2.1   Metals and viruses

In order to assess the contribution of metal additives to virus disinfection or removal in the ceramic filtration system, the effect of metals on viruses must be understood. Physiochemical water parameters such as pH, organic matter, temperature, ionic strength, etc., can affect metal speciation and reactivity. The speciation of metals was reported to impact their environmental toxicity [79,80]. Hence, it is likely that speciation of metals would impact its antiviral capacity as well. Nieto-Juarez et al. (2010) reported on the importance of dissolved Cu^{2+} ions on disinfecting MS2 bacteriophage. However, a similar assessment of Ag was overlooked [81–84].

One important parameter is solution pH. pH can not only effect speciation of Cu and Ag but also virus conformation, hence its sensitivity to disinfectants[85]. Moreover, a study by Yahya et al. (1992) reported on a synergistic effect of using Cu and Ag combined in disinfecting MS2 versus their individual use. To our knowledge, no other studies reported on conditions where synergism can happen or if it also occurs for DNA viruses. **Hence, it is important to evaluate the effect of individual metals (Cu or Ag) versus combined (Cu and Ag) on RNA viruses versus DNA viruses under variable solution pH.** This would provide clear understanding of Cu and/ or Ag antiviral efficiency when used for water treatment.

Another important factor to assess, is natural organic matter (NOM). Presence of NOM in water is inevitable. Many CPF users are located in remote or rural areas, hence, they rely on contaminated surface water or ground water as a water source [47,51,86]. This implies variability in water quality and its organic content. NOM contains functional groups such as thiols, hydroxyls, aldehydes, etc., that can form organic complexes with Cu or Ag [87,88]. This has been observed in fresh water bodies where most of Cu is bound to NOM, resulting in lower environmental toxicity of Cu[89]. Moreover, Ag interaction with NOM can result in forming Ag solids such as AgCl,

Ag$_2$S or AgS, depending on solution conditions and the reaction period [87,88]. Formation of Ag solids is undesirable since it reduces its disinfection capacity compared to Ag$^+$, as observed in *E. coli* studies [90–93]. An additional observation was that Cu binding to NOM was reported to result in production of reactive oxygen species (ROS) [94]. Presence of ROS can enhance inactivation kinetics of MS2 bacteriophage as observed in many studies [95–99].

Therefore, evaluating the effect of NOM on Cu and/ or Ag inactivation kinetics of RNA and DNA viruses is of great importance. Currently, there is a gap in literature regarding the effect of NOM on Ag or Cu inactivation kinetics of either RNA or DNA viruses. Whether or not we can anticipate reduced virus inactivation by Ag, Cu and the metal combination cannot be anticipated. Moreover, it is unclear if the possibility antiviral activity of Cu and Ag would be associated with NOM presence or not.

1.5   Research questions

- Does biofilm growth in CPFs enhances to virus removal? (**Chapter 2**)
  - o What is the relationship between biofilm age, growth conditions and virus removal in CPFs?
  - o How does consumer cleaning practices effect virus removal by biofilms in CPFs?
- Does Cu or Ag efficiently inactivate RNA and DNA viruses? What is the impact of combining Cu and Ag on inactivation of RNA and DNA viruses? (**Chapter 3**)
  - o What is the impact of water pH on Cu and Ag inactivation of waterborne viruses?
  - o Does Cu or Ag speciation change by changing pH in tested water? And does that impact inactivation kinetics?
  - o Do RNA and DNA exhibit similar susceptibility to Cu and Ag under variable pH?
- What is the impact of NOM on Cu and Ag inactivation kinetics of RNA and DNA viruses? (**Chapter 4**)
  - o Does Cu and Ag combination lead to added synergism with or without NOM?
  - o Does NOM impact Cu and Ag speciation and subsequently virus inactivation?

o   Is there production of ROS in presence of NOM with Cu and/or Ag in water? If observed, does it enhance inactivation?

- Do Cu or Ag additives contribute to removal of DNA as well as RNA viruses in CPFs? Is the removal dependent on direct filtration or timely interaction in the receptacles? (**Chapter 5**)

  o   Is adapting the commonly practiced Ag painting method suitable to incorporate Cu in ceramic filters?

1.6   Thesis outline

To enhance virus removal in CPFs, the ceramic pot filtration usage was studied over lengthy time period of filter use **(Chapter 2)**. This aimed to simulate consume conditions in using the filter for a long time period until the flow rate reduces, then cleaning it with a hand brush. We used multiple sets of filters, each with water containing different nutrient levels.

In **chapter 3**, the effect of pH on Cu and Ag inactivation kinetics was examined using two model viruses: MS2 (ssRNA) and PhiX 174 (dsDNA). Inactivation kinetics using individual metals (Cu or Ag) verses their combination (Cu and Ag) against MS2 and PhiX 174 in water matrices with different pH was measured. This provided initial understanding of what metals can serve as disinfectants in a controlled setting. To shed light on the mechanistic work of Cu or Ag, MS2 and PhiX 174 particles were examined using transmission electron microscopy before and after treatment to identify possible structural damage caused by metals.

Because water that is treated in a CPF will contain NOM, in **chapter 4**, the effect of NOM on Cu and Ag inactivation kinetics of MS2 and PhiX 174 and possible synergism of Cu and Ag was examined. Moreover, possible production of ROS and its implications for inactivation kinetics was considered and investigated. Finally, in **chapter 5** CPFs painted with Cu or Ag were evaluated for MS2 and PhiX 174 removal against blank (unpainted) filters. The evaluation also distinguished between LRVs due to filtration through metal painted CPFs and time dependent inactivation due to metal- virus interaction in water filtrate receptacles.

2 VIRUS REMOVAL BY CERAMIC POT FILTER DISKS: EFFECT OF BIOFILM GROWTH AND SURFACE CLEANING

This chapter is based on:
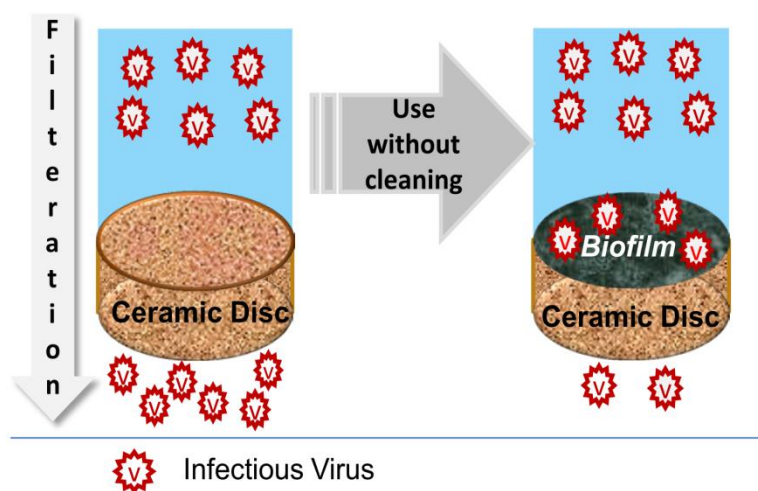
Abstract

Ceramic pot filters are household water treatment and safe storage (HWTS) systems designed to improve the microbial quality of drinking water. They yield high log reduction values (LRVs) for bacterial and protozoan pathogens but provide very little removal of viruses. This study investigated virus removal of ceramic filter discs (CFDs), using feed water with 3 different nutrient levels under extended continuous operation and limited cleaning frequency. The results show that filter use without cleaning resulted in biofilm growth and MS2 LRV values increased with increasing feed water nutrient content. Cleaning the filter surface by scrubbing led to a partial or total loss in improved LRVs, indicating the importance of this biological top layer to the removal of MS2. Overall, the removal capacity of a matured biofilm remained constant, regardless of its age. MS2 LRVs ranged between 0.9±0.2 LRV for low nutrient (LN), 1.6±0.2 LRV for medium nutrient (MN) and 2.4±0.5 LRV for high nutrient (HN) biofilms. Interestingly, a change in feed conditions for the HN filters resulted in an unprecedented high LRV of >4 LRV, which supports further investigation of the mechanistic role of biofilms in virus removal.

2.1 Introduction

Ceramic pot filters (CPF) are a cost-effective household water treatment and safe storage (HWTS) technology for users without access to microbiologically safe drinking water, such as in rural areas without central treatment works. In a meta-regression study evaluating health improvements of HWTS systems, Hunter et al (2009) concluded that the CPF provide a greater protective effect than other HWTS systems. The use of CPF reduced waterborne disease risk by a factor of 3. Compared to other HWTS systems, CPF proved to be more sustainable for long term usage and more resilient since it is less dependent on energy, availability of chemicals or weather [3,100].

CPF manufacturing and use are on the rise in developing countries, yet international production standards and quality control checks do not exist [32]. Manufacturing quality control is limited to visual inspection for cracks and flow rate checks [101]. No performance checks on the removal of microbes is conducted [32,43,102]. In lab and field studies, CPFs have been reported to provide high levels of removal for bacteria and protozoa; however, virus removal is very limited [6,43,55,103,104]. Virus removal has been assesed through challenge studies in the laboratory using bacteriophages (generally F+ coliphage MS2) as viral indicators since they resemble the removal of human enteric viruses [100]. Removal of MS2 in CPF was found to be less than 1 LRV (Log Reduction Value) under different conditions (water quality, water source, contact time, etc.) [6,41,43,55,59,102,105–107].

To qualify as protective in WHO's verification scheme for HWTS systems, CPFs would need to achieve at least 3 LRV for viruses, demonstrated by MS2 and phiX174 [100]. Reported MS2 reductions reached almost 3 LRV after 13 weeks of continuosly filtering canal water through CPFs [50], which was hypothesized to be due to the growth of biofilms on the filter during operation. Similar hypotheses were posed by Farrow et al. (2014), who claimed that reducing the cleaning frequency would lead to biofilm growth and improved virus removal.

Biofilms have demonstrated the ability to capture viruses[108], Storey and Ashbolt (2003) recovered 10^8 pfu/cm^2 of B40-8 and MS2 phages and 10^7 pfu/cm^2 phiX174 phages from biofilm coupons collected from artificially challenged drinking water piplelines. Biofilm growth in slow sand filters (SSF), membrane bioreactors (MBR) and constructed wetlands enhances the removal of micro-organisms, including viruses. Ueda (2000) measured an increase of 3.7 LRV in suspended indigenous

phage removal following biofilm growth in an MBR unit. Similarly, Purnell et al., (2015) reported a 2.3 LRV increase for MS2 and B-14 spiked in wastewater treated by biofilm-coated MBR. In slow sand filters, the surface biofilm (schmutzdecke) MS2 LRV ranged between 0.08 to 3, depending on the schmutzdecke age and water temperature [75]. Moreover, the LRV of MS2 increased by 1.5-2.5 times following biofilm growth in ultrafiltration units [111,112]. The differences in LRV between viruses under the same conditions is mainly related to morphology of the viruses, as indicated by the meta-analysis of Amarasiri et al. (2017) for a range of wastewater treatment process, including membrane filtration and membrane bioreactor treatment. The study found MS2 phages to be more difficult to remove than somatic coliphages, F-specific phages and T4 phages, making it a conservative representative for human virus removal.

Biofilm formation starts by the adhesion of bacteria to solid surfaces, which immobilises them. The bacteria may grow [67], dependent on the availability of the compounds necessary for assimilation and dissimilation such as organic matter in water [68–70]. Many CPF users rely on surface water as their water source [103,104], which may contain significant levels of organic carbon, depending on the level of contamination or eutrophication [114,115]. This implies that a biofilm will form on CPF during operation, and the biofilm formation rate will depend on the level of nutrients in the water source. The objective of the study was to examine the hypothesis that extended filtration periods and reduced cleaning frequency would lead to enhanced virus removal due to biofilm growth. Three source waters containing different nutrient levels were filtered through CFDs, and biofilm growth was monitored by tracking the flow rate of the CFD and measuring bacterial cell counts and ATP on the CFD surface. Virus removal was determined by challenging CFDs at the end of different operational periods, before and after cleaning, with MS2 phages and monitoring virus breakthrough. Finally, the biofilm was evaluated for the presence of MS2 to confirm the role of the biofilm as a virus attachment site and to identify the fate of viruses in the CFD system.

2.2 Materials and Methods

2.2.1 Ceramic filter disc manufacturing

For this study, CFDs were used to simulate full ceramic pots [116]. CFDs were manufactured at the FilterPure (now Wine to Water) factory in the Dominican

Republic by following the manufacturing protocol precisely. Local clay, sawdust and demineralised water were mixed in a weight ratio of 65%: 13%: 22%, respectively. Sawdust was sieved through a 0.5 mm sieve prior to mixing. The components were mixed for 5 minutes in the mechanical mixer, followed by 5 minutes of hand mixing. The mixture was moulded and pressed under 2200 psi pressure into CFDs. Moulded CFDs were left to dry for 3-5 days then fired in a kiln for at 860 °C with a ramp rate of 2.4°C/min and dwell time 1 hour. The disks were left in the kiln to cool overnight, no silver or other additives were applied after firing.

2.2.2 CFDs filtration setup

To facilitate their testing, each CFD ($\emptyset$ 125 mm & H=19 ± 2 mm) was fixed using silicone into the bottom of a double socket connector (125 mm $\emptyset$ PVC). On top of the connector, a 350 mm PVC column (125 mm inner $\emptyset$) was placed, providing a maximum water head of 4.5 L above the CFDs. The system was operated as a fed-batch system, filled daily with source water, while resting over an open top polypropylene receptacle to collect filtered water. LN, MN and HN source waters were applied, each in duplicate columns. Nutrient Broth (NB; CM0001, Thermos Scientific) was diluted in unchlorinated tap water. LN was tap water without NB, MN was tap water with 1:500 diluted NB and HN was a 1:125 dilution of NB. PO_4, NO_3 and NH_4 were measured using Hach kits LCK 348, LCK 339, LCK 303. Total (TOC) and dissolved (DOC) organic carbon, and total nitrogen (TN) were measured using a TOC-V CPH Shimadzu analyzer. Dissolved oxygen (DO) was measured using a WTW 3420 portable multimeter. Selected dilution rates aimed to simulate organic carbon concentrations in "clean" (< 10 mg/l) and contaminated (>10 mg/l) fresh water. The setup was operated inside a Thermo Fisher Heratherm OMH400 incubator at 27 °C throughout the experiment to represent a warm, tropical environment.

Low Nutrient (LN)	Medium Nutrient (MN)	High Nutrient (HN)
TOC =3.4 ± 0.1 mg C/l COD <15 mg/LO$_2$ NO$_3$= 2.8 ± 0.1 mg/L NO$_3$-N NH$_4$ < 2 mg/L NH$_4$-N TN =2.8 ± 0.1 mg N/L PO$_4$ <0.05 mg/l PO$_4$-P	TOC =8.2 ± 0.3 mg C/l COD =16.2 ± 2 mg/LO$_2$ NO$_3$= 2.7 ± 0.1 mg/L NO$_3$-N NH$_4$ < 2 mg/L NH$_4$-N TN =4.3 ± 0.1 mg N/L PO$_4$ <0.05 mg/l PO$_4$-P	TOC =24 ± 0.8 mg C/l COD =64 ± 1 mg/LO$_2$ NO$_3$= 2.7 ± 0.1 mg/L NO$_3$-N NH$_4$ < 2 mg/L NH$_4$-N TN =11 ± 0.1 mg N/L PO$_4$ =0.15 ± 0.05 mg/l PO$_4$-P
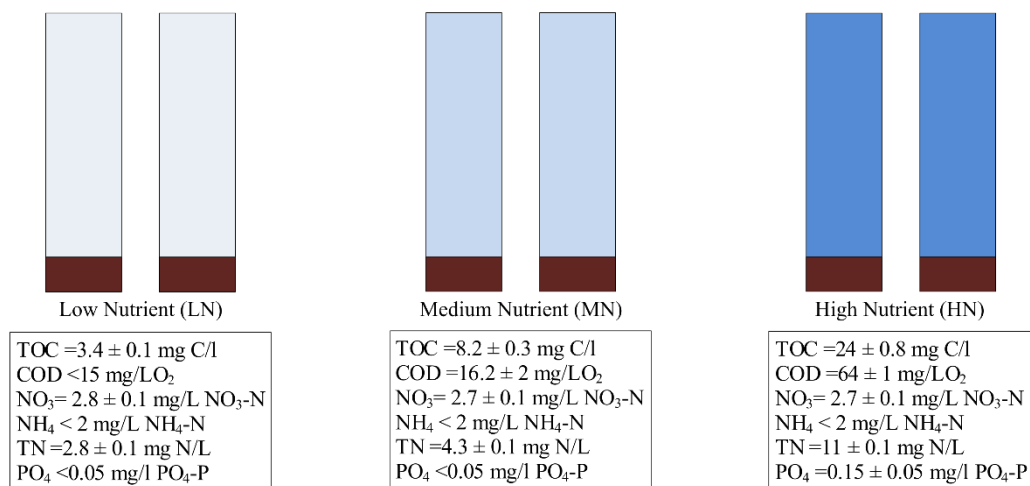
Figure 2-1 Experimental set-up and feed water characterisation *(For reference, each set of duplicate CFDs were named after their source feed water)*

2.2.3 MS2 challenge test

On the challenge test day, MS2 stock (GAP Environmental, Canada) was diluted in unchlorinated tap water (challenge water) to a concentration of 10^6 to 10^7 pfu/ml. Thus, the term "challenge water" for all experiments refers to LN water spiked with MS2 bacteriophages. The columns were each filled with 4 L and put back in the incubator at 27˚C. Filtrate volume of at least 1 total pore volume (PV) was discarded to ensure that water in the pores was replaced by MS2 challenge water. The pore volume was calculated based on the dry versus saturated weight of the CFDs and corresponded to a PV of 128 ± 2 cm^3. Filtrate samples were collected in a receptacle that had been cleaned and disinfected by subsequent rinses with 0.05% sodium hypochlorite solution, demineralized water, 100 mg/l sodium thiosulfate solution and demineralized water (3x). Receptacles were air-dried before use.

Samples were refrigerated and analysed the same day using the double agar layer (DAL) method, according to ISO 10705-1. Naladixic acid was added to the top agar to limit growth of background flora. Serial sample dilutions were plated in duplicate, and plaque-forming units (PFUs) were counted after incubation for 18 h at 37 °C. PFU results were converted into log$_{10}$ reduction values (LRVs), where LRV = log$_{10}$ (measured concentration of MS2 in the influent/measured concentration of MS2 in the filtrate).

2.2.4 **Biofilm analysis**

Biofilm growth was monitored by swabbing the CFD surface. An area of 5.31 cm^2 was swabbed using COPAN sterile Dry Swabs with a plastic applicator and rayon tip. The swab was submerged in filter-sterilised mineral water and stored at 4 ± 2˚C until analysis. Bacterial cell counts were measured with a C6 flow cytometer (BD Accuri C6, United States), with distinction between total (TCC) and intact (ICC) cell counts. ATP, TCC and ICC analyses were conducted at Het Waterlaboratorium (Haarlem, the Netherlands) following the protocol described by Liu et al. (2013).

2.2.5 **Experimental overview**

2.2.5.1 *Operational period before cleaning*

2.2.5.1.1 Initial operation (5 weeks)
Duplicate LN, MN and HN CFDs were run in fed-batch mode for 5 weeks. Daily flow rates were recorded by measuring filtrate volume over time in a graduated cylinder. MS2 LRVs were measured using the challenge test water at the end of weeks 4 and 5. Water in the columns was replaced by MS2-free source water (LN, MN and HN) directly after completing each challenge test. In addition, the surface of the HN CFDs was swabbed using rayon swabs to quantify TCC, ICC and ATP of the surface grown biofilm.

2.2.5.1.2 Long-term operation (21 weeks)
The LN and MN CFDs were operated in fed-batch mode for an additional 4 months without cleaning. HN CFDs were excluded from this experiment since their flow rates had become too low. Combining the biofilm formation periods of the current and the previous test, the biofilm age reached 21 weeks (5.25 months), which is the longest continuous testing period for ceramic filters reported to our knowledge. MS2 LRVs were determined by challenge tests on weeks 10, 16 and 21. Flow rates were measured daily, and the surface of the CFDs was sampled for biofilm analysis in weeks 10 and 21. The disk surface was swabbed after each challenge test was completed, then columns were refilled with MS2 free source water (LN and MN) to sustain biofilm growth and development.

2.2.5.2   Effect of cleaning the surface

Cleaning the filter surface and the receptacle is a regular maintenance step recommended and practised by users of CPF. Filter flow rates drop with continued use, especially when surface water is used [118,119]. Thus, it is inevitable that the CPF's internal surface needs to be cleaned periodically to restore the flow. CPF factories advise using a stiff laundry brush to scrape the surface once every 4 weeks [119]. Nevertheless, Cambodian users were reported to clean the filter every week [119]. Cleaning the filters has been studied, although the focus was on water flow restoration [43,55]. In this study, the focus is to understand the effect of removing the surface biological top layer (biofilm) on the MS2 LRV. To this end, biofilm amended CFDs were challenged with MS2 before and after cleaning the surface. The cleaning protocol was applied by brushing the surface twice using a stiff hand brush followed by a rinse with demineralised water. This protocol was repeated at each cleaning event.

After running for 21 weeks in fed-batch mode, the LN and MN CFDs surfaces were cleaned. Before and after this cleaning, biofilm swabs were obtained, flow rates were recorded and MS2 challenge tests were conducted. The cleaning event was repeated twice, following CFDs operational periods (i.e., periods of biofilm regrowth) of 4 (week 25) and 1 (week 26) weeks. Also, during these regrowth periods, MS2 challenge tests were conducted and flow rates were monitored before and after the cleaning, but biofilm swabs were obtained only before cleaning. After MS2 challenge tests for any cleaning event, CFDs were returned to fed-batch mode with MS2 free source water (LN or MN) to allow for biofilm regrowth and recovery.

HN CFDs were cleaned earlier than LN and MN CFDs given the loss of flow rate after the first experiment lasting 5 weeks. HN CFDs were subsequently fed with LN water for a month instead of regular HN feed to avoid permanent clogging of the CFDs. After this, the CFDs were reloaded with HN water for 4 and 1 weeks, each followed by cleaning events. MS2 challenge tests were run before and after each cleaning event, flow rates were monitored and biofilm swabs were taken to measure TCC and ATP.

2.2.5.3   The fate of phages in the system

After the experiments with and without cleaning, the fate of MS2 in CFDs was studied in more detail. This experiment was conducted on a 1-week-old re-grown biofilm for all CFDs. The experiment consisted of two stages: (1) MS2 challenge water feed and (2) regular feed without MS2. In the first stage, we examined the stability of the MS2 phage concentration in the feed water residing on the top of CFDs (supernatant) and monitored the MS2 concentration in the filtrate (C_f) over time/pore volume. The second stage examined the MS2 survival/recovery in the biofilm and detachment of MS2 phages from the biofilm/filter into the filtrate. Stage 2 started at the end of Stage 1 and ended when no phages were detected in biofilm or water samples.

At the onset of Stage 1, challenge water was sampled to establish the initial challenge concentration, referred to as C_0 (pfu/ml). Subsequently, duplicate samples were taken from the challenge water every hour after stirring with a sterile serological pipette. The samples were analysed for MS2 to determine the change of pfu concentration over time (C_t). Linear regression of the log concentration change (log C_t/C_0) was used to estimate the inactivation rate (λ) of MS2 in feed water at 27 $^\circ$C as described by Schijven et al. (2013).

Simultaneously, hourly samples from the filtrate were collected, mixed, volume recorded and analysed for MS2 (C_f). After sampling, a new disinfected receptacle was placed to collect the next hour's filtrate for each time point. Sampling was repeated until > 2 pore volumes (PV) of filtrate were collected, after which the challenge feed water was replaced with regular feed water without MS2 at t_1. Monitoring of the filtrate continued beyond t_1, i.e., Stage 2 of the experiment, in order to assess detachment (C_d) and breakthrough of MS2 from the biofilm/filter.

At the time of feed water replacement (t_1), 3.64 cm^2 of each CFD was swabbed to collect a biofilm sample. Swabs were transferred to a sterile glass tube containing filter-sterilised mineral water then sonicated 3-4 times for 2 minutes using a Bransonic 521 water bath. Sonicated water was collected in sterile tubes placed on ice, mixed, the volume was recorded and analysed for MS2 phages. Results were converted from PFU/ml into PFU/cm^2, where PFU/cm^2 = (PFU/ml sonicated liquid volume)/ surface area swabbed (cm^2). The number of phages in the biofilm of the total CFD surface (N_b) was calculated from the PFU/cm^2 × CFD Surface Area (cm^2).

A MS2 balance was calculated using the total number of phages loaded onto the CFD (N_i) with correction for the inactivation over time (λ), the total number of phages in the filtrate in stage 1 (N_f), the total number of detached phages (N_d, in the Stage 2 filtrate) and the total number of phages recovered from the biofilm (N_b).

2.3   Results and discussion

2.3.1   Operational period before cleaning

Fig. 2-2 depicts the average MS2 LRV after the initial operational period of 4 and 5 weeks of CFD filtration of LN, MN and HN source water. After 4 weeks of initial operation, the average MS2 LRV remained below 0.5 for both LN and MN CFDs, whereas the HN CFDs achieved an average LRV of 1.4. A week later, the MS2 LRV for LN and MN CFDs had increased to 0.9 and 1.5, respectively. The HN CFDs also showed an increased LRV (to 2), although due to the variation between duplicates, this increase is not as apparent.
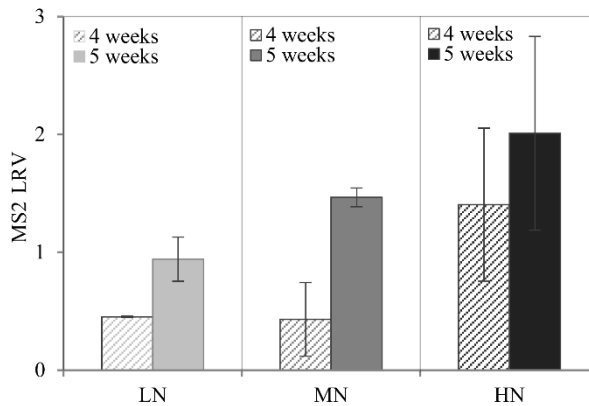
Figure 2-2 MS2 bacteriophages removal after 4 and 5 weeks of continuous loading (n=2). Error bars represent standard deviations (SD).
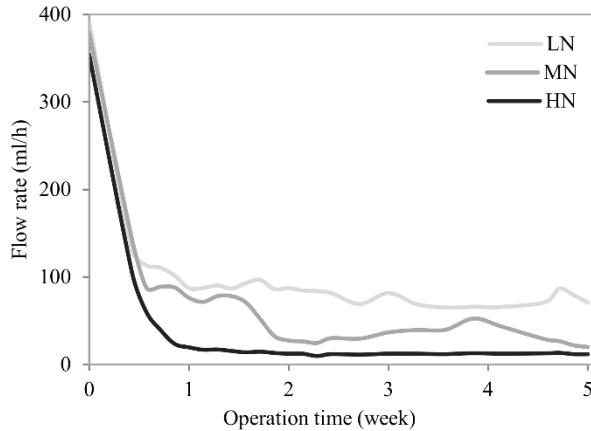
Figure 2-3 Flow rate of CFDs during the initial 5 weeks (Plotted values represent averages of duplicate CFDs)

Continuous loading of the CFDs had an impact on the flow rate as illustrated in **Fig. 2-3**. In the first four days, LN, MN and HN CFDs lost 68%, 75% and 83% of their initial flow rate, respectively. The flow rate of HN CFDs continued to drop for 1 week before stabilising. Meanwhile, LN and MN CFD flow rates slowly dropped further during the 5 weeks. Flow rate resistance was higher with higher nutrient feed (LN< MN<HN), suggesting increased biofilm growth with increased nutrient concentration in the feed. Due to the flow rate drop in HN CFDs, these filters were conserved after their cleaning in tap water from week 5 onwards and excluded from further MS2 challenge tests.

For LN and MN CFDs, **Fig**. 2-4 depicts the average MS2 LRV and the corresponding flow rates for operational periods from 5 to 21 weeks. This additional operational period did not result in a considerable further increase of MS2 LRVs. CFDs with MN biofilms had a consistently higher MS2 LRV as well as lower flow rate than those with LN biofilms.
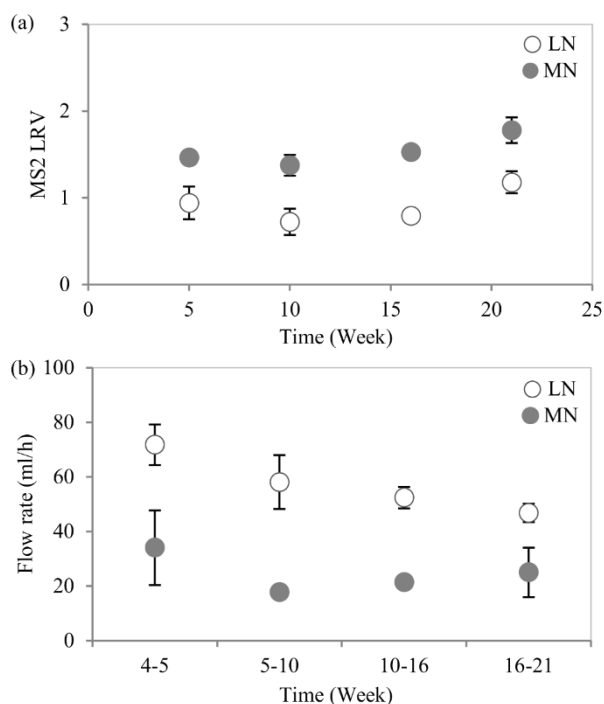
Figure 2-4 Relation between CFD (n=2) run time, (a) MS2 LRV and (b) flow rate. Error bars represent SD.

The TCC of the biofilms increased considerably between weeks 0 and 10 both for MN (>2 logs) and LN (>1.5 logs) biofilms (**Fig**. 2-5). Similarly, the ATP of the biofilms had a greater increase for MN (2.7 log) than for LN (0.97 log) biofilms (**Fig**. 2-5). Between weeks 10 and 21, the TCC and ATP of LN biofilms increased by 0.6 and 0.4 logs, respectively. Meanwhile, the TCC of MN biofilms decreased by 0.3 logs while its ATP increased by 0.2 logs. The increase in ATP, despite reduction in TCC, could be due to the release of ATP from damaged cells or a higher ATP per intact cell, possibly resulting from larger intact cells. So, while LN biofilms slowly continued their growth beyond 10 weeks, MN biofilms stabilized and had slightly lower cell counts. This is consistent with the changes in flow rate values shown in **Fig**. 2-4b. Flow rates continued decreasing for LN CFDs beyond week 10 but were relatively stable for MN CFDs.

By combining the results of the HN-5-week biofilm with the previous test as well as the results of the tests after cleaning (see next paragraph), a more inclusive image about continuous loading without cleaning and nutrient concentration of the feed

can be projected. ATP measurements provide insight into biofilm biological activity (Liu et al., 2013). Measured HN-ATP after 5 weeks was 1 and 3 logs higher than MN and LN ATP, respectively, at 21 weeks (**Fig**. 2-5). Also, the ratio between ICC and TCC was higher in 5-week-old HN biofilms (56%) compared to (42% and 8%) for MN and LN in 21-old biofilms (**Fig**. 2-5). Even though the TCC of LN biofilms (21 weeks) was comparable to that of MN biofilms (21 weeks) and HN biofilms (5 weeks), ATP levels, ICCs and MS2 LRVs (**Fig**. 2-2 and 2-4) were higher in HN than in MN and LN biofilms, accordingly.

These findings show that the initial nutrient concentration of the feed is the key factor in biofilm growth rate, thickness and associated MS2 LRVs rather than the length of the growth period [70,121]. Higher nutrient feeds led to the growth of thicker biofilms on CFDs, and therefore probably a greater amount of extracellular polymeric substances (EPS) [122]. The magnitude and properties of produced EPS is attributable to an assembling microbial community which varies in relation to growth nutrient concentration [123,124]. Increased EPS facilitates virus uptake due to its sorption capacity, surface charge and hydrophobicity, which are key factors for virus removal [72,109,125–129]. In addition, biofilms grown under high nutrient feed have a thicker boundary layer and therefore less mass transfer and stronger resistance, leading to lower flow rates [122,130].
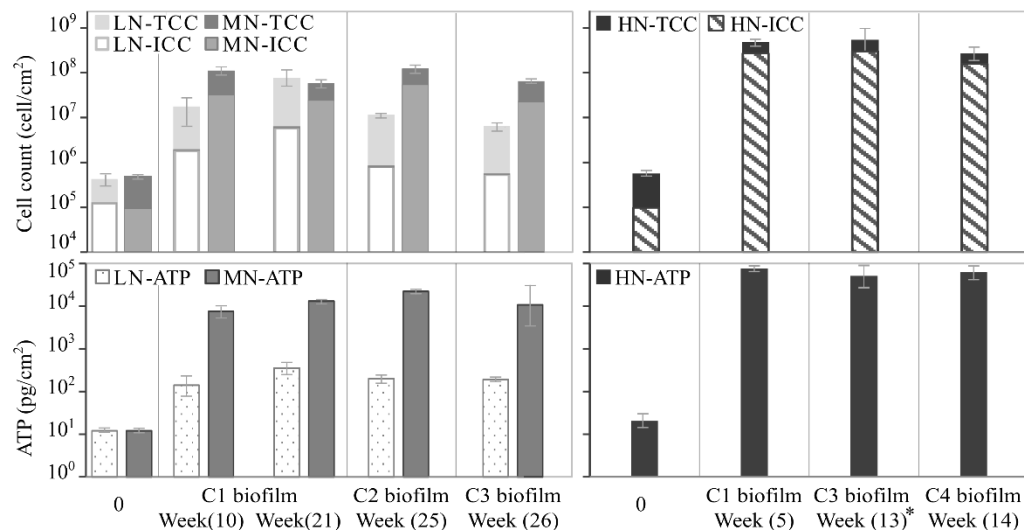
Figure 2-5 Biofilm analyses for LN, MN (left) and HN biofilms (right) excluding CFDs cleaned surface sampling at cleaning events (Cn). C(n) biofilm refers to the surface biofilm grown on the CFDs before the cleaning events (Cn). The age of Cn biofilm is the difference between the experimental weeks shown on the X-axis as the cleaning event Cn is considered a reset point. That is the text below addressing LN or MN C2 biofilm week 25 and C3 biofilm week 26 are referred to as 4 weeks and 1 week biofilm. *Age of HN biofilm at C3 is 4 weeks due to the 4 weeks LN gap after C1. Error bars represent SD

2.3.2 Effect of cleaning the surface

LN and MN CFDs were cleaned for the first time after 21 weeks (C1) and subsequently in weeks 25 (C2) and 26 (C3). MS2 LRVs after cleaning were <0.5 for C2 and C3 but 0.8 and 1.2 for LN and MN C1, respectively (see **Fig**. 2-6). Biofilm age before C1 was the longest (21 weeks), compared to 4 weeks before C2 and 1 week before C3. Thus, biofilm age potentially resulted in greater compactness due the dynamic processes of attachment and detachment over time [122], which became harder to remove only by scrubbing. Biofilm analyses at C1-cleaned surface confirms the presence of biofilm residuals, as TCC and ATP measured: 5.7×10^6 cell/cm^2 (SD 2×10^6), 38 ± 7 pg/cm^2 for LN-CFDs and 2.8×10^6 cell/cm^2 (SD 5×10^5), 145 ± 7 pg/cm^2 for MN-CFDs. This confirms that the biofilm layer, which is partially removed during a scrubbing event, plays a vital role in the removal of MS2 in CFDs.

Biofilm regrowth and recovery after 4 weeks of reloading was faster for MN CFDs than for LN CFDs. Measured TCC and ATP (**Fig**. 2-5- week 25) for MN biofilms at 4 weeks were slightly higher than for the 21-week-old biofilm but lower for LN biofilms. Biofilm regrowth after 1 week reached the same TCC and ATP as the biofilm after 4 weeks for LN CFDs but was lower for MN CFDs (**Fig**. 2-5-week 26). MS2 LRVs followed a similar pattern to that observed for biofilm regrowth. LN MS2 LRVs were lower for 4-week-old biofilm than 21-week-old biofilm, but higher than 1-week-old biofilm (**Fig**. 2-6). For MN, average MS2 LRVs were similar for 21-week- and 4-week-old biofilms but slightly lower for 1-week-old biofilm (**Fig**. 2-6). The fast recovery and regrowth of biofilm is probably due to biofilm bacteria retained after C1, which enabled fast recolonisation of the CFD surface with biofilm bacteria [131,132]. It is probable that reloading with feed water provided essential nutrients to deep biofilm layers, creating new channels and pores in the structure and hence accelerating bacterial growth [131,132].
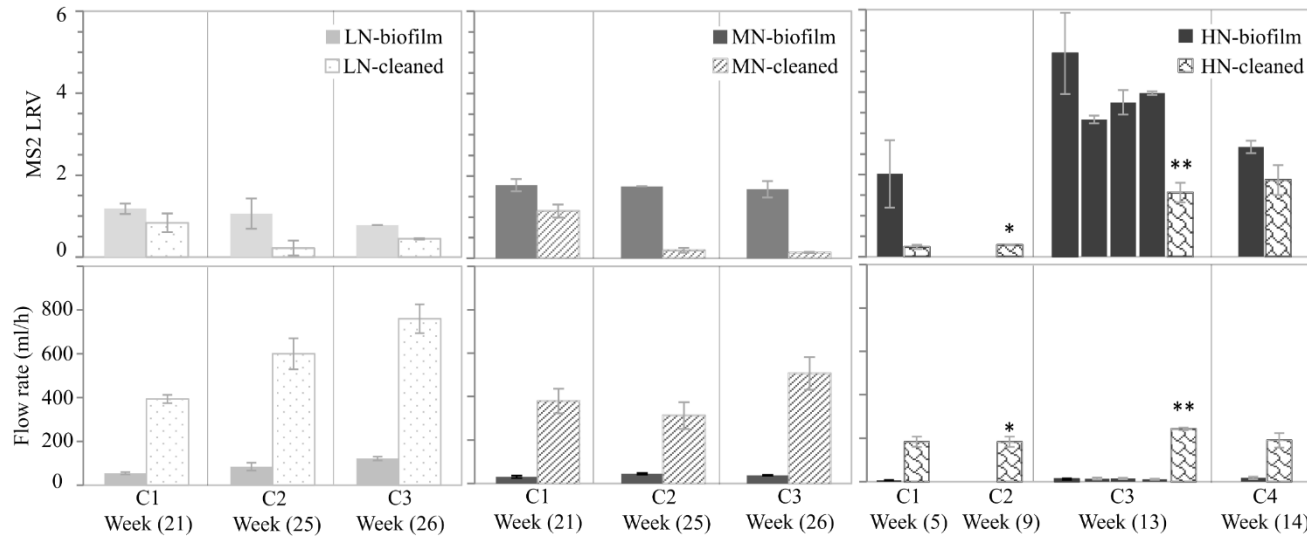
Figure 2-6 Effect of scrubbing the surface on MS2 LRV (top row) and flow rates (bottom row). Left column is LN CFDs, middle column is MN CFDs and right column is HN CFDs. Cn is the number of the cleaning event. Each cleaning event follows a challenge test with a grown biofilm before it, except for HN CFDs between C1 and C2. The age of Cn biofilm is the difference between the experimental weeks shown in the X-axis as the cleaning event Cn is considered a reset point. That is the text below addressing LN or MN C2 biofilm week 25 and C3 biofilm week 26 are referred to as 4 weeks and 1 week biofilm. *HN CFDs were fed with LN water for 4 weeks before C2. **before C3 biofilm was grown for 4 weeks and challenged weekly. Error bars represent SD.

Early scrubbing of HN CFDs after 5 weeks (C1) reduced the average MS2 LRV by 1.5 logs. Cleaning HN CFDs after 4 weeks of operation with LN (C2) resulted in the same MS2 LRVs as C1 (<0.3 logs: **Fig**. 2-6). Reduction in biofilm MS2 LRVs by cleaning was the highest at C3 (2.4 logs), despite its relatively high absolute value of 1.6 logs (**Fig**. 2-6). C4 also reduced average HN MS2 LRVs by 0.8 logs yet retained an average MS2 LRV of 1.9 ± 0.4. MS2 LRVs of C4 is similar to values obtained from HN 5-week-old biofilm, despite the drastic difference in their flow rates (**Fig**. 2-6) and residence time. TCC at C4 was 2.1×10^7 cell/cm^2 (SD: 9×10^6), and ATP was 1550 ± 354 pg/cm^2, which is 1.3 and 2 logs lower than that of the 5-week-old HN biofilm shown in **Fig**. 2-5. According to Nickels et al. (1981), manual brushing of a fouled surface eliminates the majority of the biomass, but a microbial community remains that excretes more EPS by 2 to 3 fold compared to the preceding community. Thus, it is possible that a shift in community by selection due to repetitive cleaning led to higher MS2 LRVs, even with reduced biomass and high flow rates.

Interestingly, reloading HN CFDs after C2 with HN feed water for 1 week increased the LRV significantly, reaching 5±1. The unprecedented high removal after C2 persisted for a month throughout 4 challenge tests (1-4W), achieving an average MS2 LRV of 4. TCC and ATP measurements at the end of this period (4 weeks) were similar to other HN biofilm measurements (**Fig**. 2-5-week 13). In fact, ATP was slightly lower at the 4 weeks biofilm (post LN) than 5- or 1-week-old biofilm. Thus, the current biofilm analyses provide no explanation for the high MS2 LRV. It is possible that the period using LN feed introduced an alteration in the base microbial community retained after cleaning (C1) that persisted throughout the month and allowed for rapid growth of specific biofilm bacteria on the filter surface. However, repeating the procedure by cleaning (C3) the CFD and reloading with HN for 1-week increased LRVs to 2.7 (**Fig**. 2-6), below the previously achieved 4 LRV.

A potential observation of interest was that the dissolved oxygen measurements of supernatants during the initial operation of LN, MN and HN CFDs were 8.15 ± 0.05, 4.25± 0.25 and 0.4 ±0.18 mgO$_2$/l respectively, showing evidence of anoxic or hypo-oxic conditions in HN CFDs. Switching to LN feed water may have diversified the biofilm base community or induced bacteria to shrink and adopt a spore-like state, awaiting conditions that were suitable for active growth [124]. However, no measurements were made to verify this hypothesis.

HN cleaning events (C1 to C4; **Fig.** 2-6) did not restore the flow rate to initial values. It is possible that build-up of irreversible (deeper, internal) clogging by biofilm did not allow for the same increase of flow rate after repeated scrubbing events observed in MN and LN CFDs. Repeated cleaning events increased flow rates for LN and MN CFDs, yet independent of achieved MS2 LRVs (**Fig**. 6). The correlation between flow rates and MS2 LRVs of cleaned CFDs was weak and insignificant (r^2=0.2 and p=0.08). Correlation was also weak but significant for biofilm amended CFDs (r^2=0.4, p=0.0009). Thus, reduced flow rates do not necessarily indicate higher MS2 LRVs. On the other hand, flow rates were clearly correlated to biofilm TCCs (r^2=0.7, p= 5× 10^{-8}). TCC and ATP had moderate, but significant correlation with MS2 LRVs (r^2=0.5, p= 6× 10^{-5} and r^2=0.5, p= 0.0001, respectively). These results highlight the effect of biofilm growth on changing flow rates and MS2 LRVs.

Flow rates reductions in CPFs have been linked to pore fouling with particulate matter, organic build-up and inorganic precipitation (i.e.$CaCO_3$ or insoluble iron) [58,60,134]. MS2 LRVs have been found to increase when flow rate decreased [55,60], although statistical significance and biofilm role were not considered in the assessment. In slow sand filtration, were biofilm growth is an essential element for the treatment process, Elliott et al. (2011)[135] showed that virus attenuation only began after a threshold of 1-2 weeks biofilm ageing period. Jenkins et al. (2011) observed that longer contact time (lower filtration rates) allowed for a higher attachment of virus to sand, hence higher LRVs. Schijven et al. (2013) proved experimentally and through a mathematical modelling that microorganism removal is best determined by biofilm (Schmutzdecke) age and temperature, rather than flow rates. This aligns with our observation that virus LRVs are not affected by flow rate but by biofilm growth, which in term increases residence time and reduces flow rate.

However, the flow rate plays an important role in terms of practicality and application. Slow performance of the filters can lead users to abandon using the filter [136]. The manufacturer recommends flow rates range within 1-3 L/h [32,137]. If the conversion between the flow rates of CPF full unit and CFDs flow rates is used, this is equivalent to 24 to 72 ml/h in the CFD, because 36 ml/h in the CFD corresponds to approximate 1.5 l/h [49]. Flow rates observed throughout HN- biofilm CFD are below the lower limit (24 ml/h) which diminishes the applicability of the CFDs. CFDs with LN biofilm had flow rates > 85 ml/h, while CFD with MN biofilm provided approximately 40 ml/h, except for 21 weeks old biofilm which had 55 and 31 ml/h,

respectively (**Fig**. 2-6). Thus, there's potential for application of CFP's with LN and MN water feed with sufficient flow, while benefiting from improved virus LRVs. This is not the case for HN filters, unless cleaned.

2.3.3 The fate of phages in the system

Depending on the CFD flow rates, challenge water resided on top of the CFDs for 3-12h. **Fig**. 2-7a shows that the decrease in MS2 concentration in the feed water of LN, MN and HN CFDs were λ: 0.064, 0.064 and 0.15 log/h respectively. The faster inactivation rate for HN biofilms can be due to the additional strong attachment of MS2 to the HN CFD surface biofilm [138]. Because water used in all challenge tests is LN water spiked with MS2 phages, the difference between inactivation rates is only attributed to the behaviour of the surface biofilms grown under different nutrient conditions.
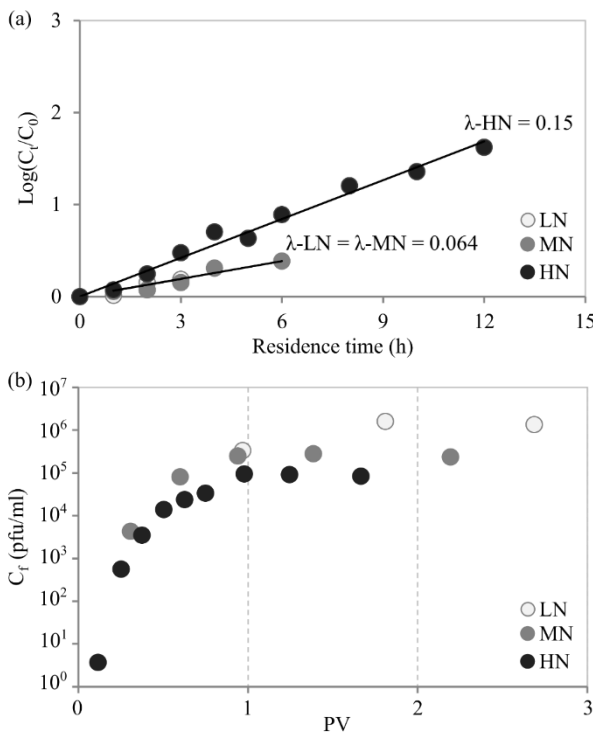
Figure 2-7 Stage 1 MS2 concentrations in supernatant and filtrate ((a) MS2 LRV in challenge water residing on top of LN, MN, HN biofilms (b) MS2 filtrate concentration (Cf) after passing through CFDs with LN, MN and HN biofilms)

The concentration of phages in the filtrate increased over time/pore volume (**Fig**. 2-7b). After 1 pore volume (PV), the MS2 concentration in MN and HN filtrate did not increase any further, while in the LN filtrate there was still some increase following 1 PV. This confirmed our approach to start filtrate sampling after the first PV to determine the LRV in challenge tests. Theoretically, the first PV of filtrate should be free of phages because the pores are filled with the previous MS2-free nutrient feed water. However, in reality, CFDs do not have an ideal plug flow. The phages measured in the filtrate through the first PV support the existence of preferential flow paths in the CFDs.

Because the duration and MS2 inactivation rate of Stage 1 varied per nutrient type (see t_1 :**Table** 2-1), the amount of phages entering the CFDs (N_i) varied as well. N_i is calculated as average = ($\sum_0^{t1} C_t$ * average V_{sup}) to exclude the effect of residence time, temperature and other processes taking place in the supernatant.

Table 1 shows that most of the phages in the feed (N_i) were removed by the biofilm/filter, with only 2-12% passing through the biofilm and filter (N_f) during the challenge phase. After the MS2 challenge was stopped, MS2 phages did survive in the biofilm (N_b); some detached and passed through the filter into the filtrate (N_d) for up to 22 d in HN CFDs. $\sum N_f + N_d + N_b$ is the total number of recovered phages, which varied between 2.6 and 12.9%. The highest unrecovered values were in HN-CFDs (97.4%) followed by MN (96.5%) and LN (87.1%) CFDs. It is possible that unrecovered phages were inactivated inside the biofilm; however, in this study, it is not possible to quantify the inactivation rate or temperature effect on MS2 inside the biofilm. Also, potential low recovery efficiency of the swabbing method [139] may have influenced the recovery rate of MS2 phages.

Table 2-1 Mass balance of MS2 phages

	t_1	t_2	N_i		N_f		N_b		N_d		Unrecovered
Unit	(h)	(days)	pfu	%	pfu	%	pfu	%	pfu	%	(%)
LN	3	1	2.7×10^9		3.6×10^8	12.4	2.2×10^1	<0.1	4.6×10^7	0.5	87.1
MN	6	8	2.0×10^9	100	6.4×10^7	3.3	2.2×10^6	0.1	2.1×10^6	0.1	96.5
HN	12	22	6.7×10^8		1.2×10^7	1.8	4.1×10^6	0.6	1.6×10^6	0.2	97.4

2.4 Conclusion

The WHO guidance for HWTS technology performance recommends ≥ 3 LRV for protective technologies and ≥5 LRV for the highest protection from viruses [100]. Under stable operational conditions, the CFDs achieved MS2 LRVs ranging between 0.9±0.2 for LN, 1.6±0.2 LRV for MN and 2.4±0.5 LRV for HN biofilms. Cleaning the surface by scrubbing led to partial or total loss in achieved LRVs, indicating the importance of this biological top layer to MS2 LRVs. Overall, repeated scrubbing resulted in a faster recovery of biofilms and associated log reductions. Recovery of MS2 from biofilm swabs confirmed the role of CFD biofilms in virus removal, although the MS2 LRV did not reach the WHO protective performance level of 3 LRV.

Biofilm formation on CPFs is inevitable and, as demonstrated, it positively contributes to the virus safety of drinking water for CPF users. Further research is required to understand the mechanisms of interaction between virus and biofilms, supported by the unprecedented high LRV of > 4 achieved after changing feed conditions. Also, future studies should factor in biofilm growth in evaluating virus removal capacity of CPFs and in recommending cleaning practices for CPF users.

3 Inactivation of RNA and DNA viruses in water by copper and silver ions and their synergistic effect

This chapter is based on:
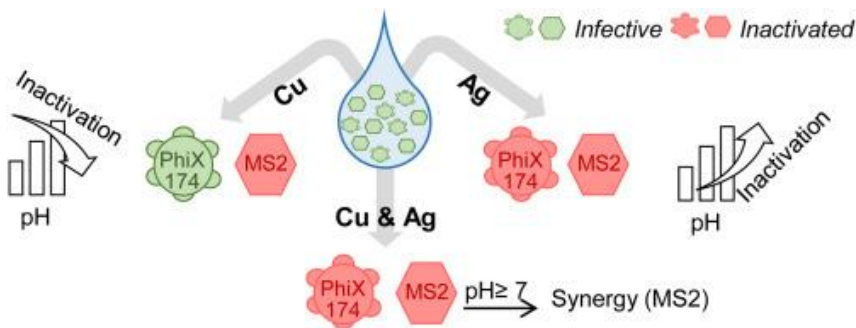
Abstract

Cu and Ag have been used as bactericidal agents since ancient times, yet their antiviral capacity in water remains poorly understood. This study tested the effect of copper (Cu) and silver (Ag) on model RNA and DNA viruses MS2 and PhiX 174 in solution at pH 6-8. Cu caused MS2 inactivation with similar rates at pH 6 and 7 but was ineffective towards PhiX 174 regardless of pH. Ag inactivated both viruses, causing denaturation of MS2 and loss of capsid spikes in PhiX 174. Ag inactivation rates were pH dependent and increased with increasing pH. At pH 8, 6.5 logs of PhiX were inactivated after 3 hours and 3 logs of MS2 after only 10 minutes. The combined use of Cu and Ag revealed synergy in disinfecting MS2 at pH ≥7. Although metal concentrations used were higher than the desired values for drinking water treatment, the results document a promising potential of Cu and Ag combinations as efficient viricidal agents in water.

3.1 Introduction

Use of metals in medicine, food and water hygiene is dated back to antiquity [140–142]. Some metals such as copper (Cu) and silver (Ag) display potent biocidal activity against bacteria [143–147], yeast, fungi [148] and viruses [143,149]. Recent studies have proven the ability of metals to disinfect multidrug-resistant bacteria [150–154], control biofilms [155,156] and have a synergistic effect when used with other biocides [157]. This has increased application of metals for disinfection in a multitude of sectors. In the water sector, Cu-Ag ionization units are used globally to control *Legionella* and other waterborne microbes that may grow in hospital water systems [143,158,159]. Cu-Ag ionization was proven more effective than other disinfectants such as UV light and chlorine [158,159]. The absence of harmful by-products from Cu and Ag at concentrations allowed in recreational water has expanded their application to reduce chlorine use in swimming pools [149,160]. Cu and Ag have also been incorporated in household water treatment systems to improve their microbial disinfection capacity [49,161].

Although Cu and Ag antiviral activity was first reported in 1963 and 1964 [162], research evaluating their effectiveness has been limited. There is a surprising absence of studies evaluating physical and chemical parameters that affect Cu and Ag antiviral activity. Reports evaluating Cu as an antiviral agent focused mainly on Cu doses [97,163] and the role of hydrogen peroxide (H_2O_2) in enhancing inactivation rates [95–99]. Cu speciation was briefly addressed by Nieto-Juarez et al. (2010) because inactivation rates of MS2 were associated with the dissolved fraction of Cu ions. Although Ag antiviral studies reported on different doses, comparing results is challenging as different studies used different solution matrices and speciation of Ag^+ ions was commonly overlooked [81–84].

The variation in testing conditions was also accompanied by contradicting results on Cu and Ag antiviral efficiency and inactivation capacity. This highlights the need for a systematic evaluation of chemical and physical parameters influencing Cu and Ag virucidal efficiency as an essential step towards their application in water. Parameters such as pH, availability of dissolved Ag^+ and Cu^{2+} ions versus their precipitates has been shown to significantly influence inactivation rates of bacteria [79,91–93,164–166]. While similar evaluation of those parameters remains unmet for viruses, a notable effect on virus inactivation can be anticipated.

The speciation of metals is a key element in determining their bioavailability, hence their toxicity and disinfection capacity [79,80]. The chemical state of the metal is also subject to change by environmental factors such as pH, temperature, ionic strength and redox potential [79,167,168]. Changing pH can also change virus conformation and its susceptibility to disinfection, making it an important factor in evaluating Cu and Ag antiviral efficiency [85]. Moreover, susceptibility to disinfectants differs for different virus types. For example, the single-stranded DNA (ssDNA) phage PhiX 174 was found to be more resistant to heat inactivation than double-stranded DNA (dsDNA) adenovirus [169] and RNA enteroviruses were more resistant to chlorine disinfection than dsDNA adenovirus [170].

Therefore, the objective of this study was to determine the efficiency of Cu and Ag ions as antiviral agents in water. Conservative model viruses MS2 phage (single-stranded RNA, ssRNA) and PhiX 174 (ssDNA) were selected as targets. Both Cu and Ag were tested individually and in combination in a solution matrix where pH was investigated as variable. Concentrations of Cu and Ag used were higher than the WHO recommendations to allow for a more feasible evaluation of metals speciation by analytical measurements. The effect of pH on metal ions availability and speciation was evaluated using experimental analysis and the chemical speciation model CHEAQS. Finally, morphology of MS2 and PhiX 174 particles was examined before and after treatment using transmission electron microscopy (TEM) to provide insights on possible structural damage by Cu and Ag.

3.2   Materials and Methods

3.2.1   Reagents

All chemicals were reagent grade and used without further purification. Copper sulfate (0.1 M), sodium phosphate monobasic monohydrate ($NaH_2PO_4.H_2O$), sodium phosphate dibasic heptahydrate ($Na_2HPO_4.7H_2O$), sodium thioglycolate, Phosphate-Buffered Saline tablets (PBS) were purchased from Sigma-Aldrich. Sodium thiosulfate solution (0.1 M) was purchased from Merck and ethylenediaminetetraacetic acid solution (EDTA) 0.1 M and silver nitrate (0.01 M) from VWR.

All experimental solutions were prepared using Milli-Q water (18 MΩ, pure lab chorus 1). Sodium phosphate buffer (PB, 1 mM) contained $NaH_2PO_4.H_2O$ and

Na$_2$HPO$_4$.7H$_2$O mixed at concentrations of 0.93 mM and 0.07 mM for pH 6, 0.58 mM and 0.42 mM for pH 7 and 0.12 mM and 0.88 mM for pH 8, respectively. Solutions were autoclaved at 121 °C for 20 minutes then stored at 4 °C until further use. When needed, further adjustment of pH was conducted using stock solution NaH$_2$PO$_4$.H$_2$O (100 mM) as a base and Na$_2$HPO$_4$.7H$_2$O (100 mM) as an acid. Silver neutralizing solution was prepared on the experimental day as described by Butkus et al. (2004). The solution contained 12 g/l of sodium thioglycolate and 0.1 M/L of sodium thiosulfate.

3.2.2 MS2 and PhiX 174 phage culturing and purification

MS2 stock was produced by infecting *Escherichia coli* C3000 (ATCC 15597), grown to early logarithmic phase (OD$_{600}$ 0.1-0.2), with MS2 suspension (ATCC 15597-B) at multiplicity of infection (MOI) 0.01 phage per cell. Following overnight replication (37 °C; 30 rpm), the lysate was harvested by centrifugation (Sorvall™ ST 16 R, 4000 x *g*, 20 min, 4 °C). The aspirated supernatant was filter sterilized through 0.22 µm sterile syringe filters (PES, VWR) then stored at 4 °C. Similarly, *E. coli* WG5 (DSM 18455) was infected at 0.2 OD$_{600}$ by PhiX 174 suspension (DSM 4497) at MOI 0.01 and incubated overnight at 37 °C and 110 rpm mixing for replication. Lysate was harvested and processed as described for MS2.

Both phage stocks were further purified by density gradient ultracentrifugation to eliminate bacterial protein residuals, broth organics or any impurities that can interfere with evaluating metals inactivation capacity. Moreover, density gradient purification reduces phage aggregation [171] which (if occurred) affects inactivation rates [172]. MS2 was suspended in iodixanol gradient (OptiPrep™- Stemcell) and PhiX 174 in cesium chloride; each adjusted to 20 % (w/v) underlined by 40% and 60% of corresponding solution. The gradient was centrifuged for 20 hours (32,000 rpm, 4 °C, Beckman coulter optima L-90 K ultracentrifuge). The corresponding phage band was gently removed using a syringe needle then re-suspended in PB buffer (pH 7). The suspension was washed twice using 30 kDa and 100 kDa Amicon® Ultrafilter columns; and centrifuged 4000 x *g*, 20 min [173]. Recovered phage was stored in PB buffer (pH 7) at 4 °C until further use. Enumeration of both phages, as well as agars and cultures used were done according to the ISO- 10705 part 1 and 2. Final concentrations of MS2 and PhiX 174 suspensions were 10^{13} pfu/ml and 10^{10} pfu/ml respectively.

3.2.3 Inactivation experiment

In the virus inactivation experiment, interaction between metals and MS2 or PhiX 174 was examined in pH and temperature controlled (25 °C) inorganic buffer (PB). The reaction took place in sterilized acid washed (10% nitric acid) glass beakers. Beakers were wrapped in aluminum foil and covered from the top with a sterile petri-dish and foil to ensure dark conditions.

MS2 and PhiX 174 were each tested separately each for inactivation by Cu, Ag, or both Cu and Ag at pH 6, 7 and 8. Additionally, interaction between MS2 and Ag was tested at pH 7.5. All conditions were examined at least in triplicates. In total 26 metal inactivation experiments were conducted of which 7 were metal free control tests.

On the experimental day, test water was prepared by adding phage suspension to PB buffer (pH 6, 7 or 8) to a final concentration of approximately 10^6 pfu/ml. 100 ml of test water were added to each beaker. For metal testing, the reaction was initiated by adding aliquots of metals to each beaker to a final concentration of Ag 4.6 µM (0.5 mg/l) and 78.7 µM (5 mg/l) for Cu. Solutions were placed inside a 25 °C incubator and stirred continuously at 60 rpm (2mag-Magnetic-Drive).

At time intervals of 0, 0.17, 0.5, 1, 3 and 6 hours, 5 ml of sample were withdrawn using sterile syringes and directly neutralized to stop the reaction. Frequency of sampling was increased in some experiments. Ag containing samples were neutralized using 2 mM of silver neutralizer [82], Cu containing samples were neutralized with 5 mM of EDTA, and Cu and Ag samples were neutralized with both solutions. Metal-free control samples were also neutralized to examine the neutralizer effect on phage recovery. After neutralizing, samples were stored on melting ice and MS2 samples were diluted in PBS buffer, and PhiX 174 in PB buffer. Phage enumeration followed the double agar layer method (DAL) by assaying duplicates of 1 ml sample and serial sample dilutions as described in ISO-10705. Limit of detection (LOD) was 1 pfu/ml and the lowest concentration (LOQ) considered reliable was 30 pfu/ml as recommended by the ISO-10705. Reported results represent the average values and standard deviations of triplicate tests. In addition, samples from metal beakers were analysed to confirm metals concentration using an ICP-OES Spectrometer (Spectro Arcos eop). Metal analysis details are provided below in the section on metals speciation.

3.2.4   Data analysis

Log removal values were calculated as Log_{10} (N_t/N_0) where N_t is the phage concentration (pfu/ml) at time t and N_0 is the concentration at time 0. First order inactivation rate constant, K_{obs} (h^{-1}) was calculated from the slope of linear regression of Ln (N_t/N_0) versus time (h). Linear regression analysis was used to calculate the Kobs with 95% confidence interval and to determine the significance of slope variation from zero. Linear regression slopes of metal free controls were compared to zero for significance of any noticeable decay. K_{obs} (mean value, SD and df) for different conditions was compared using one-way ANOVA with a Tukey test to determine if the relationship between two sets of data is statistically significant.

3.2.5   Speciation of metal ions

The ICP-OES provides a measurement of the total metal ions without distinction between ionic, dissolved, or solid precipitates. The speciation of metals is important since toxicity is often related to the metal's ionic form rather than dissolved or solid complexes [94]. Thus, a filtration test first provided an experimental assessment of dissolved metals vs solid complexes through solids exclusion by retention on the filter. Metal samples were filtered using a series of syringe filters (0.45 µM, 0.22 µM, 0.1 µM and 0.02 µM; Polyethersulfone PES), sampled after passing each filter. The same was repeated on metal samples diluted in milliQ water which was used as control to evaluate possible metal adsorption to the filters. All samples were acidified using 3 % HNO_3 and analysed using radial optical emission spectroscopy (Spectro Arcos EOP, ICP). All elements were measured at multiple wavelengths (if available). Calibration was done together with measuring the samples. In the end the concentrations were determined against an external calibration line, per element per wavelength. No internal standard was used.

Concentration of the unfiltered samples: Ag 4.6 µM (0.5 mg/l) and 78.7 µM (5 mg/l) for Cu was used as the total concentration. Lowest filtrate concentrations were considered dissolved and the difference between the total and dissolved is the filtered solid complexes. Average values and standard deviation are reported. All values are reported as a percentage (%) of the total metal concentration added.

The CHEAQS Next chemical equilibrium program was used to calculate the free ionic concentrations of Ag^+ and Cu^{2+} in the buffer matrixes used. The measured total

concentrations of Cu, Ag, Na and PO_4 were used as input together with measured pH and redox potential (SenTix ORP-T 900).

3.2.6   TEM imaging

The morphology of phage particles was examined using transmission electron microscopy (TEM, JEOL JEM-1400 plus). Because high phage concentration is required for TEM, a sub experiment was conducted using phage suspensions at 10^9 and 10^{11} pfu/ml for PhiX 174 and MS2, respectively. In brief, 100 µl of phage suspension were treated with either Ag or Cu or both. The concentrations used were approximately 20 µM of Ag and 3 mM Cu. The suspension was incubated as mentioned above but in 2-ml microcentrifuge tubes. Prior to TEM grid preparation, PhiX 174 sample buffer was exchanged for milliQ water by centrifugation (21,000 x g, 50 min, 4 °C). A second centrifugation step was applied to further wash the sample and the supernatant was discarded. For MS2 and PhiX 174, a 10 µl volume of the sample was incubated for 5 minutes on a copper mesh grid (Carbon Type-B, 400 mesh, TED PELLA). The excess liquid was extracted using filter paper, and the sample was stained using 2% uranyl acetate for 30 seconds. Imaging was repeated twice for each sample to ensure reproducibility; additional information and images are provided in supplementary information.

3.3   Results

3.3.1   Effect of pH in metal free controls

To evaluate the stability of PhiX 174 (ssDNA) and MS2 (ssRNA) under experimental conditions, metal free controls were sampled and analyzed as metal samples. Concentrations of PhiX 174 (**Fig.** 3-1a) were stable during the 6 hours testing period at each tested pH; K_{obs} similar (p > 0.05) to slope zero. The same result was observed for MS2 at pH ≥7. At pH 6, MS2 metal free control decayed over 6 hours with K_{obs} = 0.22 ± 0.01 (h^{-1}), which was significantly different from zero slope (p < 0.0001). To properly evaluate the inactivation caused by metals at pH 6, MS2 inactivation results were corrected to account for the observed decay in the control experiments.
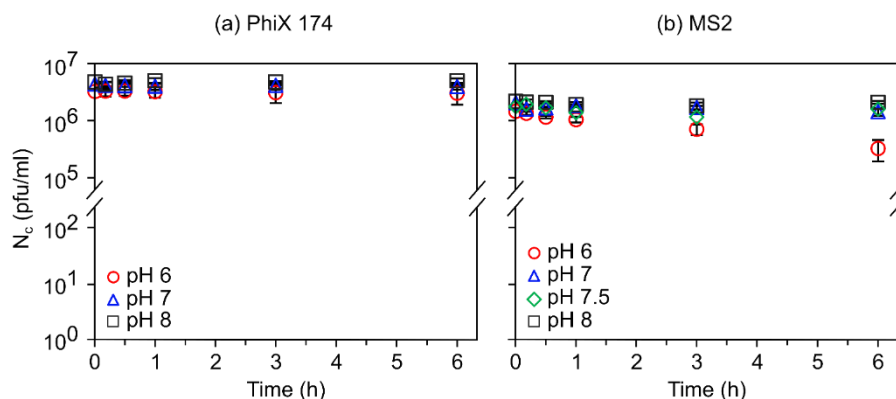
Figure 3-1 Stability of (a) PhiX 174 and (b) MS2 phage in metal free PB buffer at pH (6 – 8) and 25 °C.

The correction was applied by calculating log removal values (LRV) as $Log_{10}(N_t/N_c)$ where N_t is the phage concentration of test condition at time t and N_c is the phage concentration of control condition also at time t. K_{obs} was calculated as the slope of $Ln(N_t/N_c)$.

3.3.2 Metal ions complexation

The concentration of dissolved Cu^{2+} and Ag^+ was measured and compared against the modelling results of *CHEAQS next* chemical software. The concentration of ionic, dissolved, or solid metal ions is expressed as a percentage of the total experimental concentration; 4.6 µM (0.5 mg/l) for Ag and 78.7 µM (5 mg/l) for Cu. This provides more insight on ions availability (free ionic form) and complexation which might influence the antiviral activity of the metals.

Differences in solution pH had a clear effect on speciation of Cu and availability of Cu^{2+} ions. CHEAQS modelling results show a change in dissolved Cu from 24 % at pH 6, to 5% at pH 7 and 2% at pH 8, of which 16, 1 and 0.2% are free ionic Cu^{2+} respectively (**Fig.** 3-2). Experimental measurement of dissolved Cu yielded different percentages of dissolved Cu but the trend did align with the model predictions. Measured dissolved Cu at pH 6, 7 and 8 were 43%, 6% and 1% respectively. The higher percentage of experimentally measured dissolved Cu^{2+} could be due to the formation of copper particles smaller than the filter pore size (< 20 nm), which can

pass the filter and be analyzed as dissolved copper. Yet, both methods (model and experiment) confirm a higher percentage of available dissolved Cu^{2+} at lower pH.
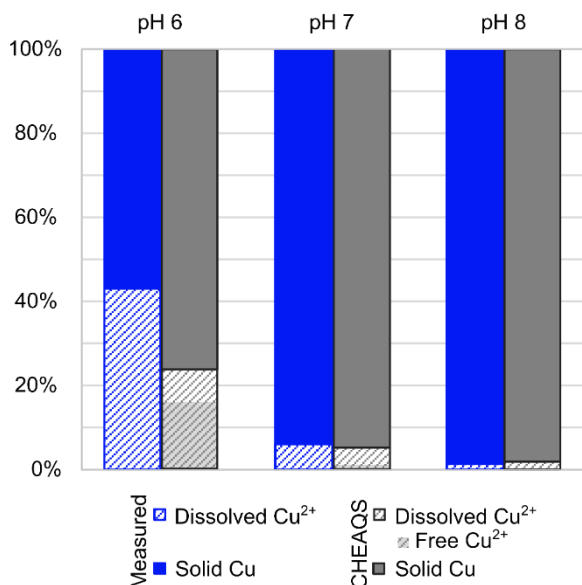
Figure 3-2 Speciation of Cu ions in solution based on experimental measurements of dissolved and solid Cu concentrations referred to as (measured), compared to the model speciation output using CHEAQS next chemical software referred to as (CHEAQS). Cu measured concentrations after 0.02 µm filtration are expressed as dissolved, while the difference between dissolved and total concentration (unfiltered sample) is considered solid Cu. Values are expressed as a percentage of the total Cu concentration which was used also as the input for CHEAQS.

For Ag, changing pH had no effect on Ag^+ speciation (see supplementary **Fig.** 3-7). CHEAQS predictions show 100 % dissolved Ag at all pH values, of which free ionic Ag^+ changed from 100% at pH 6 to 99% at pH 7 and 97% at pH 8. This slight drop was due to the formation of $AgH(PO_4)^-$ (**Fig.** 3-7). Analytical measurements also showed 100% dissolved Ag (**Fig.** 3-7). The results for Cu and Ag in the combined solutions were identical to those of Cu and Ag alone.

3.3.3 Viral inactivation by Cu

Antiviral efficiency of Cu against PhiX 174 and MS2 was compared under acidic (pH 6), neutral (pH 7) and alkaline (pH 8) conditions. Cu treatment caused no inactivation of PhiX 174, regardless of the pH (K_{obs} insignificant from control and from 0 slope, p > 0.05) (**Fig.** 3-3a). Inactivation kinetics of MS2 followed the first order, Chick Watson model (**Fig**. 3-3b). Slowest kinetics were observed at pH 8 (K_{obs}

= -0.89 ± 0.004 h^{-1}; 1.4 LRV over 6 h); significantly different from K_{obs} at pH 6 and 7 (p <0.0001). However, statistically similar (p =0.29) inactivation kinetics at pH 6 (K_{obs} = -0.79 ± 0.06 h^{-1}; 2.2 LRV over 6 h) and pH 7 (K_{obs} = -0.90 ± 0.02 h^{-1}; 2.4 LRV over 6 h) were observed. K_{obs} values were significantly different (p <0.0001) from metal free control slopes and zero slope, validating the efficiency of Cu in inactivating MS2.
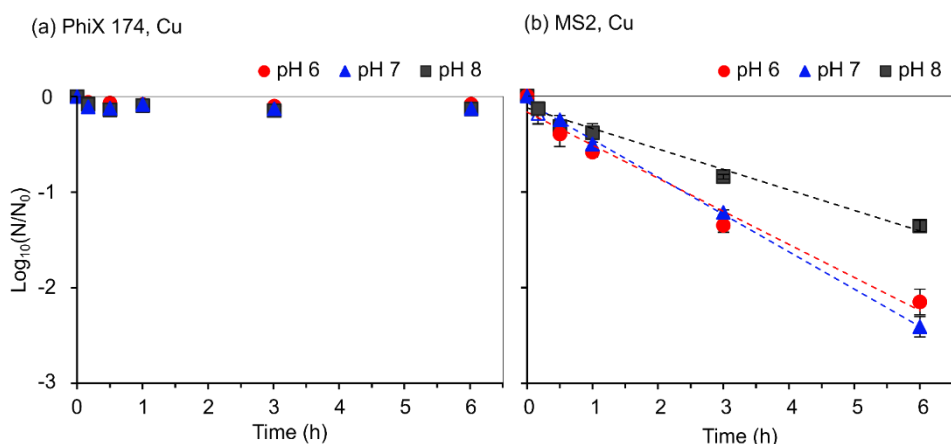
Figure 3-3 Copper inactivation of (a) PhiX 174 and (b) MS2 phage at pH 6 – 8. Inactivation rate constants: K_{obs} (h-1) ± standard deviation (SD) for MS2 is mentioned in the text. R^2 values were > 0.97 for all Kobs values. Regression lines are shown in same colour as the pH markers.

3.3.4 Viral inactivation by Ag

Ag showed a pronounced antiviral activity on both MS2 and PhiX 174. After 3 hours of exposure to Ag ions, PhiX 174 reached the lowest concentration (LOQ) and was equivalent to 6.5±0.7 logs (**Fig**. 3-4a, pH 8). Ag inactivation of MS2 also reached the LOQ (~ 5.5 ± 0.2 logs) at pH 7 and 7.5 over 3 hours (**Fig**. 3-4b). To avoid values at the LOQ, only the first hour was considered in evaluating inactivation kinetics (**Fig**. 3-4c,d).

The slowest inactivation kinetics of MS2 was observed at pH 6 (K_{obs} = -0.43 ± 0.04 h^{-1}; ~ 0.3 LRV over 1h). K_{obs} of Ag treated MS2 and metal free control at pH 6 were similar (p =0.94), hence Ag was ineffective against MS2 at pH 6. Meanwhile, significantly higher (p<0.05) kinetics were observed for PhiX 174 at pH 6, K_{obs} (-2.81 ± 0.65 h^{-1}; ~ 1.3 LRV over 1h).

At pH 7, inactivation rate constants were similar (p =0.69) for MS2 (K_{obs} = -4.99 ± 0.48) and PhiX 174 (K_{obs} =-4.09 ± 0.57). The difference in K_{obs} between pH 6 and 7 corresponds to an increase by a factor of 1.5 for PhiX 174 and by a factor 10 for MS2. K_{obs} for PhiX 174 continued to increase with the same magnitude (1.5 times) between pH 7 and 8, reaching -6.3 ± 0.37 h^{-1} at pH 8. Also, K_{obs} of MS2 doubled between pH 7 and 7.5.
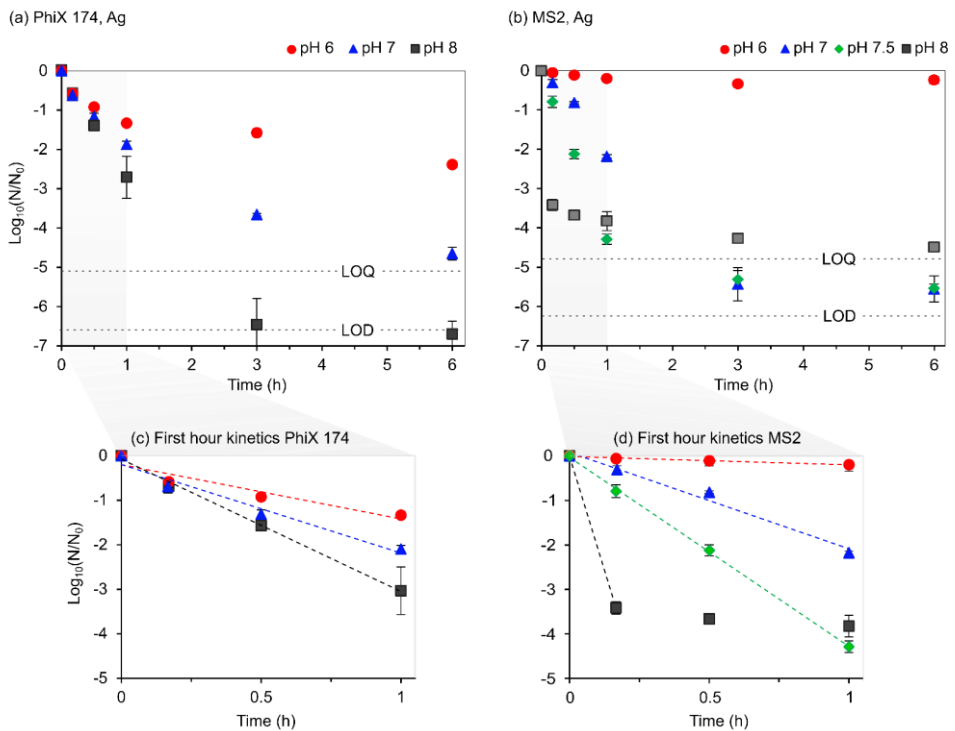
Figure 3-4 Ag inactivation of PhiX 174 and MS2. Full 6 hours LRVs are shown in top row (a and b) while modelling of first hour inactivation kinetics is shown in bottom row (c and d). Limit of detection (LOD) was 1 pfu/ml and the lowest concentration (LOQ) considered reliable was 30 pfu/ml. Kobs (h-1) values are mentioned in the text. R2 for all Kobs values was >0.96 except for PhiX 174 at pH 6 (R2 =0.90). Regression lines are in same colour as the pH markers. .

Overall, increased K_{obs} by increasing pH was significant (p<0.0001), with clear pH dependency of MS2 and PhiX 174 inactivation rates observed. Inactivation kinetics followed the Chick-Watson first-order model (**Fig.** 3-4c, d), except for MS2 at pH 8, for which inactivation declined over time. The initial 10 minutes of interaction between MS2 and Ag resulted in 3.5 LRV followed by distinct tailing and much slower kinetics (**Fig.** 3-4d).

3.3.5 Antiviral activity of Cu and Ag combined

The combination of Cu and Ag was tested to evaluate possible synergies. The experimentally observed LRVs of the Cu and Ag combination are compared to the mathematical sum of LRVs obtained from individual metal treatment, reported as (*estimated*). The first hour results of MS2 are depicted in **Fig.** 3-5. Results of PhiX 174 and the 6-hour experiment are provided in supplementary material (supplementary **Fig.** 3-8 and 3-9).

For PhiX 174, observed and *estimated* K_{obs} were similar (p > 0.7) (supplementary **Fig.** 3-9). Also, observed, and *estimated* K_{obs} for MS2 at pH 6 were similar (p >0.9) (**Fig.** 3-5a). MS2 observed inactivation kinetics at pH 7 (K_{obs} = -35.95 ± 9.4 h^{-1}; ~ 2.7 LRV in 7 minutes) was significantly higher (p<0.05) than the *estimated* inactivation kinetics (K_{obs} = -5.89 ± 0.84 h^{-1}; ~ 2.7 LRV over 1h). Similarly, observed K_{obs} was higher at pH 8 than the *estimated* rate constant (47.5 versus 16 h^{-1}). This highlights a distinct synergistic effect of using Cu and Ag combined at pH ≥ 7 compared to their individual use.

However, for the two conditions of pH 7 and 8, inactivation of MS2 diverged from first order kinetics following initial rapid inactivation. Observed inactivation of MS2 reached 3 logs after 10 minutes at pH 7 and 3 logs after 3 minutes at pH 8, both followed by subsequent tailing that decelerated the inactivation rates (**Fig.** 3-5b). MS2 diversion from first order kinetics (tailing) was initially observed using Ag at pH 8 (**Fig.** 3-4) which was reflected in the *estimated* LRVs of MS2 at pH 8 (**Fig.** 3-5a). In the three experimental conditions where MS2 inactivation rapidly reached 3 Logs (in ≤ 10 minutes), subsequent tailing was observed.
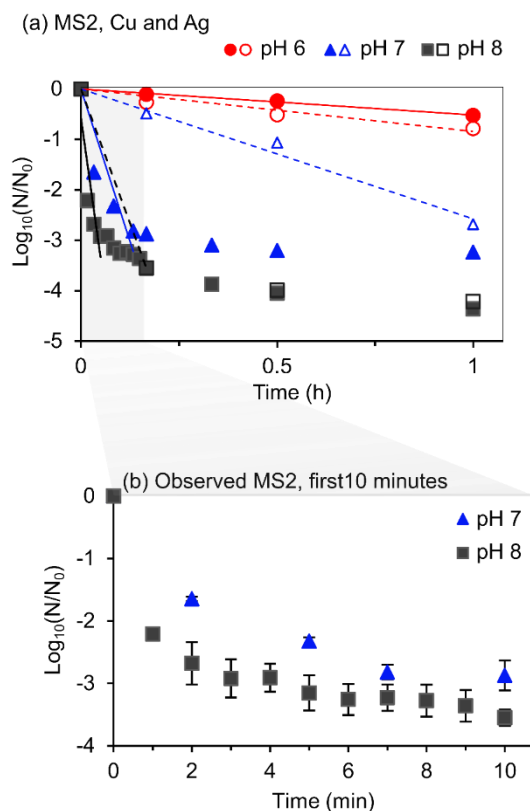
Figure 3-5 First hour inactivation of (a) MS2 by Cu and Ag ions combined as observed (closed marker) and the mathematical sum of LRVs obtained through individual treatment as estimated (open marker). (b) The first 10 minutes of observed MS2 inactivation by Cu and Ag. Regression lines are in same color as the pH markers.

3.3.6 Morphological changes of MS2 and PhiX 174

TEM imaging was used to examine morphological changes in the phage after metal treatment compared to the intact particles in metal free buffer. The examination aimed to discern possible structural damage resulting from phage interaction with metals.

As shown in **Fig.** 3-6a, MS2 control particles can be seen with intact round shaped capsid. The PhiX 174 control particles showed clear distinct capsid spikes (**Fig.** 3-6b). After exposure to Cu ions, MS2 particles appear with the same round morphology as the control but with a darkened center (**Fig.** 3-6c). This darkness is due to stain (uranyl acetate) penetration into the capsid. This could be a result of defective capsid [81] or RNA free capsid [174]. The white, non-uniform particles

appearing in the image were judged as chemical precipitates appearing on the grid. The Cu treated PhiX 174 (**Fig.** 3-6d) showed no difference from the control image except for debris or possible chemical precipitation like those in the MS2 image.
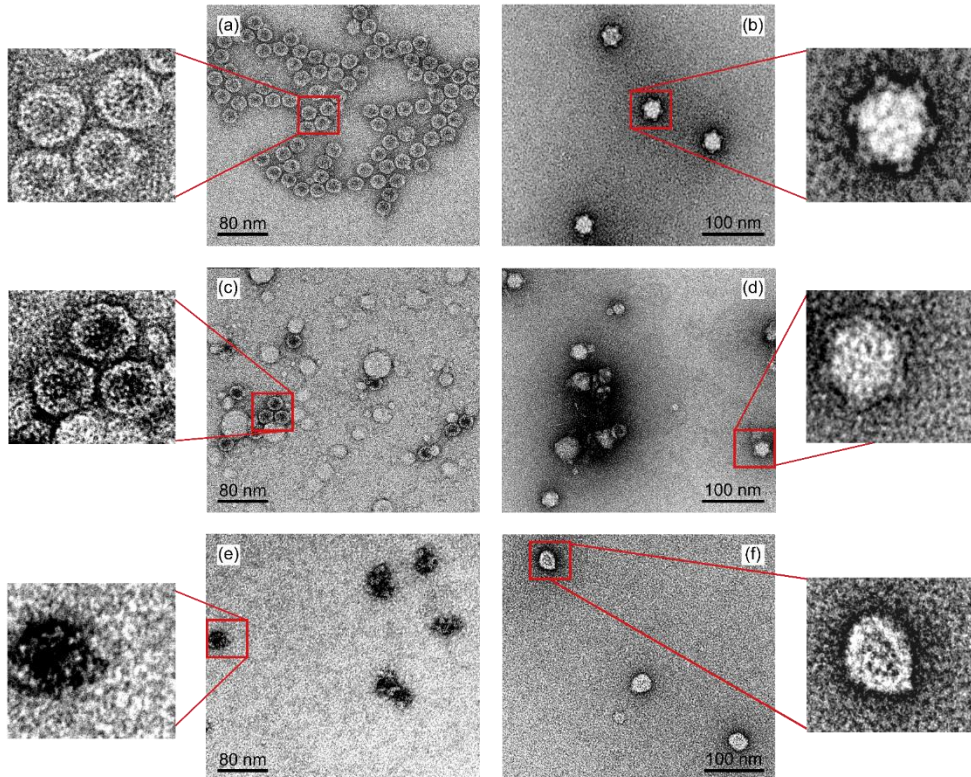
Figure 3-6 TEM images of MS2 phage (left column) and PhiX 174 (right column). Top row shows control particles (a) MS2 intact circular shape and (b) PhiX 174 intact round shell with spikes. Middle row: Cu treated (c) MS2 with dark capsid centre and white chemical precipitates on the grid and (d) PhiX 174 similar to the control except for presence of chemical precipitates and debris on the grid. Bottom row: Ag treated (e) MS2 with noticeable structural damage as capsid integrity is compromised and the particles denatured and (f) PhiX 174 lost its capsid spikes. MS2 particles were suspended in PB buffer pH 7 and PhiX 174 in PB buffer pH 8. Imaging was repeated twice to ensure reproducibility.

The Ag treated MS2 particles showed a clear difference in morphology (**Fig.** 3-6e). MS2 particles looked irregularly shaped, losing their round intact structure, and looking severely damaged. PhiX 174 particles also appeared distinctly different after Ag treatment (**Fig.** 3-6f). Although the center of the PhiX 174 capsid can still be recognized, a clear loss of capsid spikes and a change in particle size was observed.

However, no distinguishable structural damage was observed in MS2 samples containing both Cu and Ag but rather a combination of non-uniform white precipitates and denatured particles as observed in the Ag image (Image not shown).

3.4 Discussion

3.4.1 Cu inactivation of PhiX 174 and MS2

Cu inactivation of PhiX 174 and MS2 was tested to investigate the potential of Cu ions as an antiviral agent against human enteric viruses in water. Using variable pH (6-8), speciation of Cu was evaluated against inactivation rates achieved. An increase in pH was associated with reduction in free ionic Cu^{2+} and dissolved Cu.

Regardless of Cu^{2+} availability, PhiX 174 was not affected by Cu treatment. No inactivation was observed experimentally, or change in PhiX 174 morphology in TEM images. Sagripanti et al. (1993) also reported no inactivation of PhiX 174 by Cu treatment (15 mM). However, Li and Dennehy (2011) reported 3.5 LRV of PhiX 174 after adding 5 mM of $CuSO_4$ to the PhiX 174 lysate. This difference cannot be explained by Cu dose because the higher dose used by Sagripanti et al. (15 mM) and the lower dose (78.7 µM) used in our study did not cause PhiX 174 inactivation.

Of note, Li and Dennehy added Cu to the lysate which contains organics while in our study inorganic buffer was used. The interaction between organics and Cu^{2+} can lead to Cu reduction to the more toxic form Cu^{+1} and possible production of H_2O_2 [94]. H_2O_2 interacts with dissolved oxygen producing ROS, which causes phiX 174 inactivation by DNA degradation [177,178]. Cu^{2+} alone reportedly does not cause damage to the genomic DNA unless ROS were produced [79,179,180]. So, the inactivation effect of Cu on PhiX 174 reported in some studies is most probably caused by a more toxic form of Cu or production of ROS, and Cu^{2+} alone does not directly cause inactivation of PhiX 174, regardless of its concentration and solution pH.

On the other hand, MS2 was inactivated by Cu at variable rates depending on the pH. Although Cu concentration used in this study was higher than the WHO recommendation of 2 mg/l [181], LRVs achieved at the same pH might not vary when the WHO recommended limit is applied. This is because the reported MS2 inactivation rates at Cu dose ≥1 mg/l were similar due to solution saturation with

copper [97,163]. According to Nieto-Juarez et al. (2010) inactivation of MS2 by Cu is caused only by its dissolved fraction. Our analysis show that dissolved Cu was higher at pH 6 than at pH 7 by 19% (CHEAQS data). However, the observed inactivation rates of MS2 were similar at pH 6 and 7 and lower at pH 8. Based on these results, the effect of pH on MS2 inactivation rates cannot be explained by Cu^{2+} solubility alone.

Potentially, the presence of MS2 as a colloidal particle that has amino acid functional groups in the proteins of its outer capsid can influence the speciation of Cu^{2+}. A study by Badetti et al.(2019) found that amino acids can solubilize Cu^{2+} from Cu nanoparticles to form soluble complexes with Cu^{2+}. If this mechanism applies, then it is possible that more soluble Cu was available at pH 7 or 8, in presence of MS2, than the soluble Cu reported by CHEAQS data. Hence, the similarity between inactivation kinetics at pH 6 and pH 7 could be due to similar Cu solubility. However, this hypothesis doesn't provide explanation to the lower inactivation kinetics at pH 8. Hence, conformational or structural changes in the MS2 capsid could provide more conclusive explanation to inactivation rates observed.

It has been reported that at pH 6 to 8, most of the Cu^{2+} binds to histidine (His) amino acid in proteins [183], and a small fraction to cysteine (Cys) amino acids (Minoshima et al., 2016). According to Barber-Zucker et al. (2017) increasing pH from 6 to 7 and 7 to 8 enhanced Cu^{2+} interaction with His by 20% and 1% but reduced Cu^{2+} interaction with cysteine (Cys) amino acid by 2% and 1% respectively. So, it is likely that while pH 6 favored Cu^{2+} dissolution, pH 7 favored the interaction between Cu^{2+} and His, resulting in similar inactivation rates as observed in our study. The lower inactivation rates at pH 8 can be attributable to further loss of available Cu^{2+} due to reduced solubility which is not compensated by an increase of Cu^{2+} interaction with His.

The images of MS2 Cu treated particles showed preservation of the circular capsid morphology with a dark center, which could be an artificial effect from the Uranyl salts used as negative stain [185] or a result of defective capsid protein [81]. If Cu caused only conformational change (such as coordinating with amino acids), it would not be visible under TEM, making the artificial effects interpretation more likely. However, the exact structural damage cannot be determined or confirmed based on the TEM images only, so other possibilities cannot be excluded.

3.4.2 Ag inactivation of MS2 and PhiX 174

Based on the observed results, Ag appears to be a potent antiviral agent against both MS2 and PhiX 174. Ag inactivation rates followed first order Chick Watson kinetics, except for MS2 at pH 8 where tailing was observed. Virus inactivation rate tailing has been commonly explained by aggregation of virus particles induced by solution pH (close to virus isoelectric point), other physico-chemical properties of the virus type such as hydrophobicity, salt concentrations, bacterial debris, organic matter, or type or concentration of the disinfectant[172]. The purification of MS2 stock, as described in section 3.2.2, should remove bacterial debris, organics and significantly reduce aggregation [171]. Because the same MS2 stock in the inorganic buffer 1 mM PB and Ag concentration were used in experiments where tailing was not observed, it is unlikely that aggregation was the cause of observed tailing. While the exact reason behind observed tailing remains unknown, it is not determinative in evaluating Ag antiviral efficiency because it is confined to only one condition (MS2, pH 8).

Inactivation rates by Ag were pH dependent for MS2 and PhiX 174, as K_{obs} increased with increasing pH. Because Ag was available in its ionic free form (Ag^+) regardless of pH, the observed dependency cannot be explained by Ag speciation. Similar pH dependency of inactivation kinetics of bacteria by Ag was reportedly associated with the increase in the negatively charged sites on the bacteria's membrane which enhanced the interaction with Ag^+ ions [145,165,186,187]. In viruses, protonation of amino acids (loss of H^+) is responsible for the presence of negative sites in the protein capsid, depending on its pKa value. Because pKa values differ per protein structure and the solution pH [188], pKa values of MS2 and PhiX 174 amino acids were predicted using PROPKA 3.0 and provided in the supplementary material (Table 3-2, 3-3).

The higher inactivation rates observed at pH 6 for PhiX 174 compared to MS2 can be attributed to the presence of Cys residues with lower pKa value in the PhiX 174 spike protein (G) compared to the pKa of Cys residues in the MS2 capsid protein (See supplementary Table S2, S3). Although other amino acids had lower pKa, denaturation of cysteine has been linked to Ag inactivation of viruses in the literature [83,84,93,184,189]. TEM images of Ag treated PhiX 174 showed a loss of the capsid spikes. However, we only accounted for pKa values of Cys in PhiX 174 spike protein G and Cys pKa in the MS2 capsid protein. Other amino acids could also be involved, such as others with sulfhydryl groups.

The gradual increase of PhiX 174 inactivation rates with increasing pH is in agreement with the literature reported increase of the thiolates/thiols ratio which enhances the interaction between Ag^+ and Cys [188,189]. Meanwhile, the sharp increase in MS2 Kobs at pH ≥ 7 suggests involvement of both Cys and RNA in Ag^+ mediated inactivation mechanisms. Ag treated MS2 particles observed under TEM support this hypothesis because the capsid is completely distorted. It is important to note that similar to Cu, the concentration of Ag used in this study was higher than WHO recommendations for drinking water (0.1 mg/l), so lower LRVs can be anticipated when applying Ag at concentrations consistent with the WHO guidelines [82].

3.4.3 Inactivation of MS2 and PhiX 174 by Cu and Ag combined.

No synergy was observed between Cu and Ag for PhiX 174 inactivation. The combination of Cu and Ag ions exhibited a synergistic effect on MS2 inactivation at pH ≥ 7, but not at pH 6. Ag was only effective in disinfecting MS2 at pH ≥ 7 while Cu has similar efficiency at pH 6 and 7. While it is likely that synergy is primarily mediated by Ag ions rather than Cu, for synergy to occur, both metals need to be individually effective in virus disinfection. Ag^+ ions are strongly polarized compared to Cu^{2+}, so when both ions are present in solution it is highly likely that Ag^+ would interact first [79].

Synergy of Cu and Ag in inactivating MS2 was also reported by Yahya et al. (1992) at pH 8, yet the reason behind it remains unclear. Chemical speciation of Cu and Ag was like the speciation of the individual metals solutions. Also, TEM images provide no possible mechanistic explanation for the synergy observed.

Further research is needed to understand the reason behind Cu and Ag synergy. Moreover, mechanistic understanding of the tailing kinetics can help evaluate if virus inactivation by metals could be self-limiting under certain conditions. Although the promising potential of Cu and Ag antiviral efficiency is evident in this study, evaluation of complexing factors such as natural organic matter is an important consideration to address for a more complete picture of metal's antiviral efficiency and their potential application in drinking water treatment.

3.5 Conclusions

- Our study has clarified essential aspects of evaluating the antiviral activity of metals. Different solution pH did not only affect the speciation of Cu but also the sensitivity of viruses to disinfection.
- Free ionic Ag^+ strongly inactivated ssRNA MS2 and ssDNA PhiX 174 in neutral and alkaline conditions.
- There is a strong synergistic effect of Ag and Cu for the inactivation of MS2 at pH 7 and higher. No synergy was observed for PhiX 174.
- More work is needed to evaluate the efficiency of Cu and Ag in presence of organics to better characterize the further application of these metals as virucides for drinking water treatment.
- Although the concentrations used are higher than WHO recommendations, the study highlights the potential of Cu and Ag as possible virus disinfectants in (household) drinking water treatment.

3.6 Supplementary material

3.6.1 Speciation of metal ions
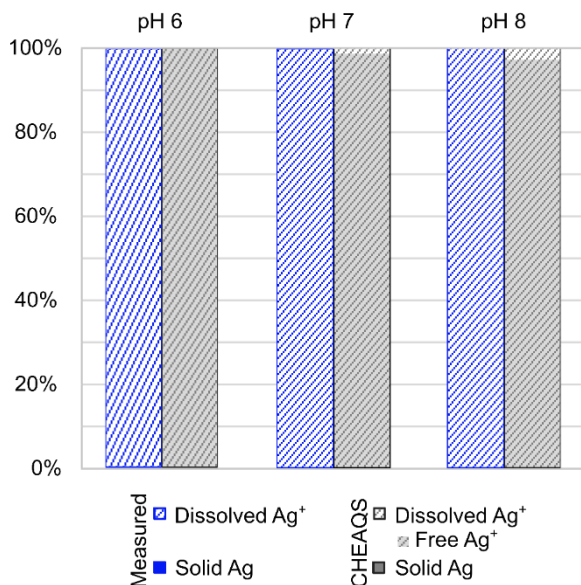
Figure 3-7 Speciation of Ag ions in solution based on experimental measurements of dissolved and solid Ag concentrations referred to as (measured) and simulated speciation using CHEAQS next chemical software. Ag measured concentrations after the passing 0.1 µm filter are expressed as dissolved, while the difference between dissolved and the unfiltered sample is considered solid complexes. Values expressed as a percentage of the total Ag concentration which was used as the input for CHEAQS as well.

Table 3-1 Detailed speciation of the dissolved Cu as output of CHEAQS next modelling.

Speciation (%)	pH 6	pH 7	pH 8
Free Cu^{2+}	16.3 %	0.9 %	0.2 %
$CuHPO_4$ (aq)	6.7 %	3.3 %	1.1 %
$Cu(OH)^+$	0.3 %	0.2 %	0.2 %
$CuSO_4$ (aq)	0.2 %	0.0 %	0.0 %
$CuH_2(PO_4)_2$ $^{2-}$	0.1 %	0.7 %	0.4 %
Total dissolved Cu (%)	23.6 %	5.2 %	1.9 %

3.6.2 Antiviral activity of Cu and Ag combined
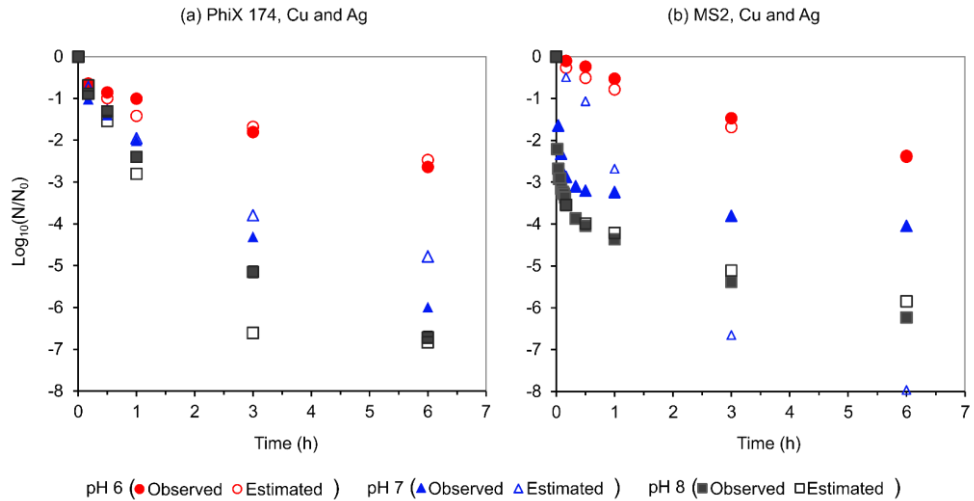
Figure 3-8 Six hours inactivation of (a) PhiX 174 and (b) MS2 by Cu and Ag ions combined (Observed) and the mathematical sum of LRVs obtained through individual treatment (Estimated).
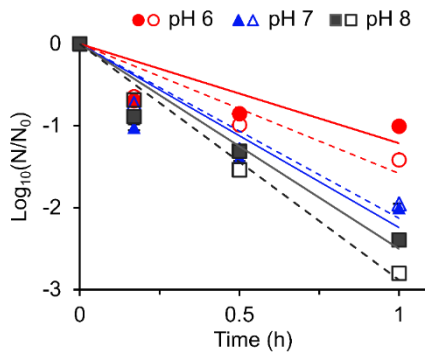
Figure 3-9 First hour inactivation kinetics of PhiX 174 by Cu and Ag combined as observed (closed marker) and the mathematical sum of LRVs obtained through individual treatment as estimated (open marker).

3.6.3   Morphological changes of MS2 and PhiX 174

The protocol for imaging MS2 and PhiX 174 samples is described in the main manuscript (Section 3.2.6). To ensure that the sample represents the inactivation experiment, samples prepared for imaging were also neutralized, diluted and quantified. Initially 300 µl of MS2 or PhiX 174 were divided into 3 parts (each of 100 µl). One aliquot was treated as control, another treated with Cu and the last with Ag. From each aliquot, a 50 µl sample was neutralized and diluted in PBS. A 10 µl volume of each dilution was deposited on agar plates containing host bacterium [190]. Lysis zones were evaluated for virus concentrations and $\log_{10}$ virus inactivation values (LRV) compared to the control.

Imaged MS2 samples had viable phage concentrations lower than the control by ~ 1.5 logs in case of Cu and ~ 5 logs in case of Ag treatment. PhiX samples had phage concentrations lower than control by ~0.2 logs in case of Cu treatment and by ~4 logs in case of Ag treatment. Images of control samples are referred to as intact.
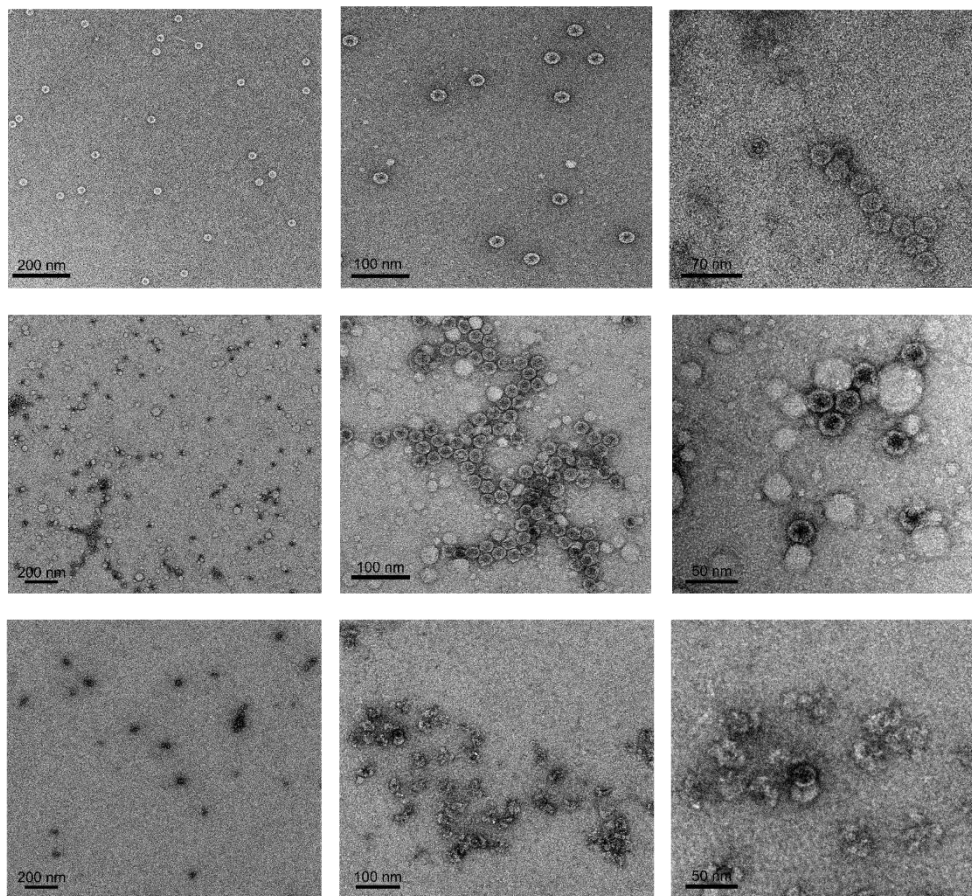
Figure 3-10 Additional TEM images of MS2 showing intact particles (top row), Cu treated particles (middle row) and Ag treated particles (bottom row).
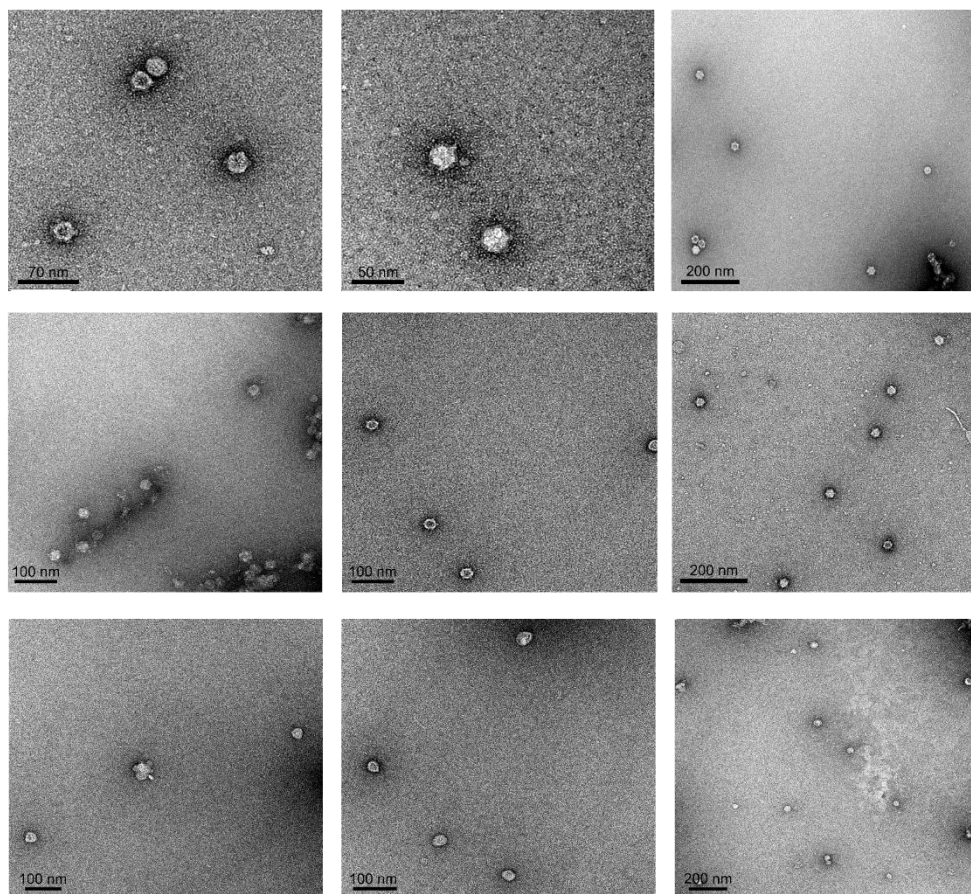
Figure 3-11 Additional TEM images of PhiX 174 showing intact particles (top row), Cu treated particles (middle row) and Ag treated particles (bottom row).

3.6.4 Modelling of amino acids pKa values for MS2 and PhiX 174

Predicting pKa values of amino acids in the protein structures of MS2 and PhiX 174 was carried out using PROPKA (version 3.0) and PARSE forcefield [191]. Protonation state was assigned at pH 6, 7 and 8. Because negligible difference in pKa values was observed using different pH values, the output is provided at pH 7 (Table S2, S3 and S4). The protein structures from the Protein Data Bank (PBD) 2MS2 and 1RB8 were provided as input for MS2 and PhiX 174, respectively.

Table 3-2 pKa values of MS2 coat protein predicted at pH 7 using PROPKA (version 3.0)

Amino acid	pKa	Amino acid	pKa
ASP 11	4.0	LYS 66	10.4
ASP 17	3.8	GLU 76	4.7
GLU 31	4.7	ARG 83	11.9
ARG 38	11.2	TYR 85	10.4
TYR 42	10.6	GLU 89	3.9
LYS 43	10.1	ASP 100	3.0
CYS 46	10.4	CYS 101	9.9
ARG 49	12.3	GLU 102	4.7
ARG 56	12.8	LYS 106	10.4
LYS 57	10.7	LYS 113	10.4
TYR 58	9.9	ASP 114	3.9
LYS 61	10.4	TYR 129	10.2
GLU 63	4.3		

Table 3-3 pKa values of PhiX 174 spike protein (G) predicted at pH 7 using PROPKA (version 3.0)

Amino acid	pKa	Amino acid	pKa	Amino acid	pKa	Amino acid	pKa
ARG 101	11.9	ASP 61	4.0	GLU 116	4.7	LYS 187	10.3
ARG 135	12.2	ASP 71	2.9	GLU 118	2.4	LYS 69	10.8
ARG 145	16.2	ASP 76	4.7	GLU 123	4.6	TYR 120	11.7
ARG 166	12.4	CYS 132	7.7	GLU 179	4.7	TYR 180	9.4
ARG 17	12.1	CYS 137	10.2	GLU 44	10.8	TYR 2	10.0
ARG 45	12.1	CYS 157	16.9	HIS 119	5.8	TYR 51	9.8
ASP 10	4.0	CYS 79	11.0	HIS 143	5.8	TYR 94	10.1
ASP 136	3.1	GLU 103	2.8	HIS 178	6.2	ARG 10	12.4
ASP 141	2.6	GLU 107	4.3	LYS 161	10.4	ARG 13	12.5
LYS 187	10.3	TYR 120	11.7	TYR 2	10.0		
LYS 69	10.8	TYR 180	9.4	TYR 51	9.8		

Table 3-4 pKa values of PhiX 174 capsid protein (F) predicted at pH 7 using PROPKA (version 3.0)

Amino acid	pKa	Amino acid	pKa	Amino acid	pKa	Amino acid	pKa
ARG 10	12.1	ARG 56	12.2	ASP 382	3.8	GLU 280	4.7
ARG 102	12.4	ARG 57	12.2	ASP 394	6.0	GLU 299	7.8
ARG 119	12.3	ARG 75	13.9	ASP 396	6.7	GLU 328	4.4

ARG 137	11.3	ARG 87	12.6	ASP 40	4.8	GLU 348	5.2
ARG 144	13.5	ASP 105	3.6	ASP 426	4.0	GLU 386	3.9
ARG 158	13.2	ASP 14	3.3	ASP 45	4.3	GLU 43	4.8
ARG 162	12.3	ASP 155	4.0	ASP 62	6.3	HIS 106	5.5
ARG 209	12.3	ASP 156	3.6	ASP 66	4.0	HIS 125	4.5
ARG 215	9.3	ASP 192	3.4	ASP 80	4.0	HIS 165	3.3
ARG 217	11.8	ASP 21	4.0	ASP 88	4.0	HIS 17	6.1
ARG 234	12.9	ASP 218	5.4	CYS 100	10.8	HIS 204	6.3
ARG 264	13.3	ASP 230	2.7	CYS 163	12.8	HIS 240	5.9
ARG 27	11.0	ASP 232	3.5	CYS 164	13.4	HIS 271	3.6
ARG 275	12.9	ASP 242	4.9	CYS 22	11.3	HIS 281	5.5
ARG 291	15.4	ASP 249	4.3	CYS 398	12.2	HIS 300	5.4
ARG 327	13.9	ASP 251	4.0	GLU 11	4.7	HIS 301	5.5
ARG 332	12.4	ASP 254	2.5	GLU 143	4.6	HIS 355	6.8
ARG 336	12.4	ASP 313	2.3	GLU 146	4.3	HIS 364	6.4
ARG 339	12.3	ASP 317	3.1	GLU 154	4.8	HIS 367	6.1
ARG 353	11.9	ASP 333	3.3	GLU 177	4.9	HIS 392	2.1
ARG 391	12.6	ASP 337	4.3	GLU 182	4.0	HIS 420	5.9
ARG 412	12.4	ASP 357	5.0	GLU 183	4.7	HIS 74	3.7
ARG 419	12.0	ASP 365	3.2	GLU 187	4.4	HIS 76	5.4
ARG 425	12.3	ASP 373	7.0	GLU 206	4.9	LYS 122	9.9
ARG 51	11.7	ASP 374	4.8	GLU 208	5.6	LYS 167	8.5
LYS 179	11.4	LYS 64	10.6	TYR 211	11.4	TYR 358	10.3
LYS 270	10.5	TYR 103	10.1	TYR 216	10.3	TYR 363	10.2
LYS 29	10.6	TYR 109	15.0	TYR 229	11.7	TYR 395	14.1
LYS 306	11.2	TYR 128	15.4	TYR 248	9.3	TYR 413	13.9
LYS 343	10.6	TYR 132	14.1	TYR 302	10.8	TYR 418	10.0
LYS 345	10.0	TYR 135	11.7	TYR 311	11.4	TYR 71	13.6
LYS 362	10.5	TYR 159	12.1	TYR 331	14.0	TYR 78	11.8
LYS 409	7.7	TYR 200	10.1	TYR 352	10.5		

4 ENHANCED VIRUS INACTIVATION BY COPPER AND SILVER IONS IN THE PRESENCE OF NOM IN WATER

This chapter is based on:

Abstract

Natural organic matter (NOM) is present in water that serves as a drinking water source. This study examined the effect of low and high NOM concentrations on inactivation kinetics of a model RNA virus (MS2) and a model DNA virus (PhiX 174) by copper (Cu^{2+}) and/ or silver (Ag^+). Cu and Ag are increasingly applied in household water treatment (HHWT) systems. However, the impact of NOM on virus inactivation kinetics by these metal ions in water remains uncertain despite the importance of their use. The presence of NOM in water led to slower virus inactivation by Ag^+ but faster virus inactivation by Cu^{2+}. The fastest inactivation of MS2 and PhiX 174, in water containing low NOM (2 mg C/ L), was observed by Cu and Ag combined synergism (K_{obs} = 3.2 ± 0.1 h^{-1}). In high NOM water (20 mg C/ L), synergism of Cu and Ag was also responsible for the highest inactivation kinetics of PhiX 174 (av. K_{obs} = 3.5 h^{-1}) but not for MS2 (K_{obs} = 4.8 h^{-1} using Cu alone). Overall, it can be concluded that the combination of Cu and Ag is promising as a virus disinfectant in treatment options allowing for multiple hours of residence time such as safe water storage tanks.

4.1 Introduction

The burden of waterborne disease remains a global threat to public health and economic prosperity. To date, 44% of the global population lacks access to safe clean drinking water [1]. Fecally contaminated water can contain harmful organisms such as deadly waterborne viruses. For example, rotavirus and norovirus are waterborne viruses that can cause fatal diarrhoeal disease, and hepatitis A or E are other waterborne viruses that cause liver disease [11–13]. Hence, it is important to provide consumers with water treatment systems with adequate protection from waterborne viruses.

Metals, such as copper (Cu) and silver (Ag), have been increasingly investigated as additives to existing filters for enhanced virus removal. Cu and/ or Ag has been added to existing household water treatment to improve virus removal in treated water [6,41,77,78,192]. Similarly, large scale membrane filters were also amended with Cu and/ or Ag for enhanced virus removal [84,193–196]. Cu and Ag were also combined with other disinfection methods such as UV light to accelerate the disinfection of viruses in water [82,83].

Multiple factors can impact the antiviral efficiency of Cu and Ag. For example, physiochemical water quality parameters such as pH, organic carbon, temperature and dissolved oxygen can impact the oxidation state and the speciation of metals [79,197,198]. Viruses can exhibit different sensitivity to different Cu or Ag chemical species [97,99,184,199]. Despite the importance of water quality in studying Cu and Ag antiviral efficiency, a systematic assessment of physiochemical parameters impacting virus inactivation kinetics remains has not been done.

In our previous study, we demonstrated the significant impact of pH on Cu and Ag inactivation kinetics of two model enteric viruses; MS2 (ssRNA) and PhiX 174 (ssDNA) [200]. Another important factor is to assess the role natural organic matter (NOM) can play in Cu and Ag antiviral efficiency. Presence of NOM in source water for HHWT systems is inevitable, and therefore an examination of its effects is crucial for Cu and Ag application [47]. Yet, to our knowledge, the effect of NOM on virus inactivation by Cu and Ag ions has not been reported.

Both; Cu and Ag have affinity to bind with ligands in NOM, changing the metal speciation [79,201]. NOM contains functionalities such as thiols, hydroxyls, aldehydes, etc., that can form organic-Ag complexes, AgCl, Ag_2S or over lengthy periods reduce

Ag to silver nanoparticles [87,88]. Formation of soluble or insoluble Ag solids have been reported as an ineffective disinfectant compared to Ag^+ [90–93]. Similarly, in fresh water bodies, most of Cu is bound to NOM which reduces its environmental toxicity [89]. Moreover, Cu binding to NOM was reported to result in production of reactive oxygen species (ROS) [94]. Presence of ROS can result in rapid inactivation of MS2 bacteriophage as observed in many studies [95–99]. Hence, it is possible that that the viricidal efficiency of Ag or Cu would be reduced by the presence of NOM. However, the possibility of ROS production by Cu-NOM interaction suggests the possible opposite effect. Currently, the antiviral efficiency or possible synergism of Cu and Ag in combination when in the presence of NOM in water cannot be predicted.

Therefore, we evaluated the antiviral efficiency of Cu and/or Ag in presence and absence of NOM using MS2 and PhiX 174 bacteriophages as a conservative model RNA and DNA virus, respectively. Cu and Ag were tested individually and combined to examine possible synergies in the presence of NOM in water. Two levels of NOM were added to water, representing low NOM (2 mg C/L) and high NOM (20 mg C/L) concentrations. The chemical speciation of Cu and/or Ag in water w/o NOM was calculated using the CHEAQS Next -chemical equilibrium program. Possible ROS production was examined through scavenger experiments and measurement of hydrogen peroxide as a step in the ROS chain.

4.2   Materials and Methods

4.2.1   Chemical reagents and microbial stocks

All chemicals were reagent grade and used without further purification as described in Soliman et al.(2020)[200]. Experimental solutions were prepared using Milli-Q water. Sodium phosphate buffer (PB; 1 mM, pH 7) contained sodium phosphate monobasic monohydrate ($NaH_2PO_4.H_2O$), sodium phosphate dibasic heptahydrate ($Na_2HPO_4.7H_2O$) mixed at concentration of 0.58 mM and 0.42 mM. PB buffer was autoclaved at 121 °C for 20 min and stored at 4 °C until further use. Potassium iodide (KI, 0.1 M) solution was prepared by dissolving KI (99%, Sigma) in MilliQ water and 0.01M molybdate solution by dissolving ammonium molybdate tetrahydrate (99.98%, Sigma) in MilliQ water.

NOM of ground water origin was obtained from the Dutch company Vitens. NOM was recovered from ion exchange brine resulting in a concentrated NOM stock of

89.9 mg/ L measured as dissolved organic carbon, which contained 88% humic substance; of which 69.3% was fulvic acid and 10.7% humic acid [202]. The 5 NOM fractions are measured and reported by Caltran et al. (2020)[202]. The NOM stocks used were prepared by diluting the concentrated NOM stock in MilliQ water, filter sterilized through sterile 0.22 μm syringe filters (PES, VWR) and stored at 4 °C until used.

Purified MS2 and PhiX 174 stocks were used as conservative enteric virus models. The culturing and purification of both phages is described in detail in Soliman et al. (2020)[200]. In brief, MS2 stock was produced by infecting host bacterium *Escherichia coli* C3000 (ATCC 15597) and PhiX 174 by infecting *E. coli* WG5 (DSM 18455). Following overnight replication, the harvested lysate was centrifuged and filter sterilized using 0.22 μm sterile syringe filters. MS2 was purified in an iodixanol gradient (OptiPrep™- Stemcell) and PhiX 174 in a cesium chloride gradient by centrifugation for 20 h (32,000 rpm, 4 °C, Beckman coulter optima L-90 K ultracentrifuge). The recovered phage was washed twice using 100 kDa Amicon® Ultrafilter columns and stored in PB buffer (pH 7) at 4 °C.

4.2.2 Impact of NOM on MS2 and PhiX 174 inactivation

The examination of NOM effect on MS2 and PhiX 174 inactivation by metals was conducted by comparing inactivation kinetics under 3 conditions: no NOM (PB buffer), low NOM (PB buffer + 2 mg C/L) and high NOM (PB buffer + 20 mg C/L). Although the presence of bacteriophages in PB buffer constituted an organic content, its concentration compared to added NOM was negligible as a result of virus purification and washing in buffer.

In addition, the stability of MS2 and PhiX 174 was examined without adding metals (control conditions). This aimed to account for any possible bacteriophage decay in the test water not caused by the metals. Overall, each bacteriophage was examined in 12 conditions (3 controls, 3 with Cu, 3 with Ag and 3 with Cu and Ag). Each condition was tested in triplicate beakers.

In a sterile glass beaker, a 60 ml volume of test water (no NOM or low NOM or high NOM) containing MS2 and PhiX 174 at a final concentration ~ 10^6 pfu/ml was added. For metal conditions, aliquots of Cu, Ag or Cu and Ag were added to a final concentration of 1 mg/l for Cu and 0.1 mg/l for Ag. All beakers were kept at 25 °C in a dark incubator and stirred continuously at 60 rpm (2mag-Magnetic-Drive) for 6

hours. At time intervals 0, 0.17, 0.5, 1, 3 and 6 h, a 5 ml of sample was withdrawn using sterile syringes and added to a sterile tube containing metals neutralizing solution. Samples containing Cu were neutralized using 150 µl EDTA (0.1M) and Ag samples using 150 µl of sodium thiosulfate (0.1M). Control samples and Cu and Ag samples were neutralized using 150 µl EDTA and 150 µl of sodium thiosulfate. The addition of neutralizer to control samples aimed to test the effect of neutralizing solutions on phage stability. All samples were diluted in PBS buffer and enumerated for each phage in duplicates.

Phage enumeration followed the ISO-10705 method, in which a 1 ml sample was assayed using the double agar layer (DAL) method. MS2 samples were enumerated using *Salmonella typhimurium* WG49 as a host and PhiX 174 using *E. coli* WG5 as host. Agars and cultures used followed the ISO- 10705 part 1 and 2 methods. Glass beakers used were sterilized, acid washed (10% nitric acid and 12.5 % hydrochloric acid), wrapped in aluminium foil and covered from the top with a sterile petri-dish and aluminium foil to ensure dark conditions.

4.2.3 Role of ROS

The interaction between Cu and NOM can lead to production of reactive oxygen species (ROS) such as hydrogen peroxide (H_2O_2) [94]. Measurements of H_2O_2 followed the Ghormley triiodide method [203] as described by Romero et al. (2011)[204]. H_2O_2 samples were obtained from metal beakers as replicates of the inactivation experiments. Every 0.5 h, a 1 ml sample was withdrawn, filtered through 0.45 µm filters and directly measured for H_2O_2. To quantify H_2O_2, 200 µl of sample was rapidly mixed with 1000 µl of KI solution and 20 µl of the molybdate solution in 2 ml disposable cuvette (VWR). Absorbance was recorded from a UV-Vis Spectrophotometer (GENESYS 10S) at 350 nm after the reading stabilized. Concentration of H_2O_2 was determined using a calibration curve (Supplementary **S1**) obtained by measuring the absorbance of H_2O_2 stock solution (Merck) at multiple dilutions.

To distinguish between inactivation kinetics caused by metals versus the additional inactivation by ROS, scavenger experiments were included. The 12 conditions mentioned above were repeated, each in triplicate beakers, with the addition of tempol as ROS scavenger. Tempol is a known redox-cycling nitroxide and used as a potent ROS scavenger to protect from oxidative damage [205–207]. In order to

determine the appropriate tempol dosage, possible tempol toxicity towards MS2 or PhiX 174 [207] and time related stability of tempol [208] were taken into account. Prior to the scavenger experiments, different doses of tempol and dosing intervals were tested (Supplementary **S2**-**S4**). Based on the results, it was determined that 1 mM of tempol dosed every 1.5 hour would provide maximum protection of MS2 or PhiX 174 without toxic effect towards either bacteriophage (as shown by the stability in tempol control tests). Therefore, inactivation experiments were replicated with the addition of 1 mM of tempol every 1.5 hour. Experimental procedure, sampling intervals, metals neutralization and phage enumeration were repeated exactly as described in the previous section. In addition, pH was measured at the beginning and end of the experiment to ensure pH stability in the presence of tempol.

4.2.4 Chemical analysis

NOM was measured as total organic carbon (TOC) using a TOC-V CPH analyzer (Shimadzu). Cu and Ag measurements were analyzed using ICP-OES (Spectro Arcos eop). Samples from NOM beakers were analyzed for all detectable elements to evaluate any additional ions present in water by adding NOM stock. Furthermore, we used the CHEAQS Next -chemical equilibrium program- to calculate the free ionic concentrations of Ag^+ and Cu^{2+} in the water matrices used. Metal – organic complexation was evaluated using model 7, (Tipping, 2011) in CHEAQS Next. Input for NOM included the measured concentration as mg C/L and measured fraction of fulvic acids as 0.69.

4.2.5 Data analysis

The measured concentration (pfu/ml) of MS2 or PhiX 174 at time t (N_t) and at time 0 h (N_0) were used to calculate bacteriophages concentrations and then the $\log_{10}$ inactivation values. To analyze inactivation kinetics, linear regression analysis was conducted with 95% confidence interval to calculate the slope of Ln (N_t/N_0) versus time, as a first order inactivation rate constant: Kobs (h^{-1}). Measured Kobs (h^{-1}) of control experiments was compared against zero (no slope) to evaluate the stability of MS2 and PhiX 174 in control conditions. Other conditions' Kobs (mean value, SD and df) were compared against each other for significant difference using an unpaired t-test.

4.3 Results

4.3.1 Impact of NOM on MS2 and PhiX 174 inactivation

The results of control (metal free) experiments showed stability of MS2 and PhiX 174 in the test waters w/o NOM (Supplementary **Fig**. 4-10). As depicted in **Fig.** 4-1, presence of NOM with Cu enhanced inactivation kinetics of MS2 and PhiX 174 compared to inactivation by Cu without NOM. MS2's $\log_{10}$ inactivation by Cu reached 1.7 ± 0.2 after 6 hours without NOM, ≥ 6 logs after 6 hours with low NOM and ≥ 6 logs after only 3 hours with high NOM (**Fig**.4-1 a). Hence, increasing NOM accelerated the MS2's inactivation by Cu. Less pronounced effect of Cu (w/o NOM) was observed on PhiX 174 compared to MS2 (**Fig**.4-1 b). For example, in presence of high NOM, Cu inactivated 1.7 ± 0.3 $\log_{10}$ of PhiX 174 after 6 hours.

Inactivation kinetics of MS2 and PhiX 174 followed the first order Chick Watson model as shown in **Fig**.4-1. The K_{obs} values are depicted in **Fig**. 4-2 as 'No Tempol' columns. MS2's K_{obs} by Cu was significantly (p <0.0001) higher in presence of high NOM (K_{obs} = −4.9 ± 0.3 h^{-1}) and low NOM (K_{obs} = −2.3 ± 0.1 h^{-1}) compared to no NOM (K_{obs} = −0.6 ± 0.04 h^{-1}). Similarly, PhiX 174's K_{obs} by Cu was significantly higher (p <0.0001) in the presence of high NOM (K_{obs} = −0.7 ± 0.1 h^{-1}) compared to no NOM (K_{obs} = −0.05 ± 0.01 h^{-1}).

However, the presence of NOM with Ag did not enhance inactivation kinetics of MS2 or PhiX 174 (**Fig**. 4-1 b and c). K_{obs} of Ag were statistically similar (p> 0.005) without NOM and with low NOM for both bacteriophages (**Fig**. 4-2 c and d). Moreover, the 6 hours Ag's $\log_{10}$ inactivation of MS2 and PhiX 174 were ≤ 2 without NOM and with low NOM. This value reduced to only 0.4 and 0.8 logs for MS2 and PhiX in presence of high NOM. As observed in **Fig**. 4-2 c and d, presence of high NOM with Ag significantly (p <0.001) reduced K_{obs} for MS2 and PhiX 174.

So far, MS2 and PhiX 174 were affected in a similar manner by presence of NOM with Cu (enhanced inactivation) or Ag (reduced inactivation kinetics). However, for the combination of Cu and Ag, NOM had different impacts on inactivation kinetics of MS2 from PhiX 174. Statistically similar (p = 0.44) inactivation of MS2 was observed by Cu and Ag without NOM and with High NOM (**Fig**.4-1 and 4-2 e). However, significantly higher (p <0.001) inactivation of MS2 was observed with low NOM. Statistically similar (p = 0.32) inactivation of PhiX 174 by Cu and Ag was

observed with low and high NOM. Overall, the inactivation of PhiX 174 by Cu and Ag with NOM was significantly higher (p <0.0001) than that without NOM (**Fig**. 4-1 and 4-2 f). Although all inactivation kinetics followed the first order Chick Watson model, MS2 inactivation by Cu and Ag without NOM followed a biphasic pattern (**Fig**. 4-1e), as also reported in our previous study[200] .
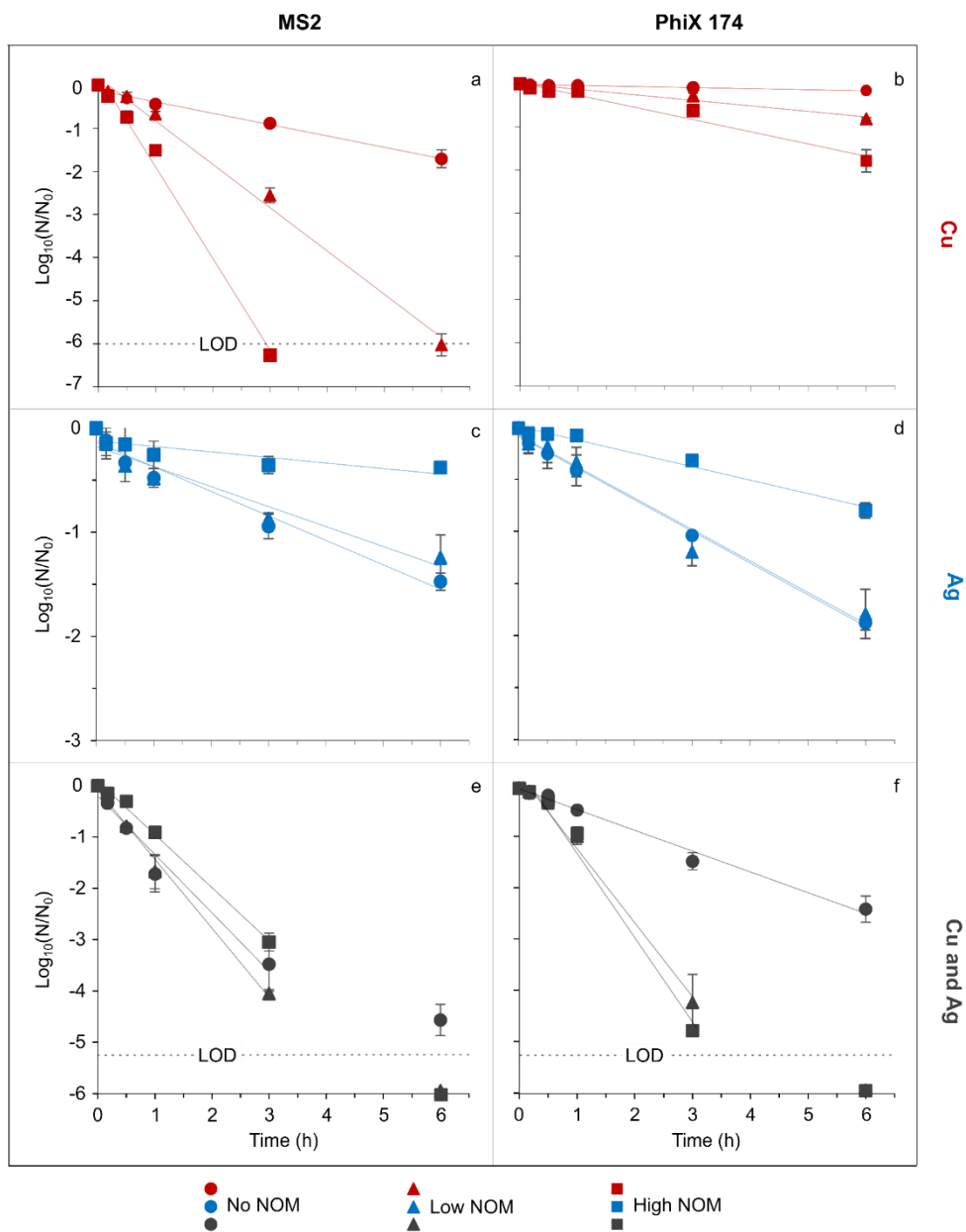
Figure 4-1 Inactivation of MS2 (a, c, and e) and PhiX 174 (b, d, and f) by Cu (a and b), Ag (c and d) and their combination Cu and Ag (e and f) in No NOM water (PB buffer), low NOM water (PB + 2 mg C/L) and high NOM water (PB + 20 mg C/L). Concentration of metals used is Cu at 1 mg/L and Ag at 0.1 mg/L at solution pH 7 and 25 °C. Limit of detection (LOD) was 1 pfu/ml. Reported results represent the average values and standard deviations of triplicate tests. Inactivation rate constants: K_{obs} (h^{-1}) ± standard deviation (SD) values are mentioned in the text and calculated based on the slope on linear regression lines. R^2 values were >0.96 for all Kobs values considered.

4.3.2   Contribution of ROS to inactivation kinetics

Tempol, a scavenger for ROS, was used to evaluate possible production of ROS and its contribution to the inactivation kinetics. **Figure** 4-2 provides an overview of the K_{obs} in presence or absence of tempol.

MS2 and PhiX 174's K_{obs} by Cu with NOM (low or high) was significantly ($p<0.001$) reduced after adding tempol (**Fig.** 4-2 a and b). In contrast, tempol did not affect the K_{obs} of MS2 or PhiX 174 by Cu without NOM. Hence, tempol effect on K_{obs} of Cu was only limited to the presence of NOM. This suggests that combining Cu and NOM leads to production of ROS and subsequently higher inactivation kinetics of MS2 and PhiX 174.

Moreover, H_2O_2 was detected when Cu was combined with NOM, but not without NOM (**Fig**. 4-3a). The measured H_2O_2 in Cu-NOM water demonstrated ROS production by Cu- NOM interaction. Higher H_2O_2 was measured in presence of high NOM with Cu, compared to low NOM. This suggests more production of ROS in presence of higher NOM, leading to faster inactivation kinetics.

H_2O_2 was not detected with Ag, regardless of NOM presence. Nevertheless, significant reduction ($p<0.05$) in Ag's K_{obs} of MS2 and PhiX 174 without NOM or with low NOM was observed after adding tempol (**Fig.** 4-2 c and d). However, this does not suggest production of ROS by Ag and low NOM since K_{obs} was also reduced by tempol without NOM.

For Cu and Ag combination, significant ($p<0.05$) reduction in MS2 and PhiX 174's K_{obs} was observed after adding tempol to water containing NOM (**Fig.** 4-2 e and f). Tempol had no effect ($p> 0.05$) on K_{obs} by Cu and Ag without NOM for either bacteriophage. This suggests production of ROS when Cu and Ag were combined with NOM. Moreover, H_2O_2 measurement in water containing Cu and Ag with NOM (**Fig.** 4-3 b), supports production of ROS when Cu and Ag were combined with NOM present.
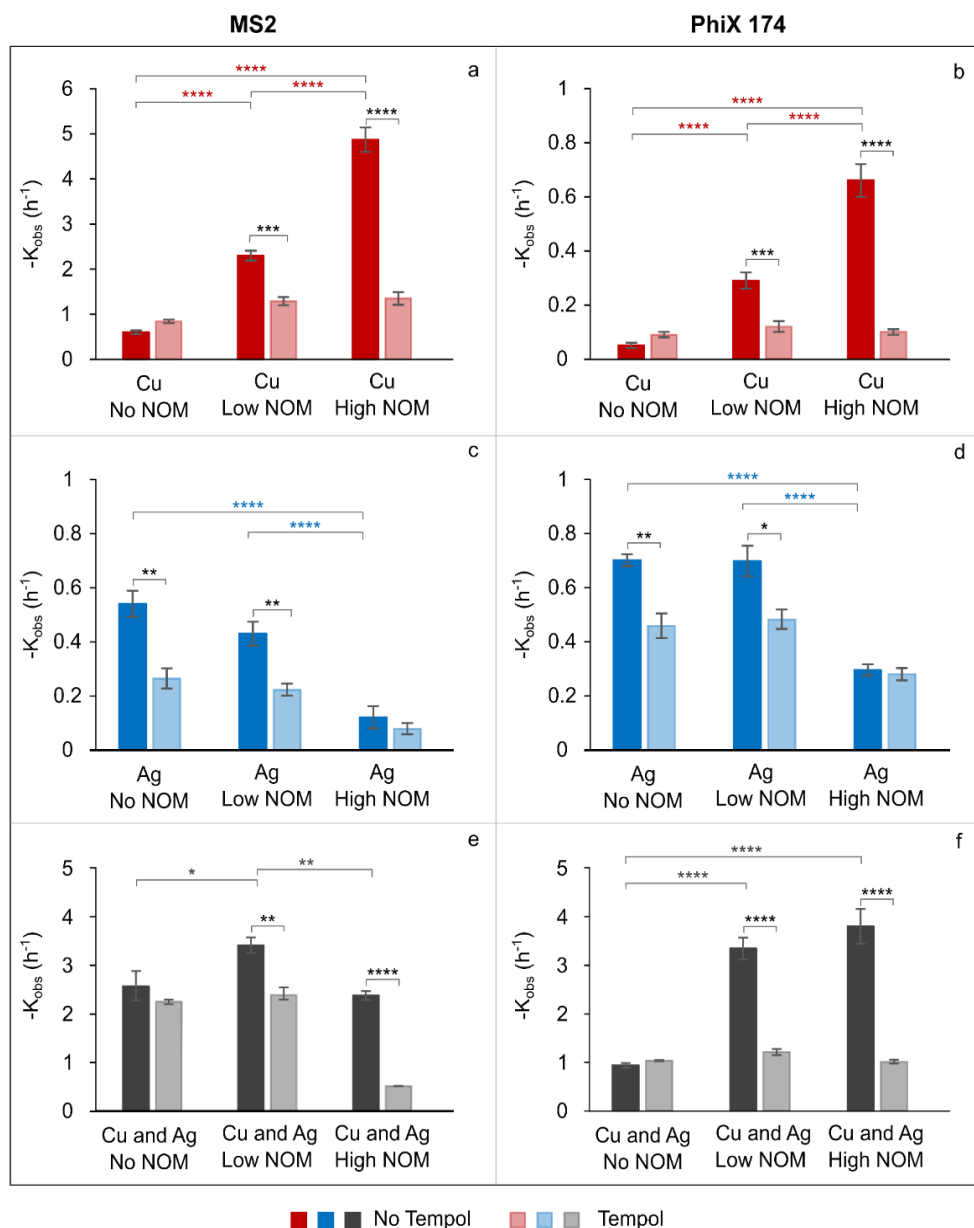
Figure 4-2 Inactivation rate constant K_{obs} (h^{-1}) of MS2 (a, c, and e) and PhiX 174 (b, d, and f) w/o tempol scavenger resulting from inactivation by Cu (a and b), Ag (c and d) and Cu and Ag (e and f) tested in no NOM water (PB buffer), low NOM water (PB + 2 mg C/L) and high NOM water (PB + 20 mg C/L). The asterisk (*) represent the significance in difference between K_{obs} (h^{-1}) values of metal experiment (* same colour as the no tempol columns) and metal experiment in presence of tempol (black *). Reported results represent the average values and standard deviations of triplicate tests. K_{obs} (h^{-1}) was calculated based on the slope of linear regression of Ln (N_t/N_0) versus time (h). R^2 values were >0.96 for all K_{obs} values considered.
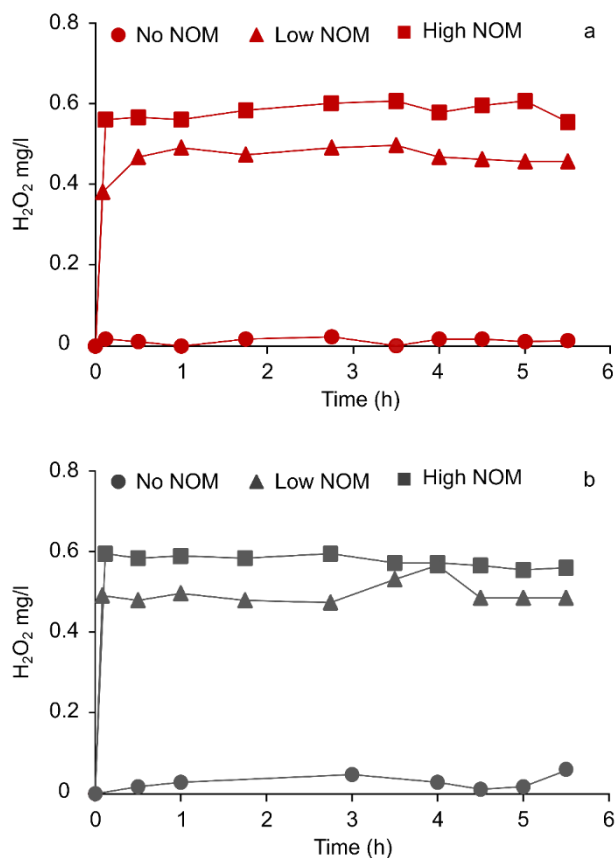
Figure 4-3 Measured H_2O_2 in (a) Cu or (b) Cu and Ag combined with no NOM, low NOM, or high NOM waters

4.3.3 Effect of NOM on synergy of Cu and Ag

The examination of Cu and Ag combination versus their individual use aimed to identify possible synergistic effect of the metal combination w/o NOM. To that end, we compared the K_{obs} experimentally obtained by using both metals (observed) against the mathematical sum of K_{obs} obtained from each metal (estimated) w/o NOM. If the observed K_{obs} is significantly higher than estimated K_{obs} by Cu and Ag in the same water matrix, it is considered to show synergism.

For MS2, Cu and Ag synergism ($p<0.05$) was observed without NOM and with low NOM only (**Fig**. 4-4a). On the other hand, for PhiX 174, strong ($p<0.0001$) Cu and Ag

synergy was observed with low and high NOM (**Fig**. 4-4b). The observed synergy for MS2 and absence of synergy for PhiX 174 by Cu and Ag (without NOM) was also reported in our previous study [200].
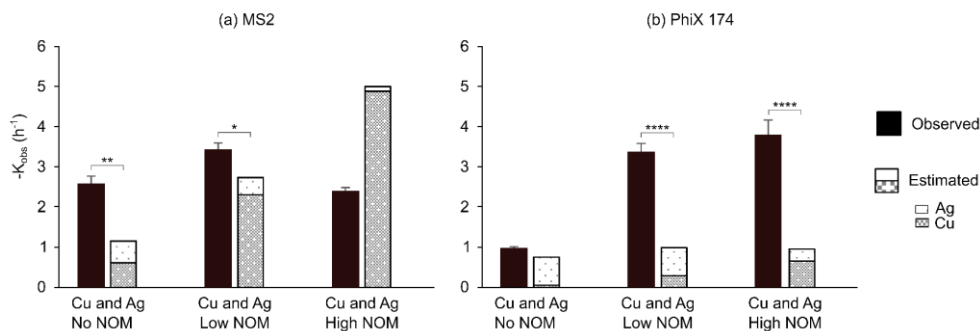
Figure 4-4 Inactivation rate constants (K_{obs}; h^{-1}) of (a) MS2 and (b) PhiX 174. Dark black columns are the K_{obs} experimentally obtained by Cu and Ag ions combined, referred to as observed. Light grey dotted column part is K_{obs} by Cu alone and white dotted column part is K_{obs} of Ag alone. The mathematical addition of the two parts adds up to the estimated K_{obs} by Cu + Ag.

4.3.4 Speciation of metal ions

The examination of metal's speciation in water w/o NOM was conducted using CHEAQS Next as chemical speciation model. Speciation of Cu and Ag was simulated in individual and combined use. The results are depicted in **Fig.** 4-5, featuring speciation of Cu when added to water individually (**Fig.** 4-5 a) and when combined with Ag (**Fig.** 4-5 c). Similarly, speciation of Ag is depicted in **Fig.** 4-5 b and d.

Without NOM, 23% of total Cu was present as dissolved Cu (**Fig**. 4-5 a). This percentage decreased to 20% and 2% in presence of low and high NOM respectively. This decrease was accompanied by increase in organic bound Cu in presence of NOM. Sixteen % of Cu was organic bound when water contained low NOM and 92% of Cu was organic bound in the presence of high NOM. So, increasing NOM in water lead to increase in the percentage of organic bound Cu. Speciation of Cu was not affected by the presence of Ag (w/o NOM) as depicted in **Fig**. 4-5 c.

The percentage of dissolved Ag^+ ions decreased from 100% -without NOM- to 85 %, with low NOM, and down to 24% with high NOM (**Fig**. 4-5 b). The reduction in Ag^+ in presence of NOM was due to the formation of organic bound Ag (15 % and 76%

respectively). Hence, presence of low NOM had negligible effect on the speciation of Ag. However, when Ag was combined with Cu, the speciation of Ag in presence of NOM differed (**Fig**. 4-5 b and d). Organic bound Ag reduced to 1% in presence of low NOM and 16% with high NOM. Hence, presence of Cu reduced the binding of Ag to NOM and enhances its dissolution.
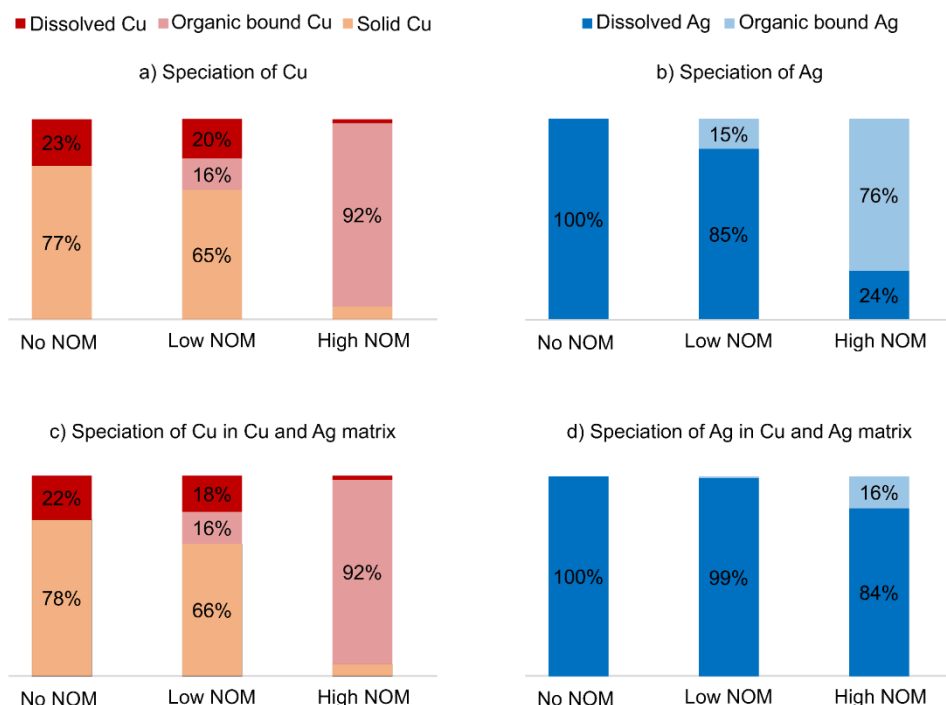
Figure 4-5 CHEAQS Next simulation (a) Cu or (b) Ag speciation when added individually each water matrix and (c) Cu or (d) Ag speciation in water matrices containing Cu and Ag combined.

4.4 Discussion

4.4.1 Copper and NOM

Without NOM, Cu had pronounced effect on MS2 inactivation but not on PhiX 174 inactivation [200]. The presence of NOM in water led to enhanced Cu inactivation of MS2 and PhiX 174. Higher NOM led to faster inactivation kinetics for both bacteriophages.

Environmentally, most Cu in water bodies or in wastewater is bound to organics [89,209]. Here, we observed that chemical interaction between Cu and NOM led to the formation of organic bound Cu, especially with high NOM (**Fig**. 4-5; 92%). Hence this leaves less dissolved free Cu^{2+} available for interaction with MS2 or PhiX 174. Although previous studies described availability of dissolved Cu^{2+} as a key factor in enhancing inactivation kinetics by Cu, we observed accelerated inactivation with higher organic bound Cu instead.

Cu binding to NOM is the starting point of a chemical interaction producing ROS [94]. In the presence of oxygen, Cu^{2+} is reduced by NOM's reducing moieties to Cu^{+1}. Then, oxygen rapidly interacts with Cu^{+1} producing super oxide which immediately reacts producing H_2O_2 as described by the following **equations 1-4** [94,210]. Moreover, these interactions could lead to production of organic radicals or toxic Cu^{+3} [210].

1) $Cu(\text{II}) + \text{R} \leftrightharpoons Cu(\text{I}) + R^+$ where R is the reducing organic moieties.
2) $Cu(\text{I}) + O_2 \longrightarrow Cu(\text{II}) + O_2^{\bullet-}$
3) $Cu(\text{II}) + O_2^{\bullet-} \longrightarrow Cu(\text{I}) + O_2$
4) $Cu(\text{I}) + O_2^{\bullet-} \longrightarrow Cu(\text{II}) + H_2O_2$

As observed in our results, interaction between NOM (low or high) and Cu led to production of H_2O_2. Higher H_2O_2 was measured in higher NOM water, similar to literature reports by Pham et al. (2012) and Xing et al.(2020)[94,210]. Moreover, tempol scavenging experiments showed that production of ROS was responsible for enhancing Cu inactivation kinetics in presence of NOM. It has been also reported by others that combination of Cu and ROS enhances inactivation of MS2 and PhiX 174, compared to Cu alone[97–99,175]. ROS causes protein oxidation and RNA damage of MS2 accelerating its inactivation [211,212].

Despite the similarity in MS2 and PhiX 174 response to Cu disinfection in NOM water, significantly higher kinetics were observed for MS2 than PhiX 174. This could be due to higher susceptibility of MS2 to certain ROS species or radicals compared to PhiX 174. For example, previous studies reported that MS2 is more susceptible to hydroxide radicals (OH$^{\bullet}$) and H_2O_2 than PhiX 174 [213,214].

4.4.2   Silver and NOM

Unlike Cu, the presence of NOM did not enhance inactivation kinetics of MS2 or PhiX 174 for Ag. In fact, slower inactivation kinetics of MS2 and PhiX 174 were

observed by Ag with high NOM. High NOM (20 mg C/L) led to a loss of 76% of Ag^+ by binding to NOM. This observation strongly suggests that complexation of Ag with NOM competes against viruses, hence leading to slower inactivation kinetics. In the case of Ag and low NOM, K_{obs} of MS2 and PhiX 174 were like that without NOM. Moreover, only 15% of Ag was organic bound in the presence of low NOM (2 mg C/l). Therefore, it is likely that loss of free dissolved Ag^+ by 15% was not significant enough to have noticeable impact on inactivation kinetics of either MS2 or PhiX 174. Complexation of Ag with NOM has been reported by multiple studies [215–217]. In fresh water, organic complexation of Ag reduces it toxicity [216,217]. These observations suggest that inactivation kinetics of Ag is dependent on the availability of free ionic Ag^+.

We also observed no H_2O_2 in the Ag and NOM conditions. To our knowledge, Ag has not been reported to produce ROS when interacting with MS2 or PhiX 174. Only in bacterial studies, Ag can produce ROS as part of the cell defence mechanism following the interaction between Ag and enzymes in the bacterial cell wall [79,218]. However, MS2 and PhiX 174 are non-enveloped and don't possess enzymes, regulatory or defence mechanism. Hence, production of ROS due to sole interaction between MS2 and PhiX 174 with Ag is unlikely.

4.4.3   Combined Cu, Ag and NOM

Cu and Ag's inactivation kinetics of MS2 was only enhanced in presence of low NOM (2 mg C/l) but not in presence of high NOM (20 mg C/L). On the other hand, high NOM and low NOM led to a similar, yet significant increase in PhiX 174's K_{obs} by Cu and Ag compared to K_{obs} without NOM.

The similarity in PhiX 174's K_{obs} between low and high NOM can be explained by the combined effect of ROS production and Ag-NOM complexation. Less free Ag^+ ions were available in water containing higher NOM but higher H_2O_2 was produced. Hence, it is possible that the balance between H_2O_2 and Ag^+ ions availability led to equivalent inactivation kinetics in presence of low and high NOM. It would have been expected that the higher H_2O_2 with high NOM compensates for the loss in Ag^+ concentration, hence resulting in similar K_{obs} in both NOM waters for MS2. Yet, that was not the case.

The variability between MS2 and PhiX 174 in reactions with Ag and Cu in the presence and absence of NOM and resulting inactivation kinetics could be due to a

production of radicals or intermediates that can be more toxic to PhiX 174 than MS2. The reaction between Ag^+ and H_2O_2 in water can result in a cascade of interactions possibly producing organic free radicals and intermediates such as bound hydroxyl radicals or Ag(II) species [219,220]. The possible production of these species and their potential effect on MS2 versus PhiX 174 functional integrity, virus infectivity and inactivation kinetics is unknown and cannot be judged based on the measurements in this study. Measurements of H_2O_2 were used as indicative of ROS production but not as conclusive representation or measurement of ROS. Hence, it is possible that other radicals not identified or quantified in this study, were produced and responsible for the inactivation rates observed by Cu and Ag in presence of NOM. However, this cannot be ascertained with certainty under the scope of the current study. Further investigation is needed to evaluate the full cascade of ROS species produced in each condition.

4.4.4 Synergy of Cu and Ag

Without NOM, Cu and Ag had a synergistic effect on MS2 (observed K_{obs} 2.5 times > estimated K_{obs}) but not on PhiX 174. With NOM (low or high) strong synergy (observed K_{obs} 3-4 times > estimated K_{obs}) of Cu and Ag was observed for PhiX 174. Meanwhile, for MS2, in presence of high NOM with Cu and Ag; observed K_{obs} was 0.5 times lower than the estimated K_{obs}, indicating slower kinetics and lack of synergy. Overall, the highest inactivation kinetics of PhiX 174 (av. K_{obs} = 3.5 h^{-1}) was observed for the Cu and Ag combination in the presence of NOM (low or high). However, the highest inactivation kinetics of MS2 (K_{obs} = 4.8 h^{-1}) was observed using Cu alone with high NOM.

It is likely that the observed Cu and Ag synergy in disinfecting PhiX 174 stems from interaction between Cu and NOM producing ROS, followed by its interaction with Ag^+. The interaction of Ag^+ ions and H_2O_2 in water was reported by Pedahzur et al. (1995)[221] to possess synergistic and long lasting effects in disinfecting *E.coli*. This suggests that simultaneous presence of Cu, Ag and ROS is crucial for fast inactivation kinetics of PhiX 174.

However, Cu and Ag's synergistic effect on MS2 was only observed without NOM and with low NOM. These are the two conditions in which free Ag^+ ions were available as 100% and 99%. Yet, the inactivation observed (**Fig**. 4-4) under these conditions with added synergy was lower than while using Cu alone with high NOM

(K_{obs} = 4.8 h^{-1}). Hence, for MS2 the fastest inactivation did not occur with synergy of Cu and Ag but rather with high ROS with Cu alone. However, the structural and mechanistic reasons for this observation are unclear based on the data available. Similar H2O2 was measured in water containing Cu and high NOM and that containing Cu, Ag, and high NOM. Yet, slower kinetics were observed for MS2 in the latter. Future structural and mechanistic study is needed to investigate the full speciation of ROS and their structural damage of MS2 and PhiX 174 in the presence of NOM, Cu and/ or Ag.

Finally, the observed log_{10} inactivation in this study document the potential of Cu at 1 mg/L and Ag at 0.1 mg/L to provide safe drinking water, complying with the WHO highly protective (5 logs) virus removal. Although contact time is in scale of hours, it is promising for safe storge treatment where longer contact time is possible. More research is needed to examine Cu and Ag antiviral efficiency in more representative water matrices (e.g., rich in ions) to further enable their application in practice.

4.5 Conclusions

- Presence of NOM in water reduced the availability of free ionic Cu^{2+} and Ag^+. Loss of free Ag^+ ions led to slower virus inactivation kinetics. However, Cu binding to NOM resulted in production of ROS and faster virus inactivation kinetics.
- In water containing low NOM (2 mg C/ L), the highest inactivation of MS2 and PhiX 174 was observed by Cu and Ag combined (a similar K_{obs} = 3.2 ± 0.1 h^{-1}).
- In water containing high NOM (20 mg C/ L), the highest inactivation kinetics of PhiX 174 (av. K_{obs} = 3.5 h^{-1}) was observed by Cu and Ag combination, while for MS2 (K_{obs} = 4.8 h^{-1}) it was observed using Cu alone.
- Synergy of Cu and Ag was observed for PhiX 174 when water contained low or high NOM, while for MS2 it was when water contained low or no NOM.
- Cu and Ag are promising virus disinfectants, especially in treatment options allowing for multiple hours of residence time such as safe water storage tanks.

4.6 Supplementary

4.6.1 Calibration curve of H_2O_2

The relationship between absorbance and H_2O_2 concentration was established by applying the Ghormley triiodide method to H_2O_2 stock solution (Merck). Absorbance of dilution series was measured by rapidly mixing a 200 µl of sample with 1000 µl of KI solution and 20 µl of the molybdate solution in a 2 ml disposable cuvette (VWR). Then, absorbance was recorded using a UV-Vis Spectrophotometer (GENESYS 10S) at 350 nm after the reading stabilized. Concentrations were plotted against measured absorbance, leading to a calibration curve equation. This equation was further used to determine the concentration of H_2O_2 in unknown samples based on the measured absorbance.
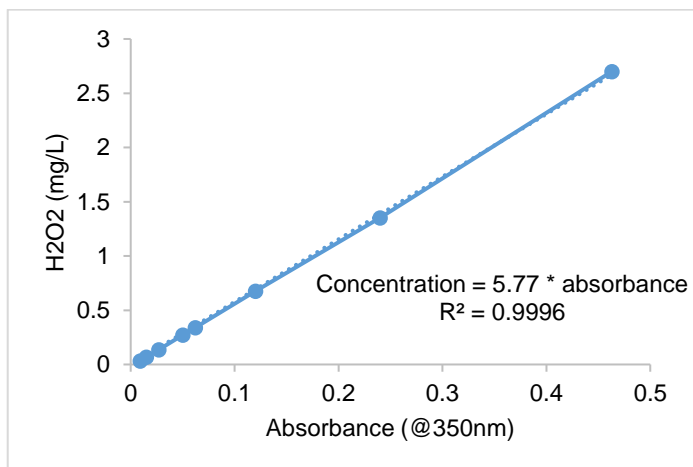
Figure 4-6 Calibration curve of H_2O_2 stock solution (Merck). Absorbance of known H_2O_2 concentrations was measured and used to produce the concentration equation

4.6.2 Tempol dosing

To evaluate possible toxicity of Tempo, an ROS chemical quencher, against MS2 and PhiX 174, stability of phages was examined in PB buffer after adding different dosages of Tempo, with observations at different times. Dosing 1 mM or 2 mM of Tempo didn't affect the stability of MS2 nor PhiX 174 (**Fig**. 4-7). Also, examining results for the dosage frequency of once every 6 hours to every 1.5 hour or every 1 hour didn't cause any notable decay for either phage.
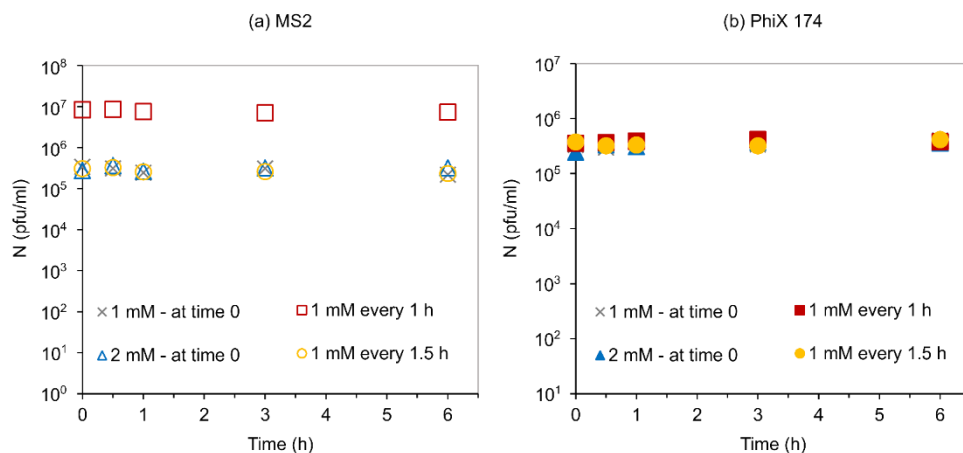
Figure 4-7 Stability of (a) MS2 and (b) PhiX 174 in no NOM water (pH 7, 25 ∘C) with different doses of tempol and variable dosing frequencies (see legend).

The choice of optimum concentration and dosing time to achieve the most protective effect was achieved by testing doses and dosing times of tempol for their virus inactivation results in Cu + NOM experiments.
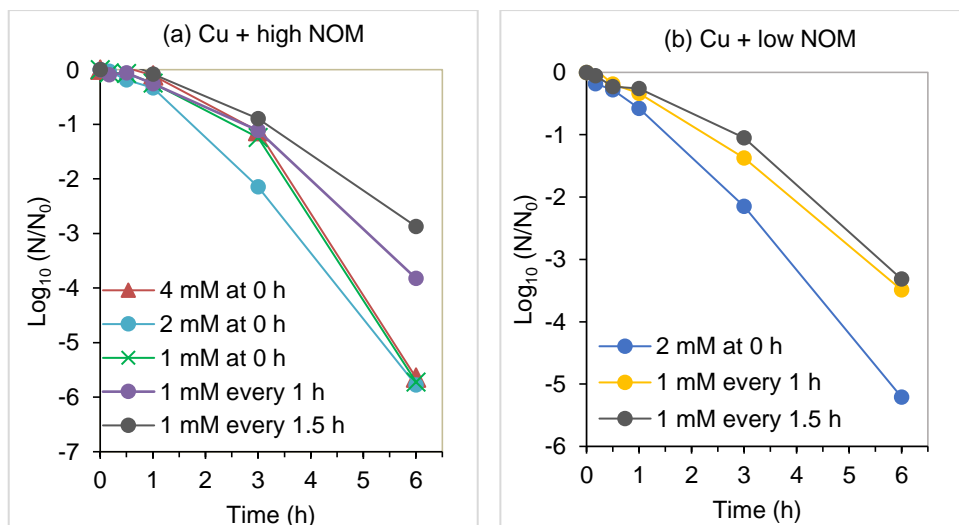
Figure 4-8 Log$_{10}$ inactivation of MS2 by Cu in (a) high NOM water (20 mg C/L) or (b) low NOM water (2 mg C/L) using different doses of tempol at different times (see legend).

As depicted in fig. 4-7, the lowest LRVs of MS2 at 6 hours were obtained when 1 mM of Tempol was added every 1.5 hours. Hence by dosing 1 mM of Tempol every

1.5 hours, MS2 is protected the most from the ROS effect. Increasing the dose or the dosage frequency didn't provide better protection but rather less.

The difference in tempol protective effect was less pronounced for PhiX 174. In fact, for high NOM, adding 1 mM of Tempol once, every 1.5 h or every 1 h had the same effect. Moreover, the difference in Log_{10} inactivation for Cu + low NOM between tempol doses was negligible.
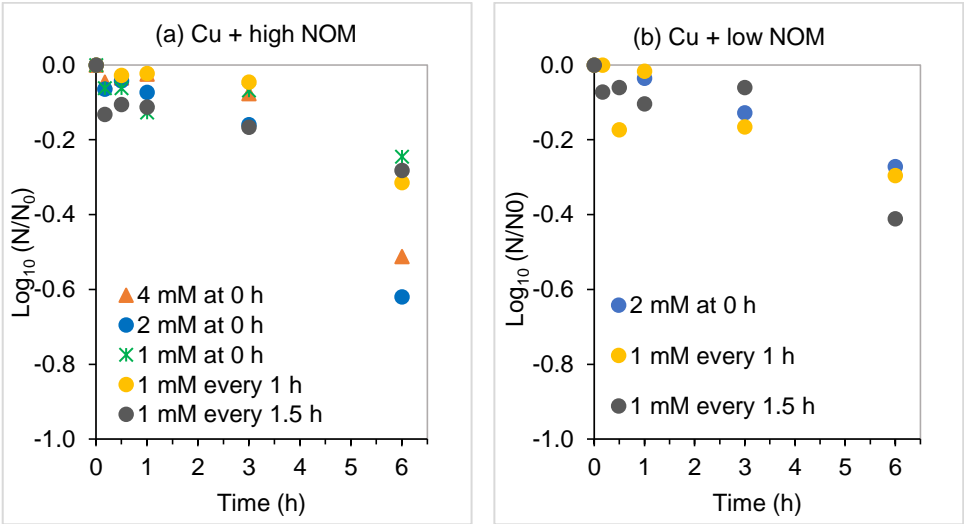
Figure 4-9 Log10 inactivation of PhiX 174 by Cu in (a) high NOM water (20 mg C/L) or (b) low NOM water (2 mg C/L) using different doses of tempol at different times (see legend).

4.6.3 Stability of MS2 and PhiX 174 in absence of metals
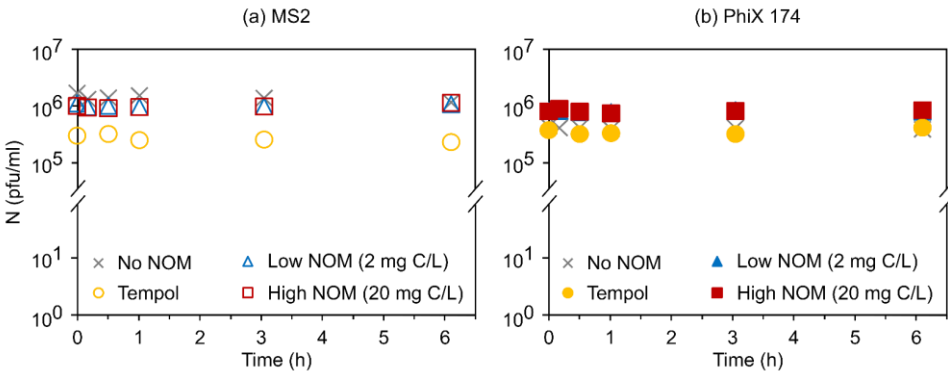
Figure 4-10 Stability of (a) MS2 and (b) PhiX 174 bacteriophage in all water matrices used (no NOM, low NOM, high NOM and with tempol).

5 COPPER AND SILVER IN CERAMIC FILTER DISCS: UTILIZING POST-TREAMENT STORAGE FOR VIRUS REMOVAL

Abstract

Ceramic pot filters are a widely used household water treatment to improve the microbial quality of water. Despite its efficiency in removing bacteria and protozoa, failure to remove viruses remains a major drawback. In the following study we investigated removal of MS2 and PhiX 174 by ceramic filter discs (CFDs) amended with metal ions; namely Cu and Ag. Both metals were applied separately by solution painting and metal leaching was determined in the effluent. Log removal values (LRV) of MS2 and PhiX 174 bacteriophage were compared in metal CFDs against blank (no metals) CFDs. Moreover, inactivation MS2 and PhiX 174 in the filter receptacles containing filtered water with leached metals was measured over 5.5 hours and compared to the blank receptacles. Cu painted CFDs had very rapid loss in Cu, reaching ≤ 0.36 mg Cu/L after 1.9 L filtered. Consequently, Cu contribution to enhancing virus removal by direct filtration was minor. However, additional inactivation of MS2 and PhiX 174 of 1.2 logs was observed over 5.5 hours of filtrate storage (containing 0.36 mg Cu/L). Meanwhile, more notable LRVs (approximately 1 log) of MS2 and PhiX 174 were observed in Ag CFDs. Additionally, inactivation in the receptacle containing 1.3 mg Ag/L reached 3.8 logs for PhiX 174 after 0.5 hour and 3 logs for MS2 after 2.5 hours. However, the concentration of Ag, 1.3 mg/L, is much higher than the recommended 0.1 mg/L maximum concentration of WHO. At a lower Ag concentration, the extent of virus inactivation may be much lower than you observed. Yet, the results of virus removal by filtration versus inactivation highlights the importance of storage time in enhancing virus removal in CPFs. It is recommended that alternative methods are needed to incorporate Cu in CPFs to improve Cu concentrations in filtrates.

5.1 Introduction

Ceramic Pot filters (CPFs) are one of the practical and sustainable household water treatment systems [51]. CPFs have many advantages such as; cheap production cost, local material and labor, simple design and manufacturing, low maintenance, easy usage etc.[14,19,24,41] The longevity of CPFs usage was reported up to 5 years efficiently treating raw water without needing replacement[51,76]. CPFs contribute to improving water quality by reducing turbidity and efficiently removing bacteria and protozoa without changing the taste or temperature of water[6,43,49,51,55,222–225].

The microbial treatment mechanism of CPFs relies on size exclusion of microbes larger than the pore size of the filter. Contaminants adsorption to the filter or entrapment in dead end pores also contributes to their removal but to less extent [47]. The majority of CPFs pores are < 20 μm but could be as small as 0.1 μm[48,49]. This allows for efficient exclusion of protozoa (10 to 200 μm) and bacteria (0.2 to 2 μm) but not viruses (0.02 to 0.1 μm)[47,51,54,55]. Although variation in CPFs pore size can result in variability of microbial performance, the more pressing issue is the complete failure to remove viruses. As indicated, the very small size of viruses allows them to pass through the filters. Hence, reported virus removal in CPFs was mostly < 0.5 log[6,55,58–60]. Meanwhile, the WHO requires a minimum of 2 logs for virus removal.

Upgrading CPFs with metals, such as silver (Ag) and recently copper (Cu) has been commonly investigated to improve microbial performance of CPFs. In fact, painting CPFs with Ag is common practice in many factories to enhance removal and disinfection of *E. coli*. However, for viruses there is uncertainty on the role Ag or Cu application to achieve increased virus removal. Reports on improved virus removal in Ag or Cu amended filters were diminished by others claiming no added efficiency[6,41,59,77,78]. One of the main issues is the lack of distinction between removal by direct filtration and time dependent inactivation by interaction of leached metals and viruses in the water of the filtrate receptacles. This distinction is important in understanding the contribution of Cu and Ag to improving virus removal. For example, *E. coli* removal in Ag amended CPFs was found to be due to time sensitive inactivation by leached Ag ions in the receptacles [6,47]. Friedman (2018)[78] observed enhancement in MS2 (model virus) removal following an overnight storage of CPFs filtrate containing leached Cu ions. Moreover, Friedman (2018) mentioned that amending CPFs with nano particles led to poor leaching of

ions compared to leaching reported by other studies applying metal in CPFs by solution painting. However, to date, application of Cu in CFDs has been only reported by Cu nanoparticles addition to the filters before the firing process. To our knowledge, applying Cu in CPFs by solution painting, as done for Ag, has not been reported.

Therefore, we manufactured ceramic filter discs (CFDs) in Nicaragua using the local production procedure for CPFs. The manufactured CFDs were painted with Ag solution or Cu solution and the ions leaching was quantified in the filtrate. CFDs were challenged with water containing two conservative model viruses; MS2 (ssRNA) and PhiX 174 (ssDNA), to test virus removal. The testing was conducted on blank CFDs then the same blank painted with Cu or Ag and re-examined for virus retention and filtrate viruses. Hence, the same CFD was used as its own control. Virus removal was measured in samples directly collected from the filter (removal by direct filtration) and in post treatment filtrate stored for an additional 5.5 hours (time sensitive virus inactivation).

5.2 Materials and Methods

5.2.1 Ceramic filter discs production and characterization

CFDs were manufactured in the Filtron factory, Nicaragua, following the local procedure. In brief, 16 liters of water, 63.5 kg of clay and 7.7 kg of sieved saw dust (sieved through a size 7 metal mesh; 3 mm) were mechanically mixed for 45 minutes. The mixture was molded by hand into a compact cube before pressing it into a pot shape. The pots were left to rest for 2 days then refined (trimmed and cleaned up) by hand. At this point the CFDs were cut out of CPFs and left to dry in the shade until the surface reaches air temperature (26 °C; Extech remote IR thermometer scan). The CFDs were arranged inside full pots and fired at 870 °C with a ramp rate 1.8 °C/min and dwell time 1 hour.

Equation 1

$$\text{Porosity (\%)} = \frac{W_s - W_d}{V_f \rho_w} * 100$$

Where W_s is saturated weight (g), W_d dry weight (g), V_f total volume of CFD (m^3) and ρ_w is water density (1 g/m^3).

The produced CFDs (Ø 125 mm) were inspected visually for cracks, followed by a porosity check using dry weight vs saturated weight (**Equation** 1). The saturated weight was measured after submerging CFDs in MilliQ water over night. The pore volume (PV) of the CFDs was estimated as the difference between Ws and Wd for each unit. The value is considered an overestimation because dead-end pores can contribute to the water weight but not to the permeability of the CFD.

5.2.2 Metal application and leaching

Four CFDs labelled F1, F2, F3 and F4 were selected based on their similarity in flow rate. F1 and F2 were painted with Cu solution while F3 and F4 with Ag. After the first virus challenge on blank CFDs, Cu and Ag were applied by painting. Hence, each filter served as its own control. Cu and Ag were applied only to the bottom of the CDFs using a metal-soaked brush. A volume of 20 mL of 0.01 M silver nitrate or 0.1 M copper sulphate were applied to the corresponding CFD. The coating was left to dry overnight at 35 °C.

Prior to metal painting, CFDs were flushed with 1 mM sodium phosphate (PB) buffer (0.58 mM $NaH_2PO_4.H_2O$ and 0.42 Mm $Na_2HPO_4.7H_2O$; pH 7). Effluent samples were analyzed using ICP-OES to evaluate additional ions leaching from CFDs and possible presence of metals in blank filters. After painting CFDs with Cu or Ag, filters were loaded with PB buffer and effluent samples were analyzed for Cu or Ag leaching, as well as, additional ions. The water matrix was also simulated using CHEAQS chemical model to evaluate possible complexation of Ag and Cu.

5.2.3 Testing of virus removal in CFDs

5.2.3.1 Tracer test

Salt tracer test aimed to understand water transport through CFDs. It accounts for the complex dynamic of CFDs pores to identify the amount of filtrate to collect before full intrusion of salt occurs. CFDs were fixed with silicon in the bottom of a pipe as described by Soliman et al. (2020)[226]. Sodium chloride (NaCl) solution was used as conservative tracer (0.36 g/L NaCl solution in MilliQ water). The tracer solution conductivity (C_0) was 1564 µS/cm, measured using a multimeter (Sen Tix 41-3). Each CFD was loaded with 4 L of tracer solution and conductivity was measured in effluent samples (C). Filtrate was collected until 1564 µS/cm was

achieved then the solution was replaced with MilliQ water. The tracer test was used to estimate the amount of water to be discarded (referred to as the first flush) before collecting samples to calculate virus removal.

5.2.3.2   Virus challenge test

Preparation of MS2 and PhiX 174 stock was done as described in Soliman et al. (2020)[200]. Test water was prepared by adding MS2 and PhiX 174 to PB buffer at a final concentration of 10^5 to 10^6 pfu/ml. Samples were taken from test water directly before adding it on top of CFDs to measure concentration at time 0 (N_0). Each CFD was loaded with 4 L of test water (PB buffer + MS2 and PhiX 174) and water was left to flow by gravity. The first 1.5 hours of effluent was discarded (first flush). Then a sterile glass beaker was introduced as receptacle to collect the filtrate. This point is the start of collecting samples for virus removal by direct filtration. At the same time, samples from water on top of CFDs were also collected to ensure influent water stability of virus concentration. The effluent was collected for half hour, sampled, and then the receptacle was moved away from the filter to store the water in the dark at 25 °C for an additional 5.5 hours. The latter aimed to study time depended inactivation in the receptacles. Log removal values (LRVs) were calculated as Log_{10} (N_t/N_0) where N_t is the concentration at time t. It should be noticed that LRVs for stored filtrate were calculated as Log_{10} ($N_t/N_{0.5}$), where $N_{0.5}$ is the concentration of the effluent at time 0.5 h after discarding the first flush. To analyze inactivation kinetics, linear regression analysis was conducted with 95% confidence interval to calculate the slope of Ln ($N_t/N_{0.5}$) versus time, known as the first order inactivation rate constant: K_{obs} (h^{-1}). Effluent samples were also analyzed using ICP-OES to measure Cu and Ag concentrations at the time of virus testing.

5.3   Results and discussion

5.3.1   CFD characterization

The calculation of CFDs pore volume (PV) provided a common metric to compare between CFDs by incorporating the hydraulic quality of the filters. PVs of CFDs were calculated based on the weight of water retained in each CFD as described in Soliman et al. (2020)[226], thereby accounting for open active pores inside the filter. Using wet weight vs dry weight to calculate PV can result in overestimation of the active pores due to the inclusion of water weight in dead-end pores. However, we

use this method due to its simplicity which makes it reproducible by local partners without requiring complicated or expensive equipment.

Table 5-1 Hydraulic properties of CFDs quantified using Ws vs Wd. F(n) refers to the filter number

CFD	F1	F2	F3	F4
PV	69	76	67	70
Porosity (%)	38	37	35	34
Flow rate (ml/min)	6.7	5.8	4.8	3.5

The measured the PV of CFDs ranged from 67 ml to 76 ml (**Table**. 5-1). The porosity of each CFD was calculated by factoring in the volume of each CFD. The calculated porosity was between 34-38 % of the total CFDs volume. These values are lower than reported porosity of CPFs by Oyanedel-Craver and Smith (2008)[227]. Hence, the CFDs used in this study might be relatively slower than other filters. The recorded flow rates, 3.5 to 6.7 ml/min, were also for a relatively slow CFDs. However, the observed variation in flow dynamics of CPFs overall makes the CFDs used in this study acceptable and representative of actual filters.

5.3.2   **Metal application and leaching**
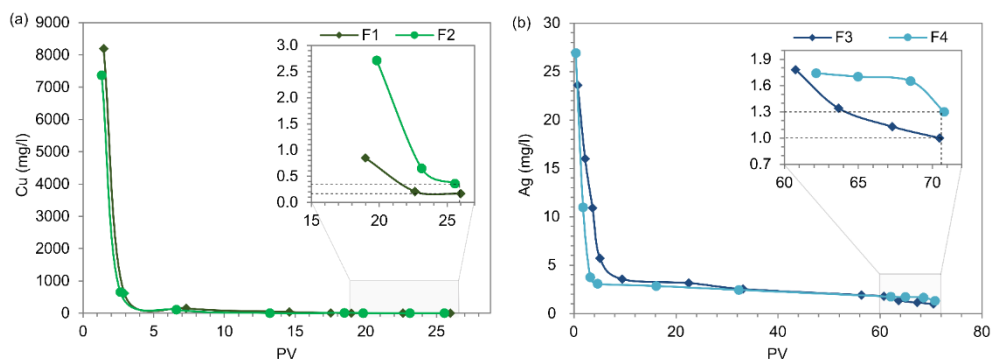
Figure 5-1 Leaching of Cu (a) and Ag (b) from CFDs loaded with PB buffer (pH =7). The magnification in (a) shows concentrations of Cu dropping after filtering 18 and 25 PVs. Similarly, the magnified part in (b) shows the decline in Ag concentration after filtering between 60 and 70 PVs

To evaluate the sustainability of impregnating CPFs with Cu and Ag, duplicate CFDs were painted with $CuSO_4$ or $AgNO_3$ solutions. Following 24 – 48 h of drying, CFDs were loaded with PB buffer and samples collected for Cu and Ag measurements in

the effluent. The optimal goal was to achieve a stable concentration of $1 - 2$ mg Cu/L and 0.1 mg Ag/L in the effluent.

As depicted in **Fig.** 5-1a, severe leaching of Cu was observed in the first few PVs. Almost 9,000 mg/L of Cu leached directly in the filtered water. This was reduced by 90% after only 2 PVs (< 160 ml effluent) where Cu concentration in the effluent reached 637 ± 17 mg Cu/L. The concentration of Cu continued to drop reaching 0.17 mg/L; F1 and 0.36 mg/L; F2 after only 25 PVs (approximately 1.9 L). These concentrations are much lower than the targeted WHO guideline of 1 mg/l. They also show that painting CFDs with Cu solution is wasteful, 99.998% of painted Cu was flushed in the effluent after only filtering 1.9 L. This proves that paining CFDs with Cu is not a sustainable nor economical method to impregnate CFDs with Cu. Moreover, it is unsafe for consumers to ingest water with such high concentrations of Cu in a short time period.

The initial leached concentrations of Ag were 25 ± 2 mg Ag/ L, significantly lower than Cu values (**Fig**. 5-1). The filtration of 5 equivalent PVs reduced initial leaching by 90%. Later, Ag continued to leach slower in the effluent. After 70 PVs (5 L), Ag concentrations reached 1 mg/l in the effluent of F3 and 1.3 mg/l in the effluent of F4. At this point Ag concentration were higher than the WHO guideline of 0.1 mg/l. The initial rapid leaching is common in newly painted filters and was previously reported by Mittelman et al. (2015) [227]. Then, as more water is filtered, silver leaching declines to a lower but stable concentration with continued filter use. Unfortunately, this experimental work did not extend to reach the low stable concentrations of metal leaching.

In practice, CPF manufactures, such as Filtron in Nicaragua, tend to apply Ag through solution painting as done in this study. Mittelman et al. (2015)[227] evaluated dissolution of Ag^+ from CFDs by $AgNO_3$ painting, and reported that applying Ag to the bottom side of CFDs is responsible for dissolution and leaching of Ag. The author also reported on a fast initial leaching of Ag, followed by slower and more steady leaching, like the observations in our study.

5.3.3 Implications of CFD's Cu and Ag painting on virus removal

5.3.3.1 Tracer test and samples collection
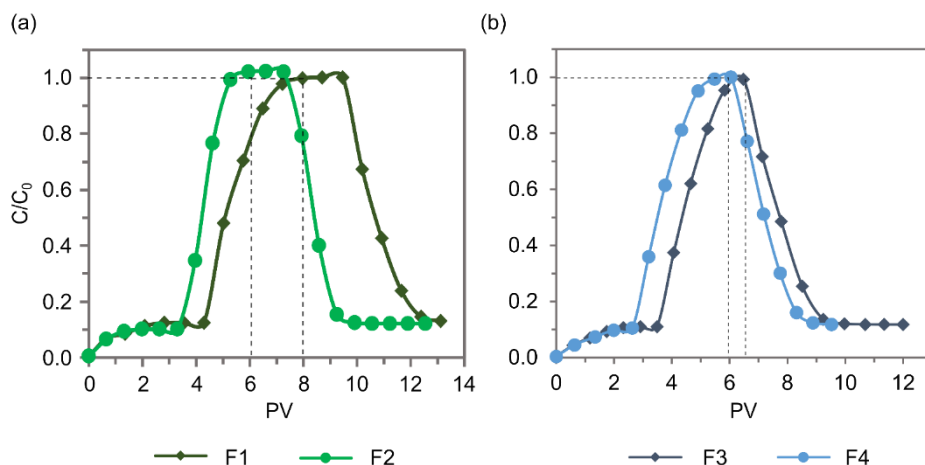
Figure 5-2 Conservative salt (NaCl) tracer test breakthrough curves

Even though the calculated PVs provide over estimation of active pores, reaching full salt intrusion required a minimum of 6 PVs (**Fig**. 5-2). This is not unusual considering the diversity in size and structure of CPFs pores which results in heterogeneous flow speed through the pores[50,116]. Hence, before collecting filtered samples for microbial analyses from CFDs, enough water was discarded to ensure that the pores are filled with test water. To that end, a minimum of 7 PV was considered as the first flush and discarded. Based on PVs and flow rates shown in **Table** 5-1, discarding 1.5 hours of filtrate would provide >7 PVs. Following the first flush, collected samples were enumerated for MS2 or PhiX 174 to evaluate their concentrations and removals.

5.3.3.2 Virus removal by filtration

To evaluate the contribution of metal paint on enhancing the virus removal in CFDs, after discarding the first flush, filtered water was enumerated for MS2 and PhiX 174. Samples obtained directly from the filters in the first 10 minutes were analyzed for virus removal by direct filtration. The remaining water collected was stored away from the filter in the dark at 25 °C, sampled periodically and analyzed for virus concentration and inactivation.

Table 5-2 LRVs of MS2 and PhiX 174 due to filtration through blank and Cu coated CFDs, F1 0.17 mg Cu/L and F2 0.36 mg Cu/L. The concentration of Cu mentioned refers to the Cu values in the analysed liquid samples

	MS2		PhiX 174	
LRV	F1	F2	F1	F2
Blank LRV	0.08	0.1	0.03	0.02
Cu LRV	0.1	0.2	0.3	0.7

Negligible removal of MS2 and PhiX 174 was observed in blank filters **(Table** 5-2), similar to most reports of other studies [6,55,58–60]. Presence of Cu in CFDs hardly improved LRVs of MS2. Although an improvement in LRVs of PhiX 174 was observed, it remained < 1 log. Friedman (2018)[78] also reported no improvement on MS2 removal by Cu amended CFDs. Lucier et al. (2017) also reported similarity in MS2 LRVs by blank and Cu amended CPFs. However, the values reported by Lucier were considerably higher (3 LRVs) than values observed in this study and Friedman's.

Table 5-3 LRVs of MS2 and PhiX 174 due to filtration through blank and Ag coated CFDs, F3 1 mg Ag/L and F4 1.3 mg Ag/L. The concentration of Ag mentioned refers to the Ag values in the analysed liquid samples

	MS2		PhiX 174	
LRV	F3	F4	F3	F4
Blank LRV	0.1	0.1	0.1	0.1
Ag LRV	0.8	0.9	1	1

In case of Ag painted CFDs, improvement of 0.9± 0.1 LRVs of MS2 and PhiX 174 was observed compared to blank CFDs (**Table** 5-3). This improvement might be due to enhanced adsorption of viruses to CFDs, inactivation or a combination of both processes. Presence of positively charged Ag^+ ions can increase virus adsorption capacity to electrostatically attract negatively charged viruses. But because Cu was also positively charged, rapid inactivation of Ag is more likely. Soliman et al. (2020)[200] reported average inactivation of MS2 and PhiX 174 of 1 LRV following 0.5-hour of interaction with 0.5 mg/L of Ag. Considering the higher concentration of Ag measured in F3 and F4 effluents, it is possible that rapid inactivation occurred during the 10- 15 minutes of interaction. Although other studies reported no improvement in MS2 LRVs from Ag amended CPFs[6,41], the removal observed in this study can be due to the relatively high concentration of Ag.

5.3.3.3 Virus inactivation in the stored filtrate by leached ions

Over the 5.5 hours of storage, no inactivation was observed in the filtrate of blank CFDs. In the filtrate of the metal-coated CFDs inactivation of MS2 and PhiX 174 was observed and followed first order Chick Watson kinetics. For the filtrate of Cu-coated CFD, a dose response was observed for both phages. In the presence of 0.17 mg Cu/L, slightly faster inactivation of MS2 (K_{obs}= 0.32 h^{-1}, 0.8 logs over 5.5 h) occurred than for PhiX 174 (K_{obs}= 0.27 h^{-1}, 0.6 logs over 5.5 h) (**Fig**. 5-3). Faster inactivation was observed in the receptacles containing 0.36 mg Cu/L of MS2 (K_{obs}= 0.46 h^{-1}, 1.1 logs over 5.5 h) and PhiX 174 (K_{obs}= 0.53 h^{-1}, 1.3 logs over 5.5 h). Although improved, neither reached the required removal of 3 logs by the WHO to qualify as a protective household water treatment. Other studies have also reported sensitivity of virus inactivation rate to Cu dosage [97,163].
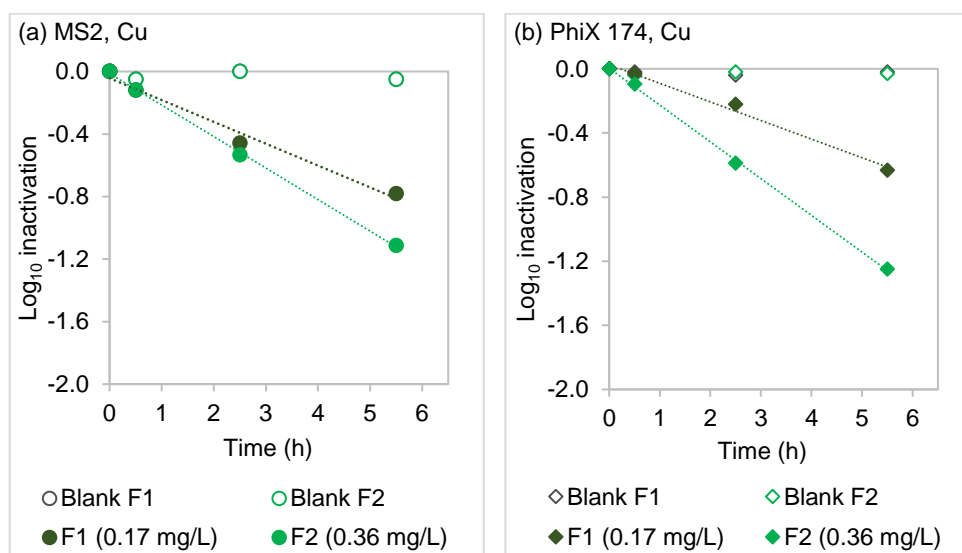
Figure 5-3. Log$_{10}$ inactivation of (a) MS2 and (b) PhiX 174 in stored filtrate of blank and Cu painted CFDs (pH= 7, T=25°C and dark conditions). Values indicated next to the filter name (F$_n$) refer to Cu concentration measured from the stored water.

The measured TOC in the filtrate was approximately 2 mg C/L (supplementary **Table** 5-4), hence in the same range as the low natural organic matter (NOM) experiments in the previous chapter. In the previous chapter, MS2 was significantly more sensitive to Cu (1 mg/L) than PhiX 174. Here, PhiX 174 showed similar sensitivity to Cu as MS2. The comparison between K_{obs} in this chapter and in chapter 4, showed

that K_{obs} of PhiX 174 is relatively higher than expected (supplementary **Table** 5-5). However, for MS2, lower K_{obs} corresponded to lower Cu concentration.

The available data does not provide a direct explanation for higher inactivation of PhiX 174 observed here. One difference from the water matrix used in Chapter 4, is the high concentrations of silica leached from CFDs in the filtrate (supplementary **Table** 5-4) which can affect the chemical speciation of Cu^{228}. However, this remains speculative and cannot be confirmed through available measurements.
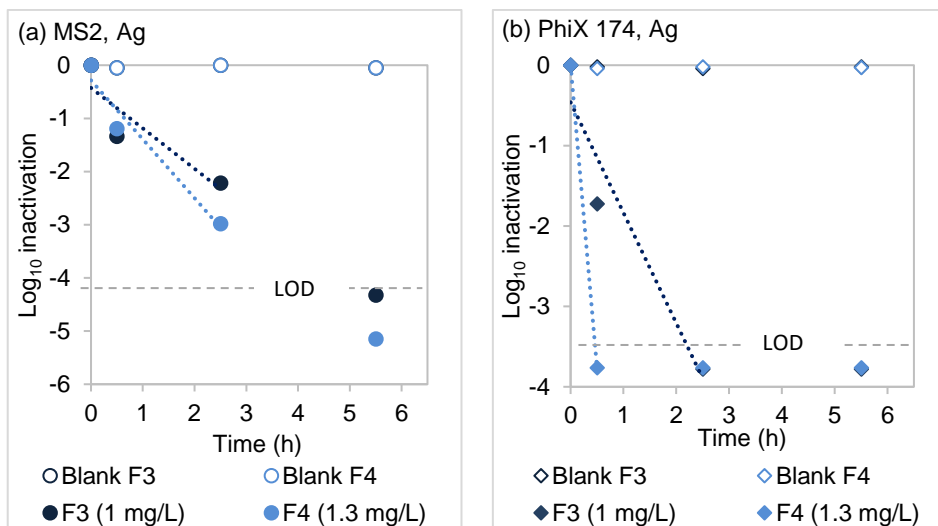
Figure 5-4 Log_{10} inactivation of (a) MS2 and (b) PhiX 174 in stored filtrate of blank and Ag painted CFDs (pH= 7, T= 25°C and dark conditions). Values indicated next to the filter name (F_n) refer to Cu concentration measured from the stored water. Limit of detection (LOD) was 1 pfu/ml.

For the filtrate of the Ag-coated CFDs, K_{obs} was calculated based on only a few data points (1-2), hence they should be considered only as indicative and not definitive. As depicted in (**Fig**. 5-4), faster Ag inactivation was observed for PhiX 174 than MS2. For F4 (1.3 mg Ag/L), after 2.5 hours, MS2 was inactivated by 3 logs (K_{obs} = 1.75 h^{-1}). However, PhiX 174 reduction exceeded 3.8 Logs (K_{obs} = 2.55 h^{-1}) after 0.5-hour storage time of F4 filtrate.

The comparison between log inactivation in the stored receptacles (with Ag) and LRVs by direct filtration highlighted the value of contact time between metals and viruses. Although Ag concentrations are higher than applicable safe drinking water conditions, the results shed the light on the role storage time plays in enhancing inactivation kinetics of MS2 and PhiX 174 by leached ions. Moreover, it should be

considered that initial adsorption values of viruses (LRVs by direct filtration) are expected to decline with time due to saturation. Hence, aiming for inactivation in the receptacles has more long-term impact than removal by attachment to the filter.

Overall, development of a post treatment method to steadily leach Cu or Ag ions in CPFs receptacles would further utilize metals applied to increase virus inactivation. Future research is needed to develop and examine the sustainability of Cu and Ag application in CPF's receptacles. Moreover, future studies should investigate the inactivation kinetics of RNA and DNA viruses using more representative water matrices.

5.4 Conclusions

- The extensive disinfection of MS2 and PhiX 174 attributed to leached ions and extended retention time in the filtered water receptacle suggests a great potential for improving safe storage of filtered water by Cu and Ag ions.
- Cu application in CFDs had minor contribution to enhancing virus removal by direct filtration compared to inactivation of viruses in the stored filtered water containing leached Cu ions.
- The high Cu and Ag concentrations measured in filtered water, especially within the first 5 PVs shows the poor retention of metals in CFDs using painting as the application method.
- Applying metals, especially Cu, by painting is costly and unsustainable because it leaches out rapidly once the filter is used.
- Although Ag enhanced LRVs by direct filtration, the high concentration of Ag in the filtrate calls for further examination with concentrations in compliance with the WHO drinking water guidelines.

5.5 SUPPLEMENTARY

Table 5-4 Full ions measurement in the stored filtrate of CFDs

mg/ L	Cu	Ag	K	Na	Cl	PO_4	SO_4	Si	K	Ca	TOC*
F1	0.17	-	0.40	42.3	0.33	83.88	0.16	40.33	0.40	0.1	2.1
F2	0.36	-	0.34	35.6	0.36	80.59	1.35	70.77	0.34	-	2.4
F3	-	1	0.36	47.6	0.4	86.6	0.11	39.3	0.36	0.66	2.3
F4	-	1.3	0.46	47.6	0.3	89	0.07	44.7	0.49	1.18	2.1

* TOC was measured in the filtrate prior to the challenge test with bacteriophages. Unfortunately, measurements of TOC of the stored filtrate are unavailable. However, we assumed it to be the same leached organics as during the challenge test.

Table 5-5 Inactivation rate constant (K_{obs}, h^{-1}) of MS2 and PhiX 174 by different Cu concentrations in water with 2 mg C/L.

Cu (mg/L)	0.17	0.36	1
MS2; K_{obs} (h^{-1})	0.32	0.46	2.3
PhiX 174; K_{obs} (h^{-1})	0.27	0.53	0.29

6 GENERAL DISCUSSION, CONCLUSIONS AND FUTURE RESEARCH

The development of HHWT had greatly contributed to reducing the global burden of waterborne disease[24–31]. CPFs were reported to be one of the most sustainable, promising, and protective HHWT technologies. There are multiple aspects that made CPFs popular and widely used. Their low cost, simple operation requirements (filling with water), simple maintenance (scrub with hand brush), accessible supply chain due to local production and long-term usage (unless broken, it can be used for years). Although the recommended lifespan of CPFs is around 2 years, filters can be in use for as long as 7 years, based on our experience in the field (**Fig**. 6-1).

Figure 6-1 Left: CPF aged 7 years in use in a restaurant in Saint louis, middle and right are CPFs in use in consumer houses in Nicaragua (2018)

Despite the advantages of CPFs, failure to remove viruses remains a major drawback. Therefore, enhancing virus removal in CPFs was the focus of this thesis work.

6.1 Biofilms

Through simulating user conditions by continuously using the filter, it was found that over time biofilms grow inside the filter. The growth of biofilms in CFDs enhanced virus removal, as observed for MS2 bacteriophages. Nutrient levels in water- high (HN), medium (MN) or low (LN)- had direct impact on the amount of biofilm and more biofilm resulted in higher LRV of MS2. After 5 operational weeks, MS2 LRVs in CFDs ranged between: 0.9 ± 0.2 for LN, 1.6 ± 0.2 LRV for MN and 2.4 ± 0.5 LRV for HN biofilms. Although biofilms contributed to improvement in MS2 LRVs, it came at a cost of reduced flow rate. Cleaning the filters restored flow rate to some extent, but led to a loss in MS2 LRVs due to the removal of the grown biofilm.

Only CFDs with HN grown biofilm achieved MS2 LRVs that qualify as WHO protective (≥ 2 LRV). However, HN CFDs had extremely low flow rates, making the filters unusable for consumers. In contrast, filters receiving LN or MN water would be usable in terms of flow rate, but won't provide enough protection from waterborne viruses even after biofilm growth.

Hence, consumers delaying filter cleaning will benefit from increased virus protection, but not significant enough for biofilm-grown systems to qualify as WHO protective under applied conditions. Furthermore, filters must be cleaned eventually, resulting in a loss of LRV. Hence, biofilm growth in CPFs cannot be advised as the (sole) method to enhance virus removal in CPFs due to its temporary protection and variable extent of growth depending on water quality, and low LRVs.

6.2   Cu and Ag

Experiments showed that the combination of Cu and Ag is very efficient for the inactivation of both RNA and DNA viruses, as shown for MS2 and PhiX 174. The highlight of the metal-ion examinations was the observed synergy of the Cu and Ag combination, and the interaction with NOM. Synergy of Cu and Ag was observed for PhiX 174 when water contained low (2 mg C/L) or high NOM (20 mg C/L). For MS2, when water contained low or no NOM, the synergy was mainly attributable to NOM in water and secondarily to water pH. For MS2, in water without NOM, synergy was observed only at pH ≥7. In water without NOM, no synergy of Cu and Ag was observed for PhiX 174, regardless of the pH.

Depending on the water source, NOM content would vary. Ground water typically has low NOM (≤3 mg C/L)[229,230]. Fresh surface water can have NOM between 0.1 to 20 mg C/L or more, depending on its level of contamination[115,229,230].   Hence presence of low or high NOM can be anticipated in source waters of ceramic filters, and it is unlikely that filtration through the ceramic filters would completely remove the NOM[231,232]. Hence, the filtrates of ceramic filters (or similar HHWT filtration processes) are expected to contain low levels of NOM. In the low NOM water, the combination of Cu and Ag reached the highly protective WHO requirements (≥ 4 logs) over 3 hours for both MS2 and PhiX 174. In the high NOM water matrix, PhiX 174 reached the WHO highly protective (≥ 4 logs) and MS2 the WHO protective (> 2 logs) inactivation over 3 hours. Hence, usage of Cu (1 mg/L) and Ag (0.1 mg/L) in

combination would be advised, along with low NOM water to benefit from the added synergy of Cu and Ag in combination to inactivate both DNA and RNA viruses.

Although application of Ag in CPFs improved virus removal by direct filtration, LRVs observed were ≤ 1 log. Ag was only a potent disinfectant as free ionic Ag^+ at water pH ≥ 7. Ag^+ binding to NOM resulted in slower inactivation of MS2 and PhiX 174. Hence, presence of NOM or other ions in water, such as Cl or S, which binds Ag^+ would further reduce its antiviral efficiency [90–93,215–217]. Moreover, the observed virus inactivation kinetics by Ag (0.1 mg/L) were relatively slow, unless higher concentrations of Ag were used. But, exceeding an Ag concentration of 0.1 mg/L of is not advised by WHO due to the associated health hazards such as Argyria disease [13,233]. Overall, it can be concluded that relying on Ag alone to provide protection from waterborne viruses would not lead to sufficient protection at concentration levels below 0.1 mg Ag/L.

Cu ions were found to bind to NOM in water as well. However, this binding led to production of ROS which accelerated the inactivation of MS2 and PhiX 174. In fact, inactivation of MS2 by Cu in water with 20 mg C/L NOM was the highest LRV (higher than Cu and Ag as well). However, Cu alone provided slower inactivation than Cu and Ag combination for MS2 in low NOM water and water without NOM. Cu alone was also inert towards PhiX 174, in water without NOM, and provided slower inactivation than Cu and Ag combination in water with low or high NOM. Hence, in all studied scenarios except one, the synergy of Cu and Ag led to a faster inactivation of MS2 and PhiX 174 than Cu alone. Moreover, the addition of Cu to CPFs had negligible impact on LRVs of MS2 and PhiX 174 by direct filtration.

Nonetheless, application of Cu in CPFs by painting resulted in rapid leaching of Cu into the filtered water. As a result, initial filtrate contained very high concentrations of Cu which diminished rapidly after filtering a few liters of water. Jackson et al. (2019)[234] applied Cu to CPFs by mixing $Cu(NO_3)_2$ with clay prior to the pots firing. This resulted in consistent release of Cu ions in the filtrate but with lower concentrations (10 µg Cu/L) than desired (1 mg Cu/L). Similarly, Jackson et al. (2019)[234] reported that mixing $AgNO_3$ with clay prior to firing resulted in more sustainable and slow release of Ag compared to painting with Ag solution. However, this method of application resulted into the formation of Cu or Ag nanoparticles[234] which might leach in the filtrate. Hence, the optimal method of Cu and Ag application in CPFs needs further investigation.

Overall, application of Cu and Ag in combination is recommended to provide protection from waterborne viruses. Application method of Cu and Ag to the filters should allow for long contact time (> 3 hours) to ensure effective inactivation of waterborne DNA and RNA viruses. The application of Cu and Ag can also be expanded to other systems which allows for long contact time such as rain water harvesting tanks or safe water storage units.

Finally, since the presence of NOM in water is to be expected, biofilm growth in CPFs is inevitable. Biofilm growth can provide some additional protection against waterborne viruses. However, it shouldn't be prioritized over the usability of the filter (i.e., allowing for acceptable flow rate).

6.3 Future research

The work presented in this thesis has highlighted the role Cu and Ag ions could play in providing consumers with protection from waterborne DNA and RNA viruses. Leaching of Cu and/or Ag from CPFs should be investigated in long term studies allowing to pass the initial stage of rapid metal leaching to reach a low but stable metal concentration in water. Then, determine how much it might add to virus inactivation in filtered water that is stored over time. Leaching of Cu and Ag from CPFs should be investigated for consistency of metal ions release and it's associated virus removal/ inactivation.

Alternatively, the development of a simple approach to incorporate Cu and Ag in the receptacles of CPFs could allow for new methods of metal application as a post-treatment option independently. For example, through electrochemical dosing where the dosing can be controlled through phone as demonstrated by Zhou et al. (2020)[235]. This can allow for Cu and Ag application in other HHWT filters or systems. It is important to provide an inexpensive and simple application system with sustainable slow release for long term applications.

Moreover, building on the findings presented here, future research should investigate the impact of ionic strength, composition of organics, and other ions (such as Cl or S) on virus inactivation kinetics by Cu and Ag. Presence of Cl ions can reduce the antiviral efficiency of Ag due to the loss in free Ag^+ ions and formation of $AgCl_2$ solids. In case of Cu, presence of Cl ions has been shown by Xing et al. (2020)[210] to change ionic strength of water and thereby impact Cu binding to organics and production of ROS. Hence, it is important to examine the antiviral

efficiency of Cu and Ag in presence of other ions. This would increase the current understanding of factors impacting Cu and Ag antiviral efficiency and help expand their application to community scale or more centralized systems for water treatment.

Finally, it is important to evaluate possible health risks associated with biofilm growth in CPFs. Biofilms can provide protection and breeding ground for harmful pathogenic organisms[67,124,125]. In our study, we observed biofilm growth on the inner side of CFDs (in contact with untreated water) and not on the outer side of the filter (in contact with treated water). Hence it is possible that CPFs would provide microbially clean water with improved virus LRVs in the presence of biofilms. Yet, it is important to have dedicated field studies for risk assessment of biofilm growth in CPFs. This observation is not only limited to CPFs but extends to other HHWT technologies, especially other single stage treatment units.

7 REFERENCES

1.   WHO. *Progress on Household Drinking-Water, Sanitation and Hygiene: Five Years into the SDGs*.; 2021. www.who.int/publications/i/item/progress-on-household-drinking-water-sanitation-and-hygiene-five-years-into-the-sdgs.

2.   WHO. *Combating Waterborne Disease at the Household Level: The International Network to Promote Household Water Treatment and Safe Storage*. World Health Organization; 2007.

3.   Hunter PR. Household Water Treatment in Developing Countries: Comparing Different Intervention Types Using Meta-Regression. *Environ Sci Technol*. 2009;43(23):8991-8997. doi:10.1021/es9028217

4.   Sobsey MD, Stauber CE, Casanova LM, Brown JM, Elliott MA. Point of use household drinking water filtration: a practical, effective solution for providing sustained access to safe drinking water in the developing world. *Environ Sci Technol*. 2008;42(12):4261-4267.

5.   Goswami KP, Pugazhenthi G. Credibility of polymeric and ceramic membrane filtration in the removal of bacteria and virus from water: A review. *J Environ Manage*. 2020;268:110583. doi:10.1016/j.jenvman.2020.110583

6.   Van der Laan H, van Halem D, Smeets PWMH, et al. Bacteria and virus removal effectiveness of ceramic pot filters with different silver applications in a long term experiment. *Water Res*. 2014;51:47-54. doi:10.1016/j.watres.2013.11.010

7.   UN General 2010. Resolution 64/292: The human right to water and sanitation. *64th Sess Available http//www un org/es/comun/docs*. 2010.

8.   Unicef, Organization WH. *Progress on Drinking Water, Sanitation and Hygiene in School: Special Focus on COVID-19*. UNICEF; 2020.

9.   Organization WH. Progress on drinking water, sanitation and hygiene: 2017

update and SDG baselines. 2017.

10. Fong T-T, Lipp EK. Enteric viruses of humans and animals in aquatic environments: health risks, detection, and potential water quality assessment tools. *Microbiol Mol Biol Rev*. 2005;69(2):357-371.

11. WHO. Global networks for surveillance of rotavirus gastroenteritis, 2001-2008. *Wkly Epidemiol Rec Relev épidémiologique Hebd*. 2008;83(47):421-425.

12. WHO. *Safer Water, Better Health*. World Health Organization; 2019.

13. WHO. *Guidelines for Drinking-Water Quality: Fourth Edition Incorporating the First Addendumitle*.; 2017. www.who.int/publications/i/item/9789241549950.

14. Guerrant DI, Moore SF, Lima AA, Patrick PD, Schorling JB, Guerrant RL. Association of early childhood diarrhoea and cryptosporidiosis with impaired physical fitness and cognitive function four-seven years later in a poor urban community in northeast Brazil. *Am J Trop Med Hyg*. 1999;61(5):707-713.

15. Berkman DS, Lescano AG, Gilman RH, Lopez SL, Black MM. Effects of stunting, diarrhoeal disease, and parasitic infection during infancy on cognition in late childhood: a follow-up study. *Lancet (London, England)*. 2002;359(9306):564-571. doi:10.1016/S0140-6736(02)07744-9

16. CDC. Diarrhea : Common Illness , Global Killer. *Centers Dis Control Prev*. 2012:1-4.

17. Adelodun B, Ajibade FO, Ighalo JO, et al. Assessment of socioeconomic inequality based on virus-contaminated water usage in developing countries: A review. *Environ Res*. 2021;192:110309. doi:10.1016/j.envres.2020.110309

18. Hutton G, Haller L, Water S, Organization WH. *Evaluation of the Costs and Benefits of Water and Sanitation Improvements at the Global Level*. World Health Organization; 2004.

19. Richardson V, Hernandez-Pichardo J, Quintanar-Solares M, et al. Effect of Rotavirus Vaccination on Death from Childhood Diarrhea in Mexico. *N Engl J Med*. 2010;362(4):299-305. doi:10.1056/NEJMoa0905211

20. Esrey SA, Potash JB, Roberts L, Shiff C. Effects of improved water supply and sanitation on ascariasis, diarrhoea, dracunculiasis, hookworm infection,

schistosomiasis, and trachoma. *Bull World Health Organ*. 1991;69(5):609-621. http://www.ncbi.nlm.nih.gov/pmc/articles/PMC2393264/.

21. Machdar E, van der Steen NP, Raschid-Sally L, Lens PNL. Application of Quantitative Microbial Risk Assessment to analyze the public health risk from poor drinking water quality in a low income area in Accra, Ghana. *Sci Total Environ*. 2013;449:134-142. doi:10.1016/j.scitotenv.2013.01.048

22. Edition F. Guidelines for Drinking-water Quality. *World Health*. 2011;1(3):104-108. doi:10.1016/S1462-0758(00)00006-6

23. Mellor J, Smith J, Samie A, Dillingham R a. Coliform Sources and Mechanisms for Regrowth in Household Drinking Water in Limpopo, South Africa. *J Environ Eng*. 2013;139(September):1152-1161. doi:10.1061/(ASCE)EE.1943-7870

24. Mack A, Choffnes ER. *Global Issues in Water, Sanitation, and Health:: Workshop Summary*. National Academies Press; 2009. http://www.ncbi.nlm.nih.gov/books/NBK28455/.

25. Mintz ED, Reiff FM, Tauxe R V. Safe water treatment and storage in the home: a practical new strategy to prevent waterborne disease. *Jama*. 1995;273(12):948-953.

26. Clasen T, Roberts I, Rabie T, Schmidt W, Cairncross S. Interventions to improve water quality for preventing diarrhoea. *Cochrane Database Syst Rev*. 2006;3.

27. Clasen T, Schmidt W-P, Rabie T, Roberts I, Cairncross S. Interventions to improve water quality for preventing diarrhoea: systematic review and meta-analysis. *Bmj*. 2007;334(7597):782.

28. Wright J, Gundry S, Conroy R. Household drinking water in developing countries: a systematic review of microbiological contamination between source and point-of-use. *Trop Med Int Heal*. 2004;9(1):106-117.

29. WASH SSINU. UNICEF. 2008.

30. Green V. Household water treatment and safe storage options for northern region ghana: consumer prefernce and relative cost. 2008.

31. Wright J, Gundry S, Conroy R. Household drinking water in developing countries: a systematic review of microbiological contamination between source and point-of-use. *Trop Med Int Heal*. 2004;9(1):106-117. doi:10.1046/j.1365-3156.2003.01160.x

32. Rayner J, Skinner B, Lantagne D. Current practices in manufacturing locally-made ceramic pot filters for water treatment in developing countries. *J Water, Sanit Hyg Dev*. 2013;3(2):252. doi:10.2166/washdev.2013.178

33. Arnold BF, Colford JM. Treating water with chlorine at point-of-use to improve water quality and reduce child diarrhea in developing countries: a systematic review and meta-analysis. *Am J Trop Med Hyg*. 2007;76(2):354-364.

34. WHO | Treatment technologies. http://www.who.int/household_water/research/technologies_intro/en/#. Vt26Gjk5Ook.mendeley. Accessed March 7, 2016.

35. Clasen T, Parra GG, Boisson S, Collin S. Household-based ceramic water filters for the prevention of diarrhea: A randomized, controlled trial of a pilot program in Colombia. *Am J Trop Med Hyg*. 2005;73(4):790-795. doi:73/4/790 [pii]

36. Clasen T, Boisson S. Household-based ceramic water filters for the treatment of drinking water in disaster response: an assessment of a pilot programme in the Dominican Republic. *Water Pract Technol*. 2006;1(2):wpt2006031.

37. Enger KS, Nelson KL, Clasen T, Rose JB, Eisenberg JNS. Linking quantitative microbial risk assessment and epidemiological data: Informing safe drinking water trials in developing countries. *Environ Sci Technol*. 2012;46(9):5160-5167. doi:10.1021/es204381e

38. Du Preez M, Conroy RM, Wright JA, Moyo S, Potgieter N, Gundry SW. Use of ceramic water filtration in the prevention of diarrheal disease: a randomized controlled trial in rural South Africa and Zimbabwe. *Am J Trop Med Hyg*. 2008;79(5):696-701.

39. Abebe LS, Smith JA, Narkiewicz S, et al. Ceramic water filters impregnated with silver nanoparticles as a point-of-use water-treatment intervention for HIV-positive individuals in Limpopo Province, South Africa: a pilot study of technological performance and human health benefits. *J Water Health*. 2014;12(2):288-300. doi:10.2166/wh.2013.185

40. WHO | Evaluating household water treatment options. http://www.who.int/water_sanitation_health/publications/2011/household_water/en/#.Vt2ORZRUbU0.mendeley. Accessed March 7, 2016.

41. Brown J, Sobsey MD. Microbiological effectiveness of locally produced

ceramic filters for drinking water treatment in Cambodia. *J Water Health*. 2010;8:1-10. doi:10.2166/wh.2009.007

42. Rayner J. Current practices in manufacturing of ceramic pot filters for water treatment. 2009.

43. van Halem D, van der Laan H, Heijman SGJ, van Dijk JC, Amy GL. Assessing the sustainability of the silver-impregnated ceramic pot filter for low-cost household drinking water treatment. *Phys Chem Earth, Parts A/B/C*. 2009;34:36-42. doi:10.1016/j.pce.2008.01.005

44. Tsao NH, Malatesta K, Anuku NE, Soboyejo W. Virus filtration in porous iron (III) doped ceramic water filters. *Adv Mater Resesarch*. 2016;1132:284-294. doi:10.4028/www.scientific.net/AMR.1132.284

45. Clark KN, Elmore AC. Bacteria removal effectiveness of ceramic pot filters not applied with colloidal silver. *Water Sci Technol Water Supply*. 2011;11(6):765-772.

46. Bielefeldt AR, Kowalski K, Summers RS. Bacterial treatment effectiveness of point-of-use ceramic water filters. *Water Res*. 2009;43(14):3559-3565.

47. Venis RA, Basu OD. Mechanisms and efficacy of disinfection in ceramic water filters: A critical review. *Crit Rev Environ Sci Technol*. 2020:1-41.

48. Fahlin CJ. Hydraulic Properties Investigation of the Potters For Peace Colloidal Silver Impregnated, Ceramic Filter. *Unpubl Thesis, Univ Color Boulder, Boulder, CO, USA*. 2003.

49. Oyanedel-Craver V a., Smith J a. Sustainable colloidal-silver-impregnated ceramic filter for point-of-use water treatment. *Environ Sci Technol*. 2008;42(3):927-933. doi:10.1021/es071268u

50. van Halem D. Ceramic silver impregnated pot filters for household drinking water treatment in developing countries. 2006.

51. Yang H, Xu S, Chitwood DE, Wang Y. Ceramic water filter for point-of-use water treatment in developing countries: Principles, challenges and opportunities. *Front Environ Sci Eng*. 2020;14(5):1-10.

52. Unuabonah EI, Ugwuja CG, Omorogie MO, Adewuyi A, Oladoja NA. Clays for efficient disinfection of bacteria in water. *Appl Clay Sci*. 2018;151:211-223.

53. WHO. WHO | WHO International Scheme to Evaluate Household Water Treatment Technologies. 2016;(ISBN 978 92 4 150994 7).

http://www.who.int/household_water/scheme/household-water-treatment-report-round-1/en/#.VtmmIDJjl5c.mendeley. Accessed March 4, 2016.

54. Tiong A. ENVIRONMENTAL ASPECTS AND FEATURES OF CRITICAL PATHOGEN GROUPS.

55. van Halem D, van der Laan H, Soppe AIA, Heijman SGJ. High flow ceramic pot filters. *Water Res*. 2017;124:398-406. doi:10.1016/j.watres.2017.07.045

56. Unicef. Use of Ceramic Water Filters in Cambodia (field note). *F Note*. 2007.

57. Bielefeldt AR, Kowalski K, Schilling C, Schreier S, Kohler A, Scott Summers R. Removal of virus to protozoan sized particles in point-of-use ceramic water filters. *Water Res*. 2010;44(5):1482-1488. doi:10.1016/j.watres.2009.10.043

58. van Halem D, van der Laan H, Heijman SGJ, van Dijk JC, Amy GL. Assessing the sustainability of the silver-impregnated ceramic pot filter for low-cost household drinking water treatment. *Phys Chem Earth*. 2009;34(1-2):36-42. doi:10.1016/j.pce.2008.01.005

59. Salsali H, McBean E, Brunsting J. Virus removal efficiency of Cambodian ceramic pot water purifiers. *J Water Health*. 2011;9(2):306. doi:10.2166/wh.2011.087

60. Farrow C, McBean E, Salsali H. Virus removal efficiency of ceramic water filters: Effects of bentonite turbidity. *Water Sci Technol Water Supply*. 2014;14(2):304-311. doi:10.2166/ws.2013.206

61. Bitton G. Adsorption of viruses onto surfaces in soil and water. *Water Res*. 1975;9(5-6):473-484. doi:10.1016/0043-1354(75)90071-8

62. Schaub SA, Sagik BP. Association of enteroviruses with natural and artificially introduced colloidal solids in water and infectivity of solids-associated virions. *Appl Microbiol*. 1975;30(2):212-222.

63. Rusinol M, Girones R. Summary of excreted and waterborne viruses. *Glob Water Pathog Proj*. 2017.

64. Gall AM, Mariñas BJ, Lu Y, Shisler JL. Waterborne Viruses: A Barrier to Safe Drinking Water. *PLoS Pathog*. 2015. doi:10.1371/journal.ppat.1004867

65. Springthorpe S, Sattar SA. Chapter 6 Virus Removal During Drinking Water Treatment. In: ; 2007:109-126. doi:10.1016/S0168-7069(07)17006-3

66. Larimer CJ. Effect of silver nanoparticle coatings on mycobacterial biofilm attachment and growth: Implications for ceramic water filters. 2013.

67. Flemming H-C, Percival SL, Walker JT. Contamination potential of biofilms in water distribution systems. *Water Sci Technol Water Supply*. 2002;2(1):271-280. http://ws.iwaponline.com/content/2/1/271.abstract. Accessed May 26, 2016.

68. LeChevallier MW, Schulz W, Lee RG. Bacterial nutrients in drinking water. *Appl Environ Microbiol*. 1991;57(3):857-862.

69. van der Kooij D, Visser A, Hijnen WAM. Determining the concentration of easily assimilable organic carbon in drinking water. 1982.

70. Pedersen K. Biofilm development on stainless steel and pvc surfaces in drinking water. *Water Res*. 1990;24(2):239-243. doi:10.1016/0043-1354(90)90109-J

71. Wingender J, Neu TR, Flemming H-C. What are bacterial extracellular polymeric substances? In: *Microbial Extracellular Polymeric Substances*. Springer; 1999:1-19.

72. Storey M V, Ashbolt NJ. Persistence of two model enteric viruses (B40-8 and MS-2 bacteriophages) in water distribution pipe biofilms. *Water Sci Technol*. 2001;43(12):133-138.

73. Ueda T. Fate of indigenous bacteriophage in a membrane bioreactor. *Water Res*. 2000;34(7):2151-2159. doi:10.1016/S0043-1354(99)00382-6

74. Purnell S, Ebdon J, Buck A, Tupper M, Taylor H. Bacteriophage removal in a full-scale membrane bioreactor (MBR) - Implications for wastewater reuse. *Water Res*. 2015. doi:10.1016/j.watres.2015.01.019

75. Schijven JF, Van den Berg HHJL, Colin M, et al. A mathematical model for removal of human pathogenic viruses and bacteria by slow sand filtration under variable operational conditions. *Water Res*. 2013;47(7):2592-2602. doi:10.1016/j.watres.2013.02.027

76. Group CMW. Best practice recommendations for local manufacturing of ceramic pot filters for household water treatment. *Atlanta, GA*. 2011;11:252-261.

77. Ehdaie B, Su Y-H, Swami NS, Smith JA. Protozoa and virus disinfection by silver-and copper-embedded ceramic tablets for water purification. *J Environ Eng*. 2020;146(4):4020015.

78. Friedman KC. Evaluation of Antimicrobial Metals for Enhanced Performance of Household Water Treatment Methods. 2018.

79. Lemire JA, Harrison JJ, Turner RJ. Antimicrobial activity of metals: Mechanisms, molecular targets and applications. *Nat Rev Microbiol*. 2013. doi:10.1038/nrmicro3028

80. Workentine ML, Harrison JJ, Stenroos PU, Ceri H, Turner RJ. Pseudomonas fluorescens' view of the periodic table. *Environ Microbiol*. 2008. doi:10.1111/j.1462-2920.2007.01448.x

81. Swathy JR, Udhaya Sankar M, Chaudhary A, Aigal S, Anshup, Pradeep T. Antimicrobial silver: An unprecedented anion effect. *Sci Rep*. 2014. doi:10.1038/srep07161

82. Butkus MA, Labare MP, Starke JA, Moon K, Talbot M. Use of Aqueous Silver To Enhance Inactivation of Coliphage MS-2 by UV Disinfection. *Appl Environ Microbiol*. 2004;70(5):2848 LP - 2853. doi:10.1128/AEM.70.5.2848-2853.2004

83. Kim JY, Lee C, Cho M, Yoon J. Enhanced inactivation of E. coli and MS-2 phage by silver ions combined with UV-A and visible light irradiation. *Water Res*. 2008;42(1-2):356-362. doi:10.1016/J.WATRES.2007.07.024

84. Zodrow K, Brunet L, Mahendra S, et al. Polysulfone ultrafiltration membranes impregnated with silver nanoparticles show improved biofouling resistance and virus removal. *Water Res*. 2009;43(3):715-723.

85. Thurman RB, Gerba CP, Bitton G. The molecular mechanisms of copper and silver ion disinfection of bacteria and viruses. *Crit Rev Environ Control*. 1989;18(4):295-315. doi:10.1080/10643388909388351

86. Brown JM. Effectiveness of ceramic filtration for drinking water treatment in Cambodia. 2007.

87. Thalmann B, Voegelin A, Morgenroth E, Kaegi R. Effect of humic acid on the kinetics of silver nanoparticle sulfidation. *Environ Sci Nano*. 2016;3(1):203-212.

88. Akaighe N, MacCuspie RI, Navarro DA, et al. Humic acid-induced silver nanoparticle formation under environmentally relevant conditions. *Environ Sci Technol*. 2011;45(9):3895-3901.

89. Buck KN, Ross JRM, Russell Flegal A, Bruland KW. A review of total dissolved copper and its chemical speciation in San Francisco Bay, California. *Environ*

Res. 2007. doi:10.1016/j.envres.2006.07.006

90. Singh R, Kim W, Smith JA. Effect of Chloride Ions on the Point-of-Use Drinking Water Disinfection Performance of Porous Ceramic Media Embedded with Metallic Silver and Copper. *Water*. 2020. doi:10.3390/w12061625

91. Choi O, Clevenger TE, Deng B, Surampalli RY, Ross L, Hu Z. Role of sulfide and ligand strength in controlling nanosilver toxicity. *Water Res*. 2009. doi:10.1016/j.watres.2009.01.029

92. Xiu ZM, Zhang QB, Puppala HL, Colvin VL, Alvarez PJJ. Negligible particle-specific antibacterial activity of silver nanoparticles. *Nano Lett*. 2012. doi:10.1021/nl301934w

93. Xiu ZM, Ma J, Alvarez PJJ. Differential effect of common ligands and molecular oxygen on antimicrobial activity of silver nanoparticles versus silver ions. *Environ Sci Technol*. 2011. doi:10.1021/es201918f

94. Pham AN, Rose AL, Waite TD. Kinetics of Cu (II) reduction by natural organic matter. *J Phys Chem A*. 2012;116(25):6590-6599.

95. Sagripanti JL, Routson LB, Lytle CD. Virus inactivation by copper or iron ions alone and in the presence of peroxide. *Appl Environ Microbiol*. 1993.

96. Yamamoto N. Damage, repair, and recombination. II. Effect of hydrogen peroxide on the bacteriophage genome. *Virology*. 1969. doi:10.1016/0042-6822(69)90158-5

97. Nieto-Juarez JI, Pierzchla K, Sienkiewicz A, Kohn T. Inactivation of MS2 coliphage in Fenton and Fenton-like systems: Role of transition metals, hydrogen peroxide and sunlight. *Environ Sci Technol*. 2010. doi:10.1021/es903739f

98. Nguyen TTM, Park H-J, Kim JY, et al. Microbial Inactivation by Cupric Ion in Combination with H2O2: Role of Reactive Oxidants. *Environ Sci Technol*. 2013;47(23):13661-13667. doi:10.1021/es403155a

99. Kim HE, Nguyen TTM, Lee H, Lee C. Enhanced Inactivation of Escherichia coli and MS2 Coliphage by Cupric Ion in the Presence of Hydroxylamine: Dual Microbicidal Effects. *Environ Sci Technol*. 2015. doi:10.1021/acs.est.5b04310

100. WHO. Evaluating Household Water Treatment Options : Health-Based Targets and Microbiological Performance Specifications. *NML Classif WA*

675. 2011:1-68.

101. Lantagne DS. Investigation of the Potters for Peace colloidal silver impregnated ceramic filter: Report 1: Intrinsic effectiveness. Iethia Environmental, Boston, MA. *Boston, MA, USA*. 2001.

102. Bielefeldt AR, Kowalski K, Schilling C, Schreier S, Kohler A, Scott Summers R. Removal of virus to protozoan sized particles in point-of-use ceramic water filters. *Water Res*. 2010;44(5):1482-1488. doi:10.1016/j.watres.2009.10.043

103. Brown J, Sobsey M. *Independent Appraisal of Ceramic Water Filtration Interventions in Cambodia*.; 2006. doi:10.1017/CBO9781107415324.004

104. Clopeck KL. Monitoring and evaluation of household water treatment and safe storage technologies: the sustained use of the KOSIM ceramic water filter in northern region Ghana. 2009.

105. Brown J, Sobsey MD. Ceramic media amended with metal oxide for the capture of viruses in drinking water. *Environ Technol*. 2009;30(4):379-391. doi:10.1080/09593330902753461

106. Guerrero L, Rusiñol M, Hundesa A, et al. Development of improved low-cost ceramic water filters for viral removal in the Haitian context. *J Water Sanit Hyg Dev*. 2015;5(1):28-38.

107. Tsao NH, Malatesta KA, Anuku NE, Soboyejo WO. Virus Filtration in Porous Iron (III) Oxide Doped Ceramic Water Filters. *Adv Mater Res*. 2015;1132:284-294. doi:10.4028/www.scientific.net/AMR.1132.284

108. Wingender J, Flemming H-C. Biofilms in drinking water and their role as reservoir for pathogens. *Int J Hyg Environ Health*. 2011;214(6):417-423. doi:10.1016/j.ijheh.2011.05.009

109. Storey M V, Ashbolt NJ. A risk model for enteric virus accumulation and release from recycled water distribution pipe biofilms. *Water Sci Technol Water Supply*. 2003;3(3):93-100.

110. Purnell S, Ebdon J, Buck A, Tupper M, Taylor H. Bacteriophage removal in a full-scale membrane bioreactor (MBR) - Implications for wastewater reuse. *Water Res*. 2015;73:109-117. doi:10.1016/j.watres.2015.01.019

111. Lu R, Mosiman D, Nguyen TH. Mechanisms of MS2 bacteriophage removal by fouled ultrafiltration membrane subjected to different cleaning methods. *Environ Sci Technol*. 2013. doi:10.1021/es403426t

114

112. ElHadidy AM, Peldszus S, Van Dyke MI. Effect of hydraulically reversible and hydraulically irreversible fouling on the removal of MS2 and φX174 bacteriophage by an ultrafiltration membrane. *Water Res*. 2014;61:297-307. doi:10.1016/j.watres.2014.05.003

113. Amarasiri M, Kitajima M, Nguyen TH, Okabe S, Sano D. Bacteriophage removal efficiency as a validation and operational monitoring tool for virus reduction in wastewater reclamation: Review. *Water Res*. 2017. doi:10.1016/j.watres.2017.05.035

114. Chapman (Ed) D. *Water Quality Assessments - A Guide to Use of Biota , Sediments and Water in Environmental Monitoring - Second Edition*.; 1996.

115. Volk C, Wood L, Johnson B, Robinson J, Zhu HW, Kaplan L. Monitoring dissolved organic carbon in surface and drinking waters. *J Environ Monit*. 2002;4(1):43-47.

116. Rayner J, Zhang H, Schubert J, Lennon P, Lantagne D, Oyanedel-craver V. Laboratory Investigation into the Effect of Silver Application on the Bacterial Removal Efficacy of Filter Material for Use on Locally Produced Ceramic Water Filters for Household Drinking Water Treatment. *ACS Sustain Chem Eng*. 2013;1:737-745.

117. Liu G, Ling FQ, Magic-Knezev A, Liu WT, Verberk JQJC, Van Dijk JC. Quantification and identification of particle-associated bacteria in unchlorinated drinking water from three treatment plants by cultivation-independent methods. *Water Res*. 2013;47(10):3523-3533. doi:10.1016/J.WATRES.2013.03.058

118. Lantagne D, Klarman M, Mayer A, Preston K, Napotnik J, Jellison K. Effect of production variables on microbiological removal in locally-produced ceramic filters for household water treatment. *Int J Environ Health Res*. 2010;20(3):171-187. doi:10.1080/09603120903440665

119. Brown J, Sobsey M. *Improving Household Drinking Water Quality Use of Ceramic Water Filters in Cambodia*. Water and Sanitation program; 2007.

120. Liu G, Verberk JQJC, Van Dijk JC. Bacteriology of drinking water distribution systems: an integral and multidimensional review. *Appl Microbiol Biotechnol*. 2013;97(21):9265-9276. doi:10.1007/s00253-013-5217-y

121. Donlan RM. Biofilms: microbial life on surfaces. *Emerg Infect Dis*. 2002;8(9):881-890. doi:10.3201/eid0809.020063

122. Wäsche S, Horn H, Hempel DC. Influence of growth conditions on biofilm development and mass transfer at the bulk/biofilm interface. *Water Res*. 2002;36(19):4775-4784. doi:10.1016/S0043-1354(02)00215-4

123. Belkin S, Colwell RR. *Oceans and Health: Pathogens in the Marine Environment*. Springer; 2006.

124. Hall-Stoodley L, Costerton JW, Stoodley P. Bacterial biofilms: from the natural environment to infectious diseases. *Nat Rev Microbiol*. 2004;2(2):95-108.

125. Skraber S, Schijven J, Gantzer C, de Roda Husman AM. Pathogenic viruses in drinking-water biofilms: a public health risk? *Biofilms*. 2005;2(02):105-117.

126. Branda SS, Vik Å, Friedman L, Kolter R. Biofilms: the matrix revisited. *Trends Microbiol*. 2005;13(1):20-26. doi:10.1016/j.tim.2004.11.006

127. Flemming H. Biofilms. In: *Encyclopedia of Life Sciences*. Chichester, UK: John Wiley & Sons, Ltd; 2008. doi:10.1002/9780470015902.a0000342.pub2

128. Armanious A, Aeppli M, Jacak R, et al. Viruses at Solid-Water Interfaces: A Systematic Assessment of Interactions Driving Adsorption. *Environ Sci Technol*. 2015;50(2):732-743. doi:10.1021/acs.est.5b04644

129. Späth R, Flemming H-C, Wuertz S. Sorption properties of biofilms. *Water Sci Technol*. 1998;37(4):207-210. doi:10.1016/S0273-1223(98)00107-3

130. Huisman L, Wood WE. *Slow Sand Filtration*. Vol 16. World Health Organization Geneva; 1974.

131. Stiefel P, Rosenberg U, Schneider J, Mauerhofer S, Maniura-Weber K, Ren Q. Is biofilm removal properly assessed? Comparison of different quantification methods in a 96-well plate system. *Appl Microbiol Biotechnol*. 2016;100(9):4135-4145. doi:10.1007/s00253-016-7396-9

132. Flemming H-C, Wingender J. The biofilm matrix. *Nat Rev Microbiol*. 2010;8(9):623-633.

133. Nickels JS, Bobbie RJ, Lott DF, Martz RF, Benson PH, White DC. Effect of manual brush cleaning on biomass and community structure of microfouling film formed on aluminum and titanium surfaces exposed to rapidly flowing seawater. *Appl Environ Microbiol*. 1981;41(6):1442-1453.

134. Brown J, Sobsey M. Independent Appraisal of Ceramic Water Filtration Interventions in Cambodia. *Final report, Univ North Carolina Public Heal Dep*

Environ Sci Eng Submitt to UNICEF. 2006.

135. Elliott MA, DiGiano FA, Sobsey MD. Virus attenuation by microbial mechanisms during the idle time of a household slow sand filter. *Water Res*. 2011;45(14):4092-4102. doi:10.1016/J.WATRES.2011.05.008

136. Casanova LM, Walters A, Naghawatte A, Sobsey MD. Factors affecting continued use of ceramic water purifiers distributed to tsunami-affected communities in Sri Lanka. *Trop Med Int Heal*. 2012;17(11):1361-1368. doi:10.1111/j.1365-3156.2012.03082.x

137. Salvinelli C, Elmore AC. Assessment of the impact of water parameters on the flow rate of ceramic pot filters in a long-term experiment. *Water Sci Technol Water Supply*. 2015. doi:10.2166/ws.2015.107

138. Schijven JF, Hassanizadeh SM. Removal of Viruses by Soil Passage: Overview of Modeling, Processes, and Parameters. *Crit Rev Environ Sci Technol*. 2000;30(1):49-127. doi:10.1080/10643380091184174

139. Ismaïl R, Aviat F, Michel V, et al. Methods for recovering microorganisms from solid surfaces used in the food industry: A review of the literature. *Int J Environ Res Public Health*. 2013;10(11):6169-6183. doi:10.3390/ijerph10116169

140. Konieczny J, Rdzawski Z. Antibacterial properties of copper and its alloys. *Arch Mater Sci Eng*. 2012.

141. Gadi B, Jeffrey G. Copper, An Ancient Remedy Returning to Fight Microbial, Fungal and Viral Infections. *Curr Chem Biol*. 2009. doi:10.1557/mrs2005.10

142. Arendsen LP, Thakar R, Sultan AH. The Use of Copper as an Antimicrobial Agent in Health Care, Including Obstetrics and Gynecology. *Clin Microbiol Rev*. 2019. doi:10.1128/cmr.00125-18

143. Borkow G, Gabbay J. Copper as a Biocidal Tool. *Curr Med Chem*. 2005. doi:10.2174/0929867054637617

144. Vincent M, Hartemann P, Engels-Deutsch M. Antimicrobial applications of copper. *Int J Hyg Environ Health*. 2016. doi:10.1016/j.ijheh.2016.06.003

145. Pathak SP, Gopal K. Evaluation of bactericidal efficacy of silver ions on Escherichia coli for drinking water disinfection. *Environ Sci Pollut Res*. 2012. doi:10.1007/s11356-011-0735-6

146. Wijnhoven SWP, Peijnenburg WJGM, Herberts CA, et al. Nano-silver - A

review of available data and knowledge gaps in human and environmental risk assessment. *Nanotoxicology*. 2009. doi:10.1080/17435390902725914

147. Hwang MG, Katayama H, Ohgaki S. Inactivation of Legionella pneumophila and Pseudomonas aeruginosa: Evaluation of the bactericidal ability of silver cations. *Water Res*. 2007. doi:10.1016/j.watres.2007.05.052

148. Marambio-Jones C, Hoek EMV. A review of the antibacterial effects of silver nanomaterials and potential implications for human health and the environment. *J Nanoparticle Res*. 2010. doi:10.1007/s11051-010-9900-y

149. Silvestry-Rodriguez N, Sicairos-Ruelas EE, Gerba CP, Bright KR. Silver as a disinfectant. *Rev Environ Contam Toxicol*. 2007. doi:10.1007/978-0-387-69163-3_2

150. Mikolay A, Huggett S, Tikana L, Grass G, Braun J, Nies DH. Survival of bacteria on metallic copper surfaces in a hospital trial. *Appl Microbiol Biotechnol*. 2010. doi:10.1007/s00253-010-2640-1

151. Wright JB, Lam K, Burrell RE. Wound management in an era of increasing bacterial antibiotic resistance: A role for topical silver treatment. *Am J Infect Control*. 1998. doi:10.1053/ic.1998.v26.a93527

152. Kaneko Y, Thoendel M, Olakanmi O, Britigan BE, Singh PK. The transition metal gallium disrupts Pseudomonas aeruginosa iron metabolism and has antimicrobial and antibiofilm activity. *J Clin Invest*. 2007. doi:10.1172/JCI30783

153. Bauer TS, Menagen B, Avnir D, Hayouka Z. Random peptide mixtures entrapped within a copper-cuprite matrix: new antimicrobial agent against methicillin-resistant Staphylococcus aureus. *Sci Rep*. 2019. doi:10.1038/s41598-019-47315-0

154. Mehtar S, Wiid I, Todorov SD. The antimicrobial activity of copper and copper alloys against nosocomial pathogens and Mycobacterium tuberculosis isolated from healthcare facilities in the Western Cape: an in-vitro study. *J Hosp Infect*. 2008. doi:10.1016/j.jhin.2007.10.009

155. Lehtola MJ, Miettinen IT, Keinänen MM, et al. Microbiology, chemistry and biofilm development in a pilot drinking water distribution system with copper and plastic pipes. *Water Res*. 2004. doi:10.1016/j.watres.2004.06.024

156. Harrison JJ, Ceri H, Stremick CA, Turner RJ. Biofilm susceptibility to metal

toxicity. *Environ Microbiol*. 2004. doi:10.1111/j.1462-2920.2004.00656.x

157. Harrison JJ, Turner RJ, Joo DA, et al. Copper and quaternary ammonium cations exert synergistic bactericidal and antibiofilm activity against Pseudomonas aeruginosa. *Antimicrob Agents Chemother*. 2008. doi:10.1128/AAC.00203-08

158. Triantafyllidou S, Lytle D, Muhlen C, Swertfeger J. Copper-silver ionization at a US hospital: Interaction of treated drinking water with plumbing materials, aesthetics and other considerations. *Water Res*. 2016. doi:10.1016/j.watres.2016.06.010

159. Stout JE, Yu VL. Experiences of the First 16 Hospitals Using Copper-Silver Ionization for Legionella Control: Implications for the Evaluation of Other Disinfection Modalities . *Infect Control Hosp Epidemiol*. 2003. doi:10.1086/502251

160. Yahya MT, Straub TM, Gerba CP. Inactivation of coliphage MS-2 and poliovirus by copper, silver, and chlorine. *Can J Microbiol*. 1992. doi:10.1139/m92-072

161. Pooi CK, Ng HY. Review of low-cost point-of-use water treatment systems for developing communities. *npj Clean Water*. 2018. doi:10.1038/s41545-018-0011-0

162. Yamamoto N, Hiatt CW, Haller W. Mechanism of inactivation of bacteriophages by metals. *Biochim Biophys Acta - Spec Sect Nucleic Acids Relat Subj*. 1964;91(2):257-261. doi:10.1016/0926-6550(64)90249-X

163. Armstrong M A, Sobsey MD, Casanova LM. Disinfection of bacteriophage MS2 by copper in water. *Appl Microbiol Biotechnol*. 2017;101(18):6891-6897. doi:10.1007/s00253-017-8419-x

164. Sharan R, Chhibber S, Attri S, Reed RH. Inactivation and injury of Escherichia coli in a copper water storage vessel: effects of temperature and pH. *Antonie Van Leeuwenhoek*. 2010;97(1):91-97.

165. Lin Y -s. E, Vidic RD, Stout JE, Yu VL. Negative Effect of High pH on Biocidal Efficacy of Copper and Silver Ions in Controlling Legionella pneumophila. *Appl Environ Microbiol*. 2002;68(6):2711-2715. doi:10.1128/AEM.68.6.2711-2715.2002

166. Lok CN, Ho CM, Chen R, et al. Silver nanoparticles: Partial oxidation and antibacterial activities. *J Biol Inorg Chem*. 2007. doi:10.1007/s00775-007-

0208-z

167. Delahay P, Pourbaix M, Van Rysselberghe P. Potential-pH Diagram of Silver: Construction of the Diagram—Its Applications to the Study of the Properties of the Metal, its Compounds, and its Corrosion. *J Electrochem Soc*. 1951. doi:10.1149/1.2778107

168. Albrecht T, Addai-Mensah J, Fornasiero D. Effect of pH, concentration and temperature on copper and zinc hydroxide formation/precipitation in solution. 2011.

169. Schijven J, Teunis P, Suylen T, Ketelaars H, Hornstra L, Rutjes S. QMRA of adenovirus in drinking water at a drinking water treatment plant using UV and chlorine dioxide disinfection. *Water Res*. 2019;158:34-45. doi:10.1016/J.WATRES.2019.03.090

170. Cromeans TL, Kahler AM, Hill VR. Inactivation of adenoviruses, enteroviruses, and murine norovirus in water by free chlorine and monochloramine. *Appl Environ Microbiol*. 2010. doi:10.1128/AEM.01342-09

171. Dika C, Gantzer C, Perrin A, Duval JFL. Impact of the virus purification protocol on aggregation and electrokinetics of MS2 phages and corresponding virus-like particles. *Phys Chem Chem Phys*. 2013;15(15):5691-5700.

172. Gerba CP, Betancourt WQ. Viral Aggregation: Impact on Virus Behavior in the Environment. *Environ Sci Technol*. 2017. doi:10.1021/acs.est.6b05835

173. Wick CH, McCubbin PE. Passage of MS2 bacteriophage through various molecular weight filters. *Toxicol Methods*. 1999. doi:10.1080/105172399242618

174. Hooker JM, Kovacs EW, Francis MB. Interior Surface Modification of Bacteriophage MS2. *J Am Chem Soc*. 2004. doi:10.1021/ja031790q

175. Sagripanti JL, Routson LB, Lytle CD. Virus inactivation by copper or iron ions alone and in the presence of peroxide. *Appl Envir Microbiol*. 1993;59(12):4374-4376. http://aem.asm.org/cgi/content/long/59/12/4374. Accessed May 23, 2016.

176. Li J, Dennehy JJ. Differential bacteriophage mortality on exposure to copper. *Appl Environ Microbiol*. 2011;77(19):6878-6883. doi:10.1128/AEM.05661-11

177. Lee H, Lee H-J, Seo J, et al. Activation of oxygen and hydrogen peroxide by

copper (II) coupled with hydroxylamine for oxidation of organic contaminants. *Environ Sci Technol*. 2016;50(15):8231-8238.

178. Ueda K, Morita J, Yamashita K, Komano T. Inactivation of bacteriophage øX174 by mitomycin C in the presence of sodium hydrosulfite and cupric ions. *Chem Biol Interact*. 1980. doi:10.1016/0009-2797(80)90029-0

179. Sagripanti JL, Goering PL, Lamanna A. Interaction of copper with DNA and antagonism by other metals. *Toxicol Appl Pharmacol*. 1991. doi:10.1016/0041-008X(91)90048-J

180. Łęczkowska A, Vilar R. Interaction of metal complexes with nucleic acids. *Annu Reports Prog Chem - Sect A*. 2013. doi:10.1039/c3ic90029k

181. WHO. Guidelines for drinking-water quality: first addendum to the fourth edition. 2017.

182. Badetti E, Calgaro L, Falchi L, et al. Interaction between copper oxide nanoparticles and amino acids: Influence on the antibacterial activity. *Nanomaterials*. 2019. doi:10.3390/nano9050792

183. Barber-Zucker S, Shaanan B, Zarivach R. Transition metal binding selectivity in proteins and its correlation with the phylogenomic classification of the cation diffusion facilitator protein family. *Sci Rep*. 2017. doi:10.1038/s41598-017-16777-5

184. Minoshima M, Lu Y, Kimura T, et al. Comparison of the antiviral effect of solid-state copper and silver compounds. *J Hazard Mater*. 2016. doi:10.1016/j.jhazmat.2016.03.023

185. Wan R, Zhao G, Chen J, Zhao Y. Research progresses of artificial nucleic acid cleavage agents. *Chinese Sci Bull*. 2000. doi:10.1007/bf03183520

186. Erickson RJ, Brooke LT, Kahl MD, et al. Effects of laboratory test conditions on the toxicity of silver to aquatic organisms. In: *Environmental Toxicology and Chemistry*. ; 1998. doi:10.1897/1551-5028(1998)017<0572:EOLTCO>2.3.CO;2

187. Brown MRW, Anderson RA. The bactericidal effect of silver ions on Pseudomonas aeruginosa. *J Pharm Pharmacol*. 1968;20(S1):1S-3S.

188. Poole LB. The basics of thiols and cysteines in redox biology and chemistry. *Free Radic Biol Med*. 2015. doi:10.1016/j.freeradbiomed.2014.11.013

189. Clem Gruen L. Interaction of amino acids with silver(I) ions. *BBA - Protein*

Struct. 1975. doi:10.1016/0005-2795(75)90268-8

190. Jebri S, Muniesa M, Jofre J. General and host-associated bacteriophage indicators of fecal pollution. *Glob Water Pathog Proj http//www waterpathogens org (Farnleitner, A Blanch, A(eds) Part 2 Indic Microb Source Track Markers), http//www waterpathogens org/book/coliphage Michigan State Univ E Lansing, MI, UNESCO*. 2017.

191. Dolinsky TJ, Nielsen JE, McCammon JA, Baker NA. PDB2PQR: An automated pipeline for the setup of Poisson-Boltzmann electrostatics calculations. *Nucleic Acids Res*. 2004. doi:10.1093/nar/gkh381

192. Jackson KN, Kahler DM, Kucharska I, Rekosh D, Hammarskjold M-L, Smith JA. Inactivation of MS2 bacteriophage and adenovirus with silver and copper in solution and embedded in ceramic water filters. *J Environ Eng*. 2020;146(3):4019130.

193. Domagała K, Jacquin C, Borlaf M, et al. Efficiency and stability evaluation of Cu2O/MWCNTs filters for virus removal from water. *Water Res*. 2020;179:115879.

194. Németh Z, Szekeres GP, Schabikowski M, et al. Enhanced virus filtration in hybrid membranes with MWCNT nanocomposite. *R Soc open Sci*. 2019;6(1):181294.

195. Sinclair T, Zieba M, Irusta S, Sebastián V, Arruebo M. High-speed water sterilization using silver-containing cellulose membranes. *Nanotechnology*. 2014;25(30):305101.

196. Rao G, Brastad KS, Zhang Q, Robinson R, He Z, Li Y. Enhanced disinfection of Escherichia coli and bacteriophage MS2 in water using a copper and silver loaded titanium dioxide nanowire membrane. *Front Environ Sci Eng*. 2016. doi:10.1007/s11783-016-0854-x

197. Allen HE, Hansen DJ. The importance of trace metal speciation to water quality criteria. *Water Environ Res*. 1996;68(1):42-54.

198. Allen HE, Hall RH, Brisbin TD. Metal speciation. Effects on aquatic toxicity. *Environ Sci Technol*. 1980;14(4):441-443.

199. Sunada K, Minoshima M, Hashimoto K. Highly efficient antiviral and antibacterial activities of solid-state cuprous compounds. *J Hazard Mater*. 2012. doi:10.1016/j.jhazmat.2012.07.052

200. Soliman MYM, Medema G, Bonilla BE, Brouns SJJ, van Halem D. Inactivation

of RNA and DNA viruses in water by copper and silver ions and their synergistic effect. *Water Res X*. 2020;9:100077. doi:https://doi.org/10.1016/j.wroa.2020.100077

201. Hou W-C, Stuart B, Howes R, Zepp RG. Sunlight-driven reduction of silver ions by natural organic matter: formation and transformation of silver nanoparticles. *Environ Sci Technol*. 2013;47(14):7713-7721.

202. Caltran I, Rietveld LC, Shorney-Darby HL, Heijman SGJ. Separating NOM from salts in ion exchange brine with ceramic nanofiltration. *Water Res*. 2020. doi:10.1016/j.watres.2020.115894

203. Ghormley JA, Stewart AC. Effects of γ-Radiation on Ice1. *J Am Chem Soc*. 1956;78(13):2934-2939.

204. Romero OC, Straub AP, Kohn T, Nguyen TH. Role of temperature and suwannee river natural organic matter on inactivation kinetics of rotavirus and bacteriophage MS2 by solar irradiation. *Environ Sci Technol*. 2011. doi:10.1021/es202067f

205. Wilcox CS, Pearlman A. Chemistry and antihypertensive effects of tempol and other nitroxides. *Pharmacol Rev*. 2008. doi:10.1124/pr.108.000240

206. Wilcox CS. Effects of tempol and redox-cycling nitroxides in models of oxidative stress. *Pharmacol Ther*. 2010. doi:10.1016/j.pharmthera.2010.01.003

207. Li Y, Zhang C, Shuai D, Naraginti S, Wang D, Zhang W. Visible-light-driven photocatalytic inactivation of MS2 by metal-free g-C3N4: Virucidal performance and mechanism. *Water Res*. 2016;106:249-258. doi:https://doi.org/10.1016/j.watres.2016.10.009

208. Matsumoto KI, Okajo A, Nagata K, et al. Detection of free radical reactions in an aqueous sample induced by low linear-energy-transfer irradiation. *Biol Pharm Bull*. 2009. doi:10.1248/bpb.32.542

209. Coale KH, Bruland KW. Spatial and temporal variability in copper complexation in the North Pacific. *Deep Sea Res Part A, Oceanogr Res Pap*. 1990;37(2):317-336. doi:10.1016/0198-0149(90)90130-N

210. Xing G, Garg S, Miller CJ, Pham AN, Waite TD. Effect of Chloride and Suwannee River Fulvic Acid on Cu Speciation: Implications to Cu Redox Transformations in Simulated Natural Waters. *Environ Sci Technol*. 2020. doi:10.1021/acs.est.9b06789

211. Fitts JP, Persson P, Brown GE, Parks GA. Structure and bonding of Cu(II)-glutamate complexes at the γ-Al2O3- water interface. *J Colloid Interface Sci*. 1999. doi:10.1006/jcis.1999.6521

212. Kim JY, Lee C, Sedlak DL, Yoon J, Nelson KL. Inactivation of MS2 coliphage by Fenton's reagent. *Water Res*. 2010. doi:10.1016/j.watres.2010.01.025

213. Mattle MJ, Vione D, Kohn T. Conceptual model and experimental framework to determine the contributions of direct and indirect photoreactions to the solar disinfection of MS2, phiX174, and adenovirus. *Environ Sci Technol*. 2015. doi:10.1021/es504764u

214. Timchak E, Gitis V. A combined degradation of dyes and inactivation of viruses by UV and UV/H2O2. *Chem Eng J*. 2012;192:164-170. doi:10.1016/j.cej.2012.03.054

215. Miller LA, Bruland KW. Organic speciation of silver in marine waters. *Environ Sci Technol*. 1995;29(10):2616-2621.

216. Reinfelder JR, Chang S Il. Speciation and microalgal bioavailability of inorganic silver. *Environ Sci Technol*. 1999;33(11):1860-1863.

217. Hogstrand C, Wood CM. Toward a better understanding of the bioavailability, physiology, and toxicity of silver in fish: implications for water quality criteria. *Environ Toxicol Chem An Int J*. 1998;17(4):547-561.

218. Park H-J, Kim JY, Kim J, et al. Silver-ion-mediated reactive oxygen species generation affecting bactericidal activity. *Water Res*. 2009;43(4):1027-1032.

219. He D, Jones AM, Garg S, Pham AN, Waite TD. Silver nanoparticle– reactive oxygen species interactions: application of a charging– discharging model. *J Phys Chem C*. 2011;115(13):5461-5468.

220. Henglein A. Reactions of organic free radicals at colloidal silver in aqueous solution. Electron pool effect and water decomposition. *J Phys Chem*. 1979;83(17):2209-2216.

221. Pedahzur R, Lev O, Fattal B, Shuval HI. The interaction of silver ions and hydrogen peroxide in the inactivation of E. coli: a preliminary evaluation of a new long acting residual drinking water disinfectant. *Water Sci Technol*. 1995;31(5-6):123-129.

222. Abebe LS, Chen X, Sobsey MD. Chitosan coagulation to improve microbial and turbidity removal by ceramicwater filtration for household drinking water treatment. *Int J Environ Res Public Health*. 2016.

doi:10.3390/ijerph13030269

223.   Bulta AL, Micheal GAW. Evaluation of the efficiency of ceramic filters for water treatment in Kambata Tabaro zone, southern Ethiopia. *Environ Syst Res*. 2019;8(1):1-15.

224.   Rayner J, Luo X, Schubert J, Lennon P, Jellison K, Lantagne D. The effects of input materials on ceramic water filter efficacy for household drinking water treatment. *Water Sci Technol Water Supply*. 2017;17(3):859-869.

225.   Lucier KJ, Dickson-Anderson SE, Schuster-Wallace CJ. Effectiveness of silver and copper infused ceramic drinking water filters in reducing microbiological contaminants. *J Water Supply Res Technol*. 2017;66(7):528-536.

226.   Soliman MYM, van Halem D, Medema G. Virus removal by ceramic pot filter disks: Effect of biofilm growth and surface cleaning. *Int J Hyg Environ Health*. 2020;224. doi:10.1016/j.ijheh.2019.113438

227.   Mittelman AM, Lantagne DS, Rayner J, Pennell KD. Silver Dissolution and Release from Ceramic Water Filters. *Environ Sci Technol*. 2015. doi:10.1021/acs.est.5b01428

228.   Xu C, Chen G, Zhao Y, et al. Interfacing with silica boosts the catalysis of copper. *Nat Commun*. 2018;9(1):1-10.

229.   Miettinen IT, Vartiainen T, Martikainen PJ. Phosphorus and bacterial growth in drinking water. *Appl Environ Microbiol*. 1997;63(8):3242-3245. doi:0099-2240/97/

230.   Brown J, Sobsey MD. Ceramic media amended with metal oxide for the capture of viruses in drinking water. *Environ Technol*. 2009;30(4):379-391. doi:10.1080/09593330902753461

231.   Mustapha S, Oladejo TJ, Muhammed NM, et al. Fabrication of porous ceramic pot filters for adsorptive removal of pollutants in tannery wastewater. *Sci African*. 2021;11:e00705.

232.   Pérez-Vidal A, Silva-Leal JA, Diaz-Gómez J, et al. Performance evaluation of ceramic pot filters combined with adsorption processes for the removal of heavy metals and phenolic compounds. *J Water Health*. 2021.

233.   Russell AD, Hugo WB. Antimicrobial Activity and Action of Silver. *Prog Med Chem*. 1994. doi:10.1016/S0079-6468(08)70024-9

234. Jackson KN, Smith JA, Edokpayi JN. New method for the deposition of metallic silver and metallic copper on full-size porous ceramic water filters. *Environ Eng Sci*. 2019;36(1):2-11.

235. Zhou J, Yang F, Huang Y, Ding W, Xie X. Smartphone-powered efficient water disinfection at the point of use. *npj Clean Water*. 2020;3(1):1-9.

CURRICULUM VITAE

Mona Soliman, born in 18th of September 1987 in Cairo, Egypt. In 2009, completed BSc in Civil engineering where her graduation thesis (honours) focused on designing water and wastewater treatment for industrial cities. This started her passionate career in water treatment. She worked water engineer and project coordinator for national and international firms. In 2013, she moved to the Netherlands to start her MSc in urban water and sanitation in UNESCO-IHE. Her thesis on phosphate recovery from wastewater was awarded the best MSc thesis by Bill & Melinda Gates foundation. Later, she started her PhD in department of sanitary engineering, TU delft, where she took the lead on setting up the white lab facility for microbial analyses of drinking water. This marked the first milestone to start the experimental work of her PhD. During her PhD, she also participated in researching the ripening process of slow sand filters. Moreover, she identified and isolated a new bacteriophage in collaboration with the phage bank, Brouns lab, TU Delft.

List of publications:

Soliman, M.Y.M., van Halem, D., Medema, G. (2020) Virus removal by ceramic pot filter disks: Effect of biofilm growth and surface cleaning. Int. J. Hyg. Environ. Health 224.2019.113438

Soliman, M.Y.M., Medema, G., Bonilla, B.E., Brouns, S.J.J., van Halem, D. (2020) Inactivation of RNA and DNA viruses in water by copper and silver ions and their synergistic effect. Water Res. X 9, 100077.

Soliman, M.Y.M., Medema, G., van Halem, D. (2021) Enhanced virus inactivation by copper and silver ions in the presence of natural organic matter in water. Submitted to Water Research journal.

Soliman, M.Y.M., Arora, H., van Halem, D., & JP Van der Hoek Optimizing the ripening period of slow sand filters (In preparation).